Interleukin-33 and Vaccine Vectors in Virus-Host Balance

Inauguraldissertation

zur

Erlangung der Würde eines Doktors der Philosophie

vorgelegt der

Philosophisch-Naturwissenschaftlichen Fakultät

der Universität Basel

von

Sandra Kallert

aus

Wilhermsdorf, Deutschland

Basel, 2015

Genehmigt von der Philosophisch-Naturwissenschaftlichen Fakultät

auf Antrag von

Prof. Christoph Dehio, Prof. Daniel Pinschewer, Prof. Benjamin Marsland

Basel, den 11.11.2014

Prof. Dr. Jörg Schibler

Table of Contents

List of Figures

List of Tables

Abbreviations

ANOVA	Analysis of Variance
APC	Antigen-Presenting Cell
art	artificial
Bcl-2	B-cell lymphoma 2
BECs	Blood endothelial cells
BHK-21	Baby Hamster Kidney cells
BSS	Balanced Salt Solution
CD	Cluster of Differentiation
cDNA	complementary DNA
Cl13	Clone 13
Clec2i	C-type lectin domain family 2 member i
Cr^{51}	Chromium-51
CTL	Cytotoxic T lymphocyte
CXCR5	Chemokine (C-X-C motif) Receptor 5
DAB	3, 3'-Diaminobenzidine
DAMP	Damage-Associated Molecular Pattern
DAPI	4',6-Diamidino-2-phenylindole
DCs	Dendritic Cells
DMEM	Dulbecco's Modifies Eagle's Medium
DNA	Desoxyribonucleic Acid
DNs	Double-Negative cells
ERK	Extracellular-signal-regulated Kinase
FACS	Fluorescence-activated cell sorting
Fc	Fragment crystallizable
FCS	Fetal Calf Serum
FFU	Focus Forming Unit
FRCs	Fibroblastic Reticlular Cells
GFP	Green Fluorescent Protein
GP	Glycoprotein
HRP	Horseradish Peroxidase
i.v.	intravenous
Ifitm	Interferon-induced transmembrane protein

IFN- α/βR	Interferon alpha/beta receptor
IFN-γ	Interferon gamma
IFN-γR	Interferon gamma receptor
IgG	Immunoglobulin
IGR	Intergenic Region
IL	Interleukin
Il1rl1	Interleukin-1 Receptor like 1
iNKT	invariant Natural Killer T cells
JNK	c-Jun N-terminal kinase
Klrb1	Killer Cell Lectin-like Receptor subfamily B, member 1
Klrg1	Killer Cell Lectin-like Receptor subfamily G, member 1
ko	knockout
LCMV	Lymphocytic Choriomeningitis Virus
LECs	Lymphatic Endothelial Cells
MAPK	Mitogen-activated protein kinases
MC-57	Mouse Fibrosarcoma Cell Line
MEM	Minimal Essential Medium
MHC	Major Histocompatibility Complex
MHV-68	Murine γ-Herpesvirus 68
moi	Multiplicity of Infection
mRNA	messenger RNA
MyD88	Myeloid Differentiation Primary Response Gene (88)
nat	natural
neoR	Neomycin Resistance Gene
NFkB	Nuclear Factor-kB
NK	Natural Killer Cells
NP	Nucleoprotein
ORF	Open Reading Frame
PAMP	Pathogen-Associated Molecular Pattern
PBS	Phosphate Buffered Saline
PCR	Polymerase Chain Reaction
PD1	Programmed Cell Death Protein 1
PE	Phycoerythrin
PFA	Paraformaldehyde
PFU	Plaque Forming Unit

PLO	Primary Lymphoid Organ
PRR	Pattern Recognition Receptor
qRT-PCR	quantitative Real Rime Polymerase Chain Reaction
r2LCMV	recombinant Bi-segmented LCMV
r3LCMV	recombinant Tri-segmented LCMV
RAG	Recombination-Activating Gene
RdRp	RNA dependent RNA polymerase
RFP	Red Fluorescent Protein
RING	Really Interesting New Gene
RNA	Ribonucleic Acid
RT-PCR	Real Time Polymerase Chain Reaction
SD	Standard Deviation
SEM	Standard Error of the Mean
SLO	Secondary Lymphoid Organ
SM1	Smarta
SPF	Specific Pathogen-Free
Tfh	T Follicular Helper Cell
TNF-α	Tumor Necrosis Factor alpha
Tspan	Tetraspanin
UTR	Untranslated Region
VLP	Virus-Like Particle
VV	Vaccinia Virus
wt	Wild-type

I General Introduction

I.1 Molecular Patterns in Virus-induced Immune Responses

In order to react to different types of danger with the initiation or enhancement of the appropriate responses, the immune system has evolved to distinguish endogenous damage from exogenous danger and trigger the activation of the respective downstream signaling cascades. Cells can therefore distinguish danger by invading microorganisms from tissue damage due to other causes such as heat or cuts.

Pathogens and microorganisms, which invade a host's organism, carry pathogen-associated molecular patterns (PAMPs). PAMPs are a set of conserved small molecular motifs that can be recognized by their respective pattern recognition receptors (PRRs) in the host. This interaction in turn leads to activation of signaling pathways and the initiation of an innate immune response (Schenten and Medzhitov 2011). Damage-associated molecular patterns (DAMPs) are a pool of structurally diverse endogenous molecules that signal tissue damage and alert the immune system of the ongoing destruction, in order to enhance immune responses. In the case of necrosis, an uncontrolled form of cell death, the dying cell releases all of its endogenous content without regulatory mechanisms, leading to the induction of an inflammatory response. The intracellular proteins that are released upon necrosis signal cell damage, which led to their terminology as "alarmins" (Oppenheim and Yang 2005, Bianchi 2007).

Both PAMPs and DAMPs bind to their respective PRRs to initiate downstream signaling. PRRs can be subdivided into membrane-bound and cytoplasmic PRRs, depending on their localization within the cell. Membrane-bound PRRs include Toll-like receptors (TLR) and C-type lectin Receptors (CLR). TLRs recognize extracellular cell-wall structures from microbes or bacterial and viral nucleic acid components which are common to pathogens but not present in host cells and lead to activation of signaling cascades (summarized in (Beutler, Jiang et al. 2006)). CLRs are expressed on a variety of different cells including immature dendritic cells and are involved in recognition of carbohydrates expressed by many pathogens including bacteria, viruses, fungi and helminthes and subsequent activation of immune responses (Chen, Lin et al. 2008, Gazi and Martinez-Pomares 2009, Drummond and Brown 2011, Paveley, Aynsley et al. 2011,

Hardison and Brown 2012). Cytoplasmic PRRs include NOD-like receptors (NLR) and RIG-I-like receptors (RLR). NLRs are intracellularly expressed receptors. They can be found in lymphocytes, macrophages, dendritic cells and also non-immune cells and they recognize sugar chains of bacterial origin. RLRs recognize viral double-stranded and single stranded RNA. Two famous members of RLRs that recognize viral patterns are RIG-I and MDA5 (Kang, Gopalkrishnan et al. 2002, Yoneyama, Kikuchi et al. 2004). RIG-I recognizes 5'-triphosphorylated dsRNA of viral origin (Hornung, Ellegast et al. 2006). MDA5 also binds to double-stranded RNA from viruses, however the detailed features of viral RNA required to activate MDA5 signaling are not fully understood yet (Runge, Sparrer et al. 2014).

Interleukin-33 (IL-33) is a member of the IL-1 family. It is expressed in the nucleus of endothelial and epithelial cells and it was found that IL-33 is a dual-function cytokine since it acts as a chromatin-associated factor within the nucleus (Carriere, Roussel et al. 2007, Moussion, Ortega et al. 2008) and as an alarm mediator once released into the extracellular space. Upon cellular destruction, cells undergo necrosis and release IL-33 (Cayrol and Girard 2009, Luthi, Cullen et al. 2009), classifying IL-33 as an alarmin (Moussion, Ortega et al. 2008). IL-33 binds to its cell surface receptor consisting of ST2 in association with the ubiquitous IL-1R accessory protein (IL1RAcP) (Schmitz, Owyang et al. 2005, Ali, Huber et al. 2007), which leads to the initiation of signaling pathways and downstream activation of nuclear factors NFkB, ERK, p38 and JNK (Palmer and Gabay 2011). Interestingly, IL-33 is released into the extracellular space as full-length protein. Opposed to what was first proposed and is known for other interleukins like IL-1β and IL-18, IL-33 is biologically active as a full-length peptide and proteolytic cleavage of IL-33 by apoptotic caspases leads to its inactivation (Cayrol and Girard 2009, Luthi, Cullen et al. 2009, Talabot-Ayer, Lamacchia et al. 2009). IL-33 was long believed to primarily act on Th2 cells and as such was regarded as a cytokine eliciting mainly Th2-associated immune responses including those leading to asthma and allergic responses (summarized in (Liew, Pitman et al. 2010, Garlanda, Dinarello et al. 2013)). However, in recent years several lines of evidence suggested that IL-33 also plays a role in Th1-associated immune responses and as such is not restricted to the Th2 context. IL-33 has been shown to enhance production of IFN-γ by iNKT cells, NK cells and CD8+ T cells (Smithgall, Comeau et al. 2008, Bourgeois, Van et al. 2009, Yang, Li et al. 2011). Importantly in 2012 we have shown that potent anti-viral immune responses require IL-33 and that signaling via the IL-33/ST2 axis is essential for the clonal expansion of virus-specific CD8+ T cells and their differentiation into functional effector cells upon antigen-

encounter during viral infection (see section 1 “The Alarmin Interleukin-33 Drives Protective Antiviral CD8+ T Cell Responses”). CD8+ T cells that are in an IL-33 deficient environment or that are unable to sense IL-33 fail to expand normally show reduced cytotoxic potential, do not differentiate into multi-functional effector T cells and are finally unable to efficiently control the virus (Bonilla, Frohlich et al. 2012).

I.2 The Role of Secondary Lymphoid Organ Stroma in Adaptive Immune Responses

Much is known about the role of the hematopoietic compartment in adaptive immune responses including B and T cells, on which immunological research has focused for a long time. However, evidence has accumulated that non-hematopoietic radio-resistant cells in secondary lymphoid organs also play a crucial role in adaptive immune responses, a component which has long been underestimated. Primary lymphoid organs (PLOs) like thymus and bone marrow and secondary lymphoid organs (SLOs) like spleen and lymph nodes are sites of organized lymphoid cell accumulations. B and T cell maturation occurs in PLOs, whereas further lymphocyte differentiation and adaptive immune responses take place in SLOs, where antigens get efficiently trapped for subsequent exposure to T and B lymphocytes (summarized in (Ruddle and Akirav 2009)). The spleen can be divided into two areas, the red pulp and the white pulp. The red pulp is the blood-filtering system of the spleen, which removes damaged cells and recycles iron (Mebius and Kraal 2005, Ruddle and Akirav 2009). The white pulp is organized as lymphoid structure with highly vascularized B and T cell compartments (Mebius and Kraal 2005, Ruddle and Akirav 2009). The radio-resistant (CD45-negative) compartment forms the structure of the spleen and consists of three different cell types: CD31+gp38- blood endothelial cells (BECs), CD31-GP38+ fibroblastic reticular cells (FRCs) and CD31-GP38- so-called double-negative cells (DNs), which are poorly characterized so far. In lymph nodes, an additional population of CD31+GP38+ lymphatic endothelial cells (LECs) can be found. BECs form the inner lining of blood vessels and are a separation between the inside of the vessel and the surrounding tissue. FRCs form the structural backbone in splenic T-cell zones. Not much is known about the function of DNs so far (Mebius and Kraal 2005). Besides forming three-dimensional networks in the splenic T cell zones, providing a scaffold for lymphocyte migration (Link, Vogt et al. 2007, Turley, Fletcher et al. 2010), stromal cells have now been shown to be modulators of inflammation and hematopoietic cells depend on stromal cells for successful entry, migration and activation in lymphoid

organs (Link, Vogt et al. 2007). FRCs are multifunctional cells that produce various chemokines, form the scaffold for T cell migration and form a conduit network for the transport of small soluble antigens throughout the SLO parenchyma (Nolte, Belien et al. 2003, Bajenoff, Egen et al. 2006). They furthermore promote survival of naïve T cells by production of IL-7 (Link, Vogt et al. 2007) and directly stimulate anti-viral immune responses by facilitating interactions between T cells and dendritic cells (DCs) (Bajenoff, Egen et al. 2006, Bajenoff, Glaichenhaus et al. 2008). In addition, several reports have demonstrated that resident stromal cells can function as antigen-presenting cells in secondary lymphoid organs such as lymph nodes and spleen and thus can directly prime and activate T cells ((Lee, Epardaud et al. 2007, Nichols, Chen et al. 2007, Cohen, Guidi et al. 2010, Fletcher, Lukacs-Kornek et al. 2010), summarized in (Turley, Fletcher et al. 2010)). In the last years several reports also postulated that FRCs get directly infected by LCMV resulting in disruption of the FRC network and loss of immunocompetence, which in turn might contribute to immunosuppression and persistence during chronic LCMV infection (Mueller, Matloubian et al. 2007, Scandella, Bolinger et al. 2008).

I.3 Adaptive Immune Responses in Acute and Chronic Viral Infection

Infections with viruses can either be of short- or long-term and are denominated acute and chronic, respectively. Whereas acute infections are cleared in a short period of time, chronic infections are characterized by prolonged viremia and may never be cleared by the host's immune system such as for human immunodeficiency virus (HIV). In certain cases such as human hepatitis B and C virus infections (HBV, HCV) or in murine infection with lymphocytic choriomeningitis virus (LCMV), the outcome may either be life-long persistence or protracted yet self-limiting infection. The magnitude and functionality of adaptive immune responses against acute and chronic viral infections show important differences, as exemplified on the basis of the afore-mentioned prototypic infection model of LCMV. Its outcome depends on the strain and dose of virus used and the MHC class I haplotype of the mouse (Zinkernagel, Pfau et al. 1985). In C57BL/6 (H-2^b) mice, the LCMV strain Armstrong or low doses of the WE strain cause acute infections, which are characterized by a rapid onset of disease, if any, and viremia that is resolved within one week. High-dose infection with LCMV strain Clone 13 or Docile results in protracted or persisting viremia, which is detectable in some tissues for more than three months (Ahmed, Salmi et al. 1984, Wherry, Blattman et al. 2003). This

difference in outcome is particularly noteworthy, since the clearance of an infection with LCMV Armstrong versus infection with LCMV Clone 13 is dependent on only two amino acid differences (Bergthaler, Flatz et al. 2010).

CD8+ T cells play an essential role for the clearance of acute and the control of persistent LCMV infection and LCMV has been shown to be an excellent inducer of virus-specific CTLs (summarized in (Doherty and Christensen 2000), (Byrne, Ahmed et al. 1984, Yewdell and Haeryfar 2005)). Upon acute infection, virus-specific CD8+ T cells get activated and clonally expand in response to the antigen stimulation. They up-regulate effector markers and differentiate into effector CD8+ T cells expressing inflammatory mediators like Interferon-γ and TNF-α and the cytotoxic molecules perforin and granzyme B for direct killing of infected cells (Kagi, Ledermann et al. 1994). The expansion phase of CTLs is followed by a contraction phase were most (90-95%) of effector CTLs undergo apoptosis and the remaining CD8+ T cells differentiate into memory T cells. Those memory cells enable a quick re-expansion upon exposure to the antigen and consequently a quicker anti-viral response (Wherry and Ahmed 2004). Virus-specific CTLs also clonally expand in response to chronic LCMV infection. However, in the course of chronic LCMV infection many antiviral CTLs get deleted (Moskophidis, Lechner et al. 1993) and the remaining ones hierarchically lose effector functions over time and develop a functionally impaired state, both of which can be referred to as "exhaustion" of virus-specific CTLs (Zajac, Blattman et al. 1998). In consequence the remaining cells are impaired in their ability to directly lyse infected cells, proliferate in response to antigen-stimuli and produce inflammatory and anti-viral cytokines like IL-2, TNF-α and IFN-γ (Zajac, Blattman et al. 1998, Wherry, Blattman et al. 2003). Taken together, the continuous exposure to high loads of antigen during chronic infection leads to the progressive dysfunction or eventual deletion of virus-specific CTLs, which in turn favors long-term persistence of the virus (Ou, Zhou et al. 2001, Fuller and Zajac 2003, Wherry, Blattman et al. 2003, Wherry, Ha et al. 2007).

Acute LCMV infections are controlled virtually exclusively by CD8+ T cell-dependent mechanisms, in presence or absence of functional CD4+ T cells (Moskophidis, Cobbold et al. 1987, Ahmed, Butler et al. 1988, Rahemtulla, Fung-Leung et al. 1991). In contrast, clearance of chronic LCMV infection requires both CD4+ and CD8+ T cells and an only temporary unavailability of CD4+ T cells through blockade or depletion drastically affects the outcome of infection and prevents eventual resolution of the virus infection (Doherty, Allan et al. 1992, Matloubian, Concepcion et al. 1994). Several lines of

evidence suggest that chronic LCMV infections are eventually controlled 2-3 months after infection via not only CTL- but also B cell-dependent mechanisms, both of which are reliant on help from CD4+ T helper cells. Without the help of CD4+ T cells, virus-specific CTLs get depleted during chronic infection (Battegay, Moskophidis et al. 1994, Matloubian, Concepcion et al. 1994). Furthermore it has been shown that LCMV-specific antibody responses are essential for the final control and clearance of the virus and that the activation of those antibody-producing B cells depends on CD4+ T cell help (Ciurea, Hunziker et al. 2001, Bergthaler, Flatz et al. 2009). Similar to CD8+ T cells, also CD4+ T cells have been shown to enter a functionally altered state in chronic LCMV infection, which is also sometimes referred to as "exhaustion" (Brooks, Teyton et al. 2005). Priming and early CD4+ T cell activation have been demonstrated to be comparable in acute and chronic infection. This suggests that such "exhaustion" is not a consequence of an early-programmed event but of continuous antigenic exposure (Brooks, McGavern et al. 2006). Nevertheless, CD4+ T cells continue to provide help to CD8+ T cells and B cells during chronic infection, which improves control of virus replication. IL-21, which most likely is produced by CD4+ T cells, has been shown to shape the functionality of antiviral CD8+ T cells and as such to play a vital role for the control of chronic LCMV infection (Elsaesser, Sauer et al. 2009, Frohlich, Kisielow et al. 2009, Yi, Du et al. 2009). Taken together both CD4+ and CD8+ T cells play an important role in anti-viral immune responses against chronic infection and thus for successful clearance of the virus.

I.4 Arenaviruses in Basic Research and Human Disease

Arenaviruses generally infect rodents but can cause severe illness upon accidental transmission to humans. Disease severity and pathology varies amongst members of the family and can range from aseptic meningitis caused by LCMV to hemorrhagic fevers which can lead to death upon infection with Guanarito, Junin, Machupo or the most famous family member Lassa virus (Geisbert and Jahrling 2004). Arenaviruses are divided into two groups: the Old World arenaviruses like Lassa virus (LASV) and LCMV can be found in Africa. Members of the New World arenaviruses like Junin, Guanarito or Machupo virus are widespread in rodent populations of South America (Johnson, Kuns et al. 1966, Tesh, Wilson et al. 1993, Mills, Ellis et al. 1994). Junin virus is the only arenavirus for which a preventive vaccine is available for clinical use. For all others anti-viral therapy with the nucleoside analog ribavirin is the only possible treatment so far and

affords limited efficacy. Thus there is substantial need for new vaccines and powerful treatments for infections with arenaviruses. Development of these tools necessitates a more detailed knowledge of the molecular biology of the virus and of the viral factors impacting disease outcome and pathogenesis.

As already alluded to in section I.3, LCMV is a prototypic mouse model virus in research on viral infections. As for all arenaviruses, the natural host of LCMV are mice, however, several reports revealed that LCMV might also be a neglected human pathogen (Barton 1996, Wright, Johnson et al. 1997). Since its isolation in the 1930s (Rivers and McNair Scott 1935, Traub 1935) studies using this virus have uncovered many key concepts in viral immunology and pathogenesis like neonatal tolerance, MHC restriction and T cell exhaustion (summarized in (Zinkernagel 2002) and (Oldstone 2002)). LCMV has been extensively used to investigate viral molecular biology and immune responses particularly in the context of persistent infection.

I.5 Reverse Genetic Engineering of Arenaviruses

By definition, transfection of purified RNA of negative-strand viruses like LCMV cannot initiate an infectious cycle when transfected into permissive cells. This is in large parts due to their inability to directly serve as mRNA i.e. they cannot be translated when introduced into cells. In order to generate infectious viral particles of negative-stranded RNA viruses from cDNA in cultured permissive cells, the viral RNA segments must be trans-complemented with the minimal factors required for genome transcription and replication. This has complicated the investigation of negative-stranded RNA viruses with consequent delays in this research topic. With the help of a minigenome system that has been published several years ago, viral cis-acting elements and transacting factors involved in transcription, replication and formation of viral particles could finally be analyzed (Lee, Novella et al. 2000, Lee, Perez et al. 2002, Perez and de la Torre 2003, Pinschewer, Perez et al. 2003, Pinschewer, Perez et al. 2005). Also for other arenaviruses like LASV and Tacaribe virus reverse genetic systems have been established (Lopez, Jacamo et al. 2001, Hass, Golnitz et al. 2004). In 2006 the recovery of infectious LCMV entirely from cDNA was achieved using pol-I/-II or T7/pol-II-driven plasmids, respectively (referred to as “viral rescue” (Flatz, Bergthaler et al. 2006, Sanchez and de la Torre 2006)). Rescue of LCMV entirely from plasmid enabled the introduction of

mutations at will in the viral genome and the investigation of their impact on viral phenotypes and cellular and molecular bases of viral pathogenesis. In addition reverse genetics based on negative-strand RNA viruses hold great promise and are widely used for novel vaccine designs and vector platforms in the fight against viral infections and cancer (von Messling and Cattaneo 2004, Vigil, Park et al. 2007).

I.6 Recombinant Viruses as Vaccine Platforms

Since treatment for patients suffering from viral infections are limited, vaccines are considered as one of the most promising and effective tool against infectious diseases. Whereas in the past mainly live attenuated viruses were used, the importance of recombinant viruses as a novel vaccine platform is steadily increasing since the early 1980ies (Thummel, Tjian et al. 1981, Mackett, Smith et al. 1982). One of the main advantages of recombinant viruses over other technologies is the possibility to modify the genetic information of both the vector platform and the antigen at will in a controlled fashion. This is in contrast to strategies used for live-attenuated viruses where researchers rely on random mutations e.g. acquired during serial passages in order to obtain attenuated variants (Olschlager and Flatz 2013). Several recombinant virus platforms have been proven protective in animals and also in human trials. The choice of a vector platform depends on different factors. It is favorable, if the vector has a similar tropism as the target virus. Also the vector has to be able to elicit efficient immune responses against the introduced antigen in order to provide efficacy. In the fight against arenaviral hemorrhagic fevers, wild-type vesicular stomatitis virus (VSV) was modified to recombinant rVSV expressing the glycoprotein of LASV instead of the own GP (Garbutt, Liebscher et al. 2004) and vaccinated non-human primates were protected against subsequent lethal challenge with LASV (Geisbert, Jones et al. 2005). One of the oldest and most successful recombinant chimeric virus as vaccine vector is attenuated yellow fever strain 17D (YFV 17D) (Olschlager and Flatz 2013). Genes of Japanese Encephalitis Virus or Dengue Virus have been added to the YFV 17D genome, leading to protection of vaccinated animals against respective lethal challenge (Chambers, Nestorowicz et al. 1999, Guirakhoo, Zhang et al. 1999, Guirakhoo, Weltzin et al. 2000, Chambers, Liang et al. 2003). Earlier this year the chimeric YF17D/Dengue Virus vaccine has been shown to be protective in the world's first large-scale efficacy study and is expected to be licensed in the course of next year (Sanofi-Pasteur 2014a, Sanofi-Pasteur 2014b). A chimeric YFV

17D expressing GP of the arenavirus LASV also showed promising results by protection of guinea pigs against fatal LASV challenge (Bredenbeek, Molenkamp et al. 2006, Jiang, Dalebout et al. 2011).

Even though the mentioned recombinant viruses have been proven successful for vaccination against some infectious diseases, the induction of a multifunctional yet long-lasting CTL response is still to be achieved. VV-based vectors induce multifunctional CTL responses but these are of rather low magnitude (Peters, Jaoko et al. 2007, Harari, Bart et al. 2008). In addition, vaccination with rVV-based vectors induces a strong vector-specific antibody response, which renders homologous boosts problematic.

Rescue of replicative LCMV from DNA was an important achievement in order to exploit LCMV as a potential vaccine platform (Flatz, Bergthaler et al. 2006, Sanchez and de la Torre 2006). It has been demonstrated that replication-deficient LCMV elicits long-lived T cell responses while the defect in replication ensures stable attenuation and an acceptable safety profile (Flatz, Hegazy et al. 2010). The combination of several features of LCMV makes it a potential candidate for vaccine delivery. LCMV is known to induce a multifunctional and long-lasting T cell response (Homann, Teyton et al. 2001). In addition LCMV directly infects DCs, leading to their activation and presentation of the vaccine antigen by professional antigen-presenting cells, which in turn is essential for the induction of functional CD8+ T cell responses (Probst, Lagnel et al. 2003, Steinman 2007). LCMV has furthermore been shown to induce only low levels of neutralizing antibodies against the glycoprotein of LCMV but high magnitude of protective neutralizing antibody responses to foreign antigens, enabling homologous boost strategies and underlining its suitability as a potentially novel vaccine vector in clinical use (Pinschewer, Perez et al. 2004). An adequate safety profile e.g. by stable attenuation and a constant expression of the transgene are two of the most important qualifications a potential vaccine vector has to fulfill in order to be evaluated for human applications. A recombinant vaccine vector providing these features of an acceptable safety profile combined with the induction of a multifunctional protective immune response without the generation of neutralizing antibodies thus represents a promising candidate for a vaccine platform.

II Aims of the Thesis

The aims of my thesis were threefold.

Firstly, we wanted to decipher the role of IL-33 in adaptive immunity against acute and chronic viral infection.

Secondly, we aimed at investigating the cellular source of IL-33 and the impact thereof on T cell responses to chronic viral infection.

Thirdly, we intended to develop genetically and phenotypically stable transgene-expressing replication-competent arenaviruses.

1 The Alarmin Interleukin-33 Drives Protective Antiviral CD8+ T Cell Responses

Weldy V, Bonilla [1,2,*], Anja Fröhlich [3,4,*], Karin Senn [5,*], Sandra Kallert [1,2], Marylise Fernandez [1,2], Susan Johnson [1,2], Mario Kreutzfeldt [1,6], Ahmed N. Hegazy [3,4,7], Christina Schrick [1,6], Padraic G. Fallon [8], Roman Klemenz [5], Susumu Nakae [9], Heiko Adler [10], Doron Merkler [1,6,11], Max Löhning [3,4,†], Daniel D. Pinschewer [1,2,†]

[1] Department of Pathology and Immunology, University of Geneva, 1 rue Michel Servet, 1211 Geneva 4, Switzerland.
[2] World Health Organization Collaborating Center for Vaccine Immunology, University of Geneva, Switzerland.
[3] Experimental Immunology, Department of Rheumatology and Clinical Immunology, Charité–University Medicine Berlin, Berlin, Germany.
[4] German Rheumatism Research Center (DRFZ), a Leibniz Institute, Charitéplatz 1, 10117 Berlin, Germany.
[5] Institute for Cancer Research, Department of Pathology, University Hospital of Zurich, Schmelzbergstrasse 12, 8091 Zurich, Switzerland.
[6] Division of Clinical Pathology, Geneva University Hospital, 1 rue Michel Servet, 1211 Geneva 4, Switzerland.
[7] Department of Gastroenterology, Hepatology and Endocrinology, Campus Charité Mitte, Charité–University Medicine Berlin, Berlin, Germany.
[8] Institute of Molecular Medicine, St. James's Hospital, Trinity College Dublin, Dublin 8, Ireland.
[9] The Institute of Medical Science, The University of Tokyo, 4-6-1 Shirokanedai, Minato-ku, Tokyo 108-8639, and Japan Science and Technology Agency, Precursory Research for Embryonic Science and Technology (PRESTO), 4-1-8 Hncho, Kawaguchi, Saitama 332-0012, Japan.
[10] Helmholtz Zentrum München, Institute of Molecular Immunology and Clinical Cooperation Group Hematopoietic Cell Transplantation (CCG HCT), Marchioninistraße 25, 81377 München, Germany.
[11] Department of Neuropathology, University Medical Center, Georg August University, Göttingen, Germany.

[*] These authors contributed equally to this work.
† These authors contributed equally to this work.

To whom correspondence should be addressed. Email: loehning@drfz.de (M.L.); daniel.pinschewer@gmx.ch (D.P.P)

This article has been published in

Science. 2012 Feb 24;335(6071):984-9

1.1 Abstract

Pathogen-associated molecular patterns decisively influence antiviral immune responses, whereas the contribution of endogenous signals of tissue damage, also known as damage-associated molecular patterns or alarmins, remains ill defined. We show that interleukin-33 (IL-33), an alarmin released from necrotic cells, is necessary for potent $CD8^+$ T cell (CTL) responses to replicating, prototypic RNA and DNA viruses in mice. IL-33 signaled through its receptor on activated CTLs, enhanced clonal expansion in a CTL-intrinsic fashion, determined plurifunctional effector cell differentiation, and was necessary for virus control. Moreover, recombinant IL-33 augmented vaccine-induced CTL responses. Radio-resistant cells of the splenic T cell zone produced IL-33, and efficient CTL responses required IL-33 from radio-resistant cells but not from hematopoietic cells. Thus, alarmin release by radio-resistant cells orchestrates protective antiviral CTL responses.

1.2 Introduction and Results

Pathogen-associated molecular patterns (PAMPs) characterize intruding microorganisms and are important for adaptive immune responses to viral infection (Schenten and Medzhitov 2011). Conversely, endogenous molecular patterns, which indicate tissue injury, are referred to as alarmins and form a second class of damage-associated molecular patterns (DAMPs) (Oppenheim and Yang 2005). Unlike PAMPs, the potential contribution of alarmins to antiviral immune defense remains largely elusive.

Many viruses are excellent inducers of cytotoxic $CD8^+$ T lymphocytes (CTLs) (Yewdell and Haeryfar 2005), the basis of which is incompletely understood. To screen for inflammatory signals augmenting antiviral CTL responses, we used lymphocytic choriomeningitis virus (LCMV) infection of mice. We performed a genome-wide cDNA expression analysis of total spleen tissue from LCMV-infected mice and compared it to an analysis of uninfected controls. From a large panel of interleukins and pro-inflammatory cytokines, interferon-γ (IFN-γ) and IL-33 were most up-regulated (table 1.S1). The IL-33 receptor ST2, an IL-1 receptor family member also known as T1 and IL1RL1, was also up-regulated.

IL-33 is expressed in the nucleus of nonhematopoietic cells, such as fibroblasts and epithelial and endothelial cells of various tissues (Moussion, Ortega et al. 2008), but its role in antiviral CTL responses is unknown. Its bioactive pro-inflammatory form is released as a result of necrosis but not apoptosis, classifying IL-33 as an alarmin (Cayrol and Girard 2009, Haraldsen, Balogh et al. 2009, Zhao and Hu 2010). IL-33 mRNA expression peaked at 3 to 5 days after infection and grossly paralleled the kinetics of LCMV RNA (Fig. 1.1A). To test whether IL-33 was important for CTL responses to LCMV, we performed infection experiments in IL-33–deficient (*Il33*$^{-/-}$) mice (Oboki, Ohno et al. 2010). Absence of IL-33 reduced the absolute number of CTLs responding to the immunodominant LCMV epitope GP33 by >90%. The frequency of epitope-specific CTLs was reduced by >75% (Fig. 1.1B). When expressed as a nuclear factor in healthy cells, IL-33 is complexed with chromatin and modulates gene expression (Carriere, Roussel et al. 2007). Upon release from necrotic cells, however, IL-33 binds and signals through ST2 (Schmitz, Owyang et al. 2005, Dinarello 2009). To assess which one of these roles of IL-33 accounted for defective CTL responses in *Il33*$^{-/-}$ mice, we used transgenic mice expressing a soluble decoy receptor for IL-33 [*Il1rl1-Fc* mice (Senn, McCoy et al. 2000)]. *Il1rl1-Fc* mice displayed defective CTL expansion analogously to

Il33$^{-/-}$ mice (Fig. 1.S1A). Mice lacking the IL-33 receptor ST2 [*Il1rl1*$^{-/-}$ (Townsend, Fallon et al. 2000)] also mounted similarly reduced responses to all three LCMV epitopes tested (Fig. 1.1C and Fig. 1.S1 B and C). This indicated that IL-33 was released to the extracellular compartment and signaled through ST2 to amplify antiviral CTL responses.

Analogous to the responses against LCMV, an RNA virus, *Il1rl1*$^{-/-}$ mice also exhibited significantly reduced CTL responses against murine γ-herpesvirus 68 [MHV-68 (Ehtisham, Sunil-Chandra et al. 1993)], a DNA virus (Fig. 1.S1D). In further analogy to LCMV, MHV-68 induced IL-33 mRNA up-regulation (Fig. 1.S1E). The differences in CTL responses to LCMV and MHV-68 were also reflected in reduced antigen-specific cytotoxicity (Fig. 1.S1 F and G). However, CTL responses to a nonreplicating adenovirus-based vaccine vector were similar in *Il1rl1*$^{-/-}$ and wild-type (WT) mice (Fig. 1.S1H).

Given IL-33 can act as an alarmin, we hypothesized that productive viral replication may represent a unifying characteristic of LCMV and MHV-68 infection, differentiating them from adenoviral vectors. Indeed, the CTL responses of WT and *Il1rl1*$^{-/-}$ mice to replication-deficient LCMV-based vaccine vector (Flatz, Hegazy et al. 2010) were indistinguishable, and the magnitude of these responses was comparable to the magnitude of responses observed in WT LCMV-infected *Il1rl1*$^{-/-}$ mice (Fig. 1.1D). Further, *Il1rl1*$^{-/-}$mice mounted defective CTL responses against WT vaccinia virus (VV), whereas attenuated [thymidine kinase–deficient (Buller, Smith et al. 1985)] VV-based vectors induced comparable responses in *Il1rl1*$^{-/-}$ and WT controls (Fig. 1.S1I). Thus, we hypothesized that exogenously administered IL-33 could mimic viral replication to enhance vaccine-induced CTL responses. Indeed, recombinant IL-33 significantly augmented CTL responses to VV-based vectors and viruslike particles (VLPs) (Fig. 1.1 E and F.

CTLs play a pivotal role in the resolution of primary viral infection (Buller, Smith et al. 1985, Fung-Leung, Kundig et al. 1991, Ehtisham, Sunil-Chandra et al. 1993, Flatz, Hegazy et al. 2010). *Il1rl1*$^{-/-}$ mice controlled low-dose LCMV infection (Fig. 1.S1J) but displayed elevated viremia after high-dose LCMV infection and often progressed to viral persistence, whereas WT control mice eliminated the virus (Fig. 1.1G and Fig. 1.S1K). ST2-deficient mice also displayed a log increase in splenic MHV-68 titers and three logs increase in pulmonary VV titers (Fig. 1.1 H and I). LCMV-neutralizing antibody responses were comparable in *Il1rl1*$^{-/-}$ mice and WT controls (Fig. 1.S1L), suggesting

that defective CTL responses of *Il1rl1*$^{-/-}$ mice were at the root of impaired LCMV control.

LCMV can cause lethal CTL-mediated immunopathologic disease of the central nervous system when administered intracranially (Fung-Leung, Kundig et al. 1991). Five out of six WT mice developed terminal disease within 10 days, whereas all *Il1rl1*$^{-/-}$ mice survived without clinical signs of immunopathology (Fig. 1.1J).

The IL-33 receptor ST2 has predominantly been detected on mast cells and CD4^{+} T helper type 2 cells (Lohning, Stroehmann et al. 1998, Xu, Chan et al. 1998, Liew, Pitman et al. 2010), reportedly exerting pleiotropic effects on helminth-specific immunity, allergy, anaphylaxis, autoimmune, and cardiovascular disease (Liew, Pitman et al. 2010, Palmer and Gabay 2011). Conversely, ST2 expression on human and mouse CTLs has only recently been found under select in vitro culture and differentiation conditions (Yang, Li et al. 2011). Hence, we investigated which cells were sensing IL-33 for augmenting antiviral CTL responses. To this end, we reconstituted lethally irradiated mice with an approximately 1:1 mixture of WT (CD45.1^{+}) and ST2-deficient bone marrow (CD45.1^{-}) (Fig. 1.2A and Fig. 1.S2A). Compared with uninfected mice, WT cells were 10-fold overrepresented in the population of antigen-specific CTLs responding to LCMV infection (Fig. 1.2A). In contrast, the repartition of WT and *Il1rl1*$^{-/-}$ B cells remained unaltered (Fig. 1.S2A). These observations suggested that virus-reactive CTLs respond to IL-33 directly. Independent evidence was obtained when T cell receptor–transgenic GP33-specific CTLs (Pircher, Burki et al. 1989) (P14 cells) were adoptively transferred, followed by LCMV challenge (Fig. 1.2B). Impaired expansion of ST2-deficient P14 cells in WT recipients corroborated CTL-intrinsic ST2 signaling. As expected, no such differences were seen between control and ST2-deficient P14 cells in the IL-33–depleted environment of *Il1rl1-Fc* mice (Fig. 1.2B). Primary CTL responses to LCMV are CD4 T cell independent (Rahemtulla, Fung-Leung et al. 1991), and the differences in CTL responses between WT and *Il1rl1*$^{-/-}$ mice persisted when CD4^{+} T cells were depleted (Fig. 1.S2B). Altogether, these findings established a CTL-intrinsic role of ST2 signaling in the expansion of antiviral CTLs.

On day 6 after LCMV infection, we observed ST2 expression on up to 20% of virus-specific CTLs, representing the peak of expression as monitored on activated (CD62L^{low}) CTLs (Fig. 1.2 C and D, and Fig. 1.S2 C and D). In P14 cells, we detected a simultaneous peak of ST2 mRNA (Fig. 1.2E). IL-33 signaling through ST2 involves the adaptor protein MyD88 and downstream phosphorylation of p38 mitogen-activated protein kinase

(Schmitz, Owyang et al. 2005). Exposure of day 6 LCMV-infected splenocytes to IL-33 ex vivo increased phospho-p38 levels in control P14 cells but not in ST2-deficient ones (Fig. 1.2F). In concordance with induction of ST2 expression upon activation, IL-33 failed to trigger detectable phospho-p38 signals in naïve P14 cells but did so on day 6 and 8 after infection (Fig. 1.2G). MyD88 serves important CTL-intrinsic functions, but the upstream receptor(s) accounting for these effects had remained elusive (Rahman, Cui et al. 2008). In agreement with previous reports, *Myd88*$^{-/-}$ P14 cells expanded significantly less than control P14 cells when adoptively transferred into WT recipients and challenged with LCMV (Fig. 1.2H). In the IL-33–depleted environment of *Il1rl1-Fc* recipients, however, control and *Myd88*$^{-/-}$ P14 cells responded equivalently, suggesting that defective expansion of *Myd88*$^{-/-}$ P14 cells was largely attributable to a lack of ST2 downstream signaling.

CTL functionality represents an important correlate of protective capacity (Appay, van Lier et al. 2008). A substantial proportion of control P14 effector cells were plurifunctional, co-expressing IFN-γ, tumor necrosis factor (TNF)-α, IL-2, and the degranulation marker CD107a in various combinations (Fig. 1.3A). Conversely, about 95% of ST2-deficient P14 cells were monofunctional or lacked effector function (Fig. 1.3A). Reduced plurifunctionality was also observed in polyclonal antiviral CTL populations of ST2-deficient compared with WT mice (Fig. 1.S3A). Coexpression of granzyme B and CD107a indicates efficient cytotoxicity and was nearly undetectable in ST2-deficient P14 cells (Fig. 1.3B). Control P14 cells also contained significantly higher levels of the anti-apoptotic protein Bcl-2 than ST2-deficient cells (Fig. 1.3C).

We performed genome-wide cDNA expression profiling of control and ST2-deficient effector P14 cells, yielding 63 differentially expressed candidate genes (Fig. 1.S3B and table 1.S2). We validated differential expression of *Klrb1c* (NK1.1) and *Clec2i*, which influence effector cell differentiation and proliferation (Ljutic, Carlyle et al. 2005, Tian, Nunez et al. 2005); *Ifitm1* and *Ifitm3*, which mediate the antiproliferative effects of IFN-γ and pro-apoptotic signals (Dobrzanski, Reome et al. 2004); and *Tspan5*, which affects cell proliferation, migration, and adhesion (Koopman, Kopcow et al. 2003); thus corroborating the broad and profound effects of ST2 signals on the CD8^{+} effector T cell transcriptome (Fig. 1.3D). The gene that encodes KLRG-1, which is a marker of effector CTLs (Joshi, Cui et al. 2007), was also among the gene array candidates. Indeed, ST2-deficient P14 cells and virus-specific CTLs of *Il1rl1*$^{-/-}$ mice exhibited a significant reduction in KLRG-1^{high}CD127^{low} effector CTLs, failed to express NK1.1, and expressed

somewhat higher levels of the inhibitory receptor PD-1 (Fig. 1.3 E and F, and Fig. 1.S3 C to E). With transition to the memory phase, however, the size of the LCMV-specific CTL pool and the cells' KLRG-1 expression became similar in WT and *Il1rl1*$^{-/-}$ mice, and vaccinated *Il1rl1*$^{-/-}$ mice controlled LCMV challenge infection as efficiently as WT controls (Fig. 1.S3 F and G). This supported the concept that inflammatory signals are more important for primary effector CTL responses than for memory formation (Rahman, Cui et al. 2008, Rahman, Zhang et al. 2011).

To characterize the cellular source of IL-33 bolstering antiviral CTL responses, we generated reciprocal bone marrow chimeras by using WT or *Il33*$^{-/-}$ mice (Fig. 1.4A). WT recipient mice generated significantly more LCMV-specific CTLs than *Il33*$^{-/-}$ recipients, irrespective of the IL-33 competence of the bone marrow. These data suggested that radio-resistant, and thus nonhematopoietic, cells are the main source of IL-33. IL-33^{+} cells were only detected in the spleen of chimeras generated from WT recipients, irrespective of the bone marrow received (WT or *Il33*$^{-/-}$, Fig. 1.4B). IL-33^{+} cells colocalized predominantly with CD3^{+} cells but only sparsely with B cells (Fig. 1.4C and Fig. 1.S4). This was compatible with IL-33 expression by fibroblastic reticular cells (Moussion, Ortega et al. 2008), a stromal cell population of the T cell zone and known target of LCMV infection (Mueller, Matloubian et al. 2007).

1.3 Discussion

In light of the evidence for IL-33 to act as an alarmin (Haraldsen, Balogh et al. 2009, Zhao and Hu 2010), our findings offer a previously unknown molecular link to understand how viral replication, commonly thought of as "danger" (Gallucci and Matzinger 2001), can enhance CTL responses to infection. The nonredundancy with PAMPs is noteworthy, particularly in the context of viral replication, which provides abundant PAMP signals (Schenten and Medzhitov 2011). The observed LCMV dose dependency suggests that the IL-33–ST2 axis is most relevant under conditions of high viral burden. We identified nonhematopoietic cells in the splenic T cell zone expressing IL-33. Depending on the site of initiation and expansion of T cell responses, other cell types expressing IL-33 may also supply this cytokine to CTLs (Le Goffic, Arshad et al. 2011), and potential regulation by the soluble form of ST2 remains to be investigated (Becerra, Warke et al. 2008).

PAMPs act primarily on professional antigen-presenting cells and thereby are decisive for efficient priming of CTLs (Joffre, Nolte et al. 2009). IL-33 and possibly also other alarmins have complementary and nonredundant functions and, in the case of IL-33, act on antiviral CTLs directly. Taken together, this study establishes a paradigm for the role of nonhematopoietic cells providing alarmins to augment and differentiate protective CTL responses to viral infection.

1.4 Methods

1.4.1 Mice and animal experimentation

IL-33-/- mice (Oboki, Ohno et al. 2010) were obtained through the RIKEN Center for Developmental Biology (Acc. No. CDB0631K; http://www.cdb.riken.jp/arg/mutant%20mice%20list.html). *Il1rl1-/-*, *Il1rl1-Fc*, P14 and P14 *Myd88-/* mice have been described (Pircher, Burki et al. 1989, Senn, McCoy et al. 2000, Townsend, Fallon et al. 2000, Rahman, Cui et al. 2008). Animal experiments were performed at the Universities of Geneva and Zurich and at the Charité and German Rheumatism Research Center Berlin in accordance with the Swiss and German laws for animal protection, respectively, and with permission from the local veterinary offices.

1.4.2 Gene expression analysis

Affymetrix GeneChip Mouse Gene 1.0 ST and Applied Biosystems TaqMan RT-PCR assays were utilized for assessing gene expression. TaqMan results were normalized to GAPDH. RNA from FACS-sorted T cells was pre-amplified using the Sigma Aldrich Transplex WTA kit.

1.4.3 Viruses, vaccine vectors and cytokine treatment

LCMV-WE was administered at a dose of 200 PFU intravenously (low dose) unless specified. For intracerebral infection, 10^5 PFU of LCMV Armstrong were given. $2x10^6$ PFU of recombinant (thymidine kinase-deficient) vaccinia virus vector expressing LCMV-GP (Flatz, Hegazy et al. 2010) and $4x10^5$ PFU wild type vaccinia virus strain WR were given intravenously. 10^5 PFU of MHV-68 were given intraperitoneally, $3x10^5$ PFU of rLCMV vectors (Flatz, Hegazy et al. 2010) were administered intravenously, and vaccination with 200 µg of VLPs carrying GP33 (Storni, Lechner et al. 2002) was performed subcutaneously. Infectious LCMV, vaccinia virus and MHV-68 titers, and LCMV RNA were quantified as described (Adler, Messerle et al. 2000, Flatz, Hegazy et al. 2010). Recombinant IL-33 (eBioscience, 4 µg per dose) was administered daily intraperitoneally, starting on day 1 after vaccination.

1.4.4 T cell assays, antibody measurements and phospho-p38 MAPK detection

Epitope-specific T cells were enumerated using MHC class I tetramers (Beckman Coulter) and dextramers (Immudex), and by intracellular cytokine assays (Flatz, Hegazy et al. 2010). CTL activity was measured in primary ex vivo Cr^{51} release assays. EL-4 cells serving as targets in primary ex vivo CTL assays were loaded with the LCMV-epitope GP33 (KAVYNFATC) or with a mixture of MHV-68 peptides p79 (TSINFVKI) and p56 (AGPHNDMEI). LCMV-neutralizing antibodies were determined in plaque reduction assays (Pinschewer, Perez et al. 2004). For FACS detection of phospho-p38 MAPK, cells were serum starved for 5 hours prior to adding recombinant mouse IL-33 (R&D Systems) or mock for 30 min., then were fixed, permeabilized and stained using Phosflow Lyse/Fix buffer, Phosflow perm buffer III and PE anti-phospho-p38 (all from BD Pharmingen). For flow cytometric detection of cell surface ST2, splenocytes were pre-incubated with anti-mouse Fcγ-receptor antibody (clone 2.4G2) followed by staining with digoxigenin-coupled anti-mouse ST2 antibody (clone DJ8, mdbisoscience). For detection, a PE-coupled anti-digoxigenin Fab antibody (Roche) was used. To augment the PE signal we performed two rounds of amplification using the PE FASER Kit (Miltenyi Biotec). As a specificity control for surface ST2 detection by the above procedure (Fig. 1.S2C, D), Fc block was washed away, and surface ST2 was blocked by incubation of the splenocytes with uncoupled ST2 antibody (10 µg/ml). Subsequently, unbound antibody was washed away and the cells were stained as described above. For detection of surface ST2 on MHC class I tetramer-binding CD8+ T cells, ST2 surface staining and amplification were performed first, followed by extensive washing with PBS/2% BSA. Only subsequently the splenocytes were incubated with the respective MHC class I tetramer. Further antibodies for flow cytometry were from BD Pharmingen, Biolegend, eBiosciences.

1.4.5 Immunohistochemistry

PFA-fixed tissues were subject to antigen retrieval (microwave), perioxidase inactivation (PBS/3% H2O2) and blocked (PBS/10% FCS). Goat anti–mouse IL-33 (R&D Systems), rat anti–human/mouse CD3 (Serotec) and rat anti-mouse/human B220/CD45R (eBioscience) served as primary antibodies and were visualized by an avidin-biotin technique with 3,3′ -diaminobenzidine (nuclear haemalaun counterstaining) for light microscopy or with species-specific Alexa555- or Alexa488-conjugated secondary

antibodies (Invitrogen) together with DAPI (Sigma-Aldrich) in fluorescence/confocal microscopy.

1.4.6 Bone marrow chimeras and adoptive cell transfer

Recipients of bone marrow ($5x10^6$ cells) were lethally irradiated (11 Gy) the day before transfer, and residual T cells were depleted (100 µg T24 anti-Thy1 antibody intraperitoneally). We purified P14 CD8+ T cells for transfusion (10^4 cells per recipient) by magnetic cell sorting (Miltenyi Biotec).

1.4.7 Statistical analysis

One-way ANOVA with Bonferroni's or Dunnett's post-test were used for multiple comparisons as indicated, unpaired two-tailed student's t test to compare two groups, and logrank tests for survival curves (Graphpad Prism software vs. 4.0b). $p<0.05$ was considered statistically significant (*), $p<0.01$ as highly significant (**).

1.5 Figures

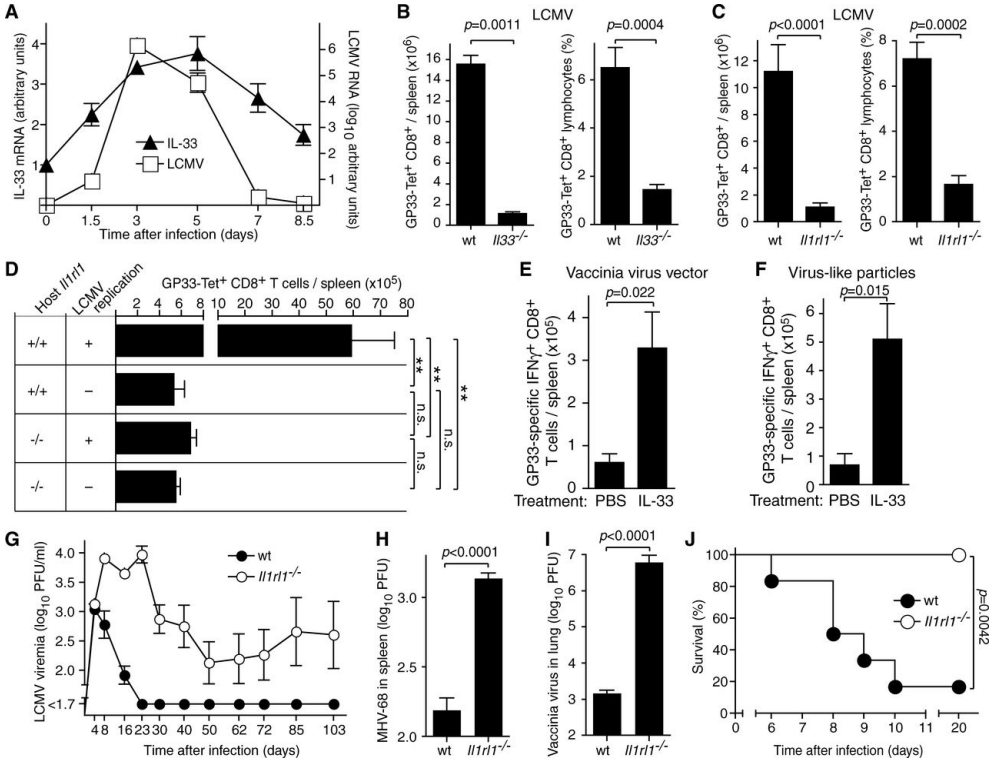

Figure 1.1: The IL-33–ST2 pathway drives protective CTL responses to replicating viral infection.

(**A**) Kinetic analysis of IL-33 and LCMV RNA expression in the spleen after LCMV infection. Symbols represent the mean ± SEM of four mice. *N* = 1 (*N* refers to the number of times an experiment was performed). (**B** and **C**) The number of GP33-specific CTLs in the spleen, as detected by peptide–major histocompatibility complex (MHC) tetramer staining, on day 8 after LCMV infection. Bars represent mean ± SEM of five mice. *N* = 1 (B) or 3 (C). (**D**) Epitope-specific CTLs of WT and *Il1rl1*$^{-/-}$ mice responding to replicating WT LCMV infection or to replication-deficient rLCMV vectors. Bars represent the mean ± SEM of five mice. *N* = 2. *P* < 0.0001 by one-way analysis of variance (ANOVA). Results of Bonferroni's posttest are indicated. n.s., not significant; **P* < 0.05; ***P* < 0.01. (**E** and **F**) WT mice were vaccinated with recombinant VV vector expressing LCMV-GP (E) or with GP33-carrying VLPs (F) on day 0 and were treated with IL-33 or diluent [phosphate-buffered saline (PBS)] daily from day 1 to 7, and CTL responses were determined on day 8. Bars represent the mean ± SEM of four to five mice. *N* = 2 (E) or 1 (F). (**G**) Viremia after infection with 2 × 10^6 plaque-forming units (PFU) of LCMV-WE. Symbols represent the mean ± SEM of five mice. *N* = 2. (**H**) Splenic MHV-68 titers on day 10 after infection. Bars represent the mean ± SEM of five mice. *N* = 1. (**I**) Pulmonary VV titers on day 8 after infection. Bars represent the mean ± SEM of four to five mice. *N* = 1. (**J**) Incidence of choriomeningitis after intracerebral LCMV infection. Terminally diseased animals were killed in accordance with Swiss law. Survival was compared by using the log rank test. Groups of six mice were used. One of two similar experiments is shown. Unpaired two-tailed student's *t* test was used for statistical analysis in (B), (C), (E), (F), (H), and (I).

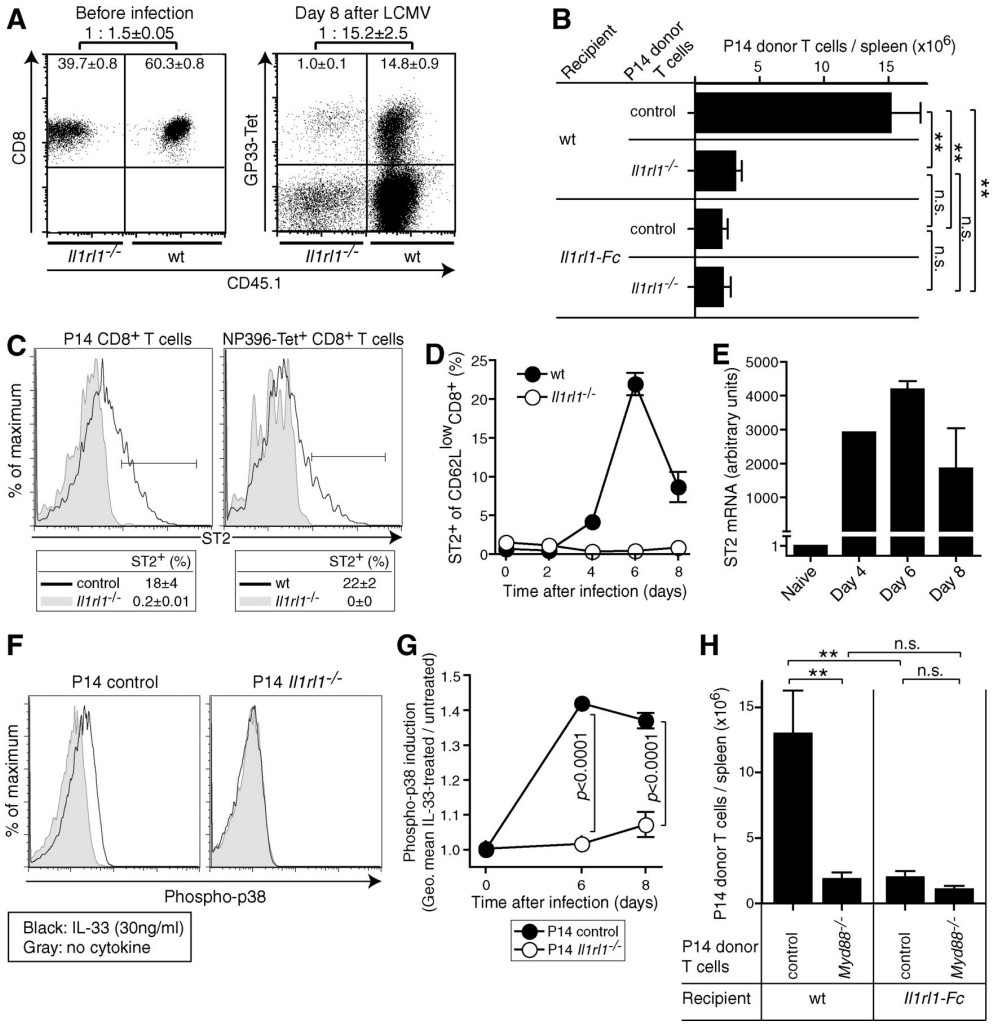

Figure 1.2: CD8$^+$ T cell–intrinsic signaling through ST2 and MyD88 augments antiviral CTL responses.

(**A**) Irradiated recipients were reconstituted with WT (CD45.1$^+$) and *Il1rl1*$^{-/-}$ (CD45.1$^-$) bone marrow. Flow cytometric analysis of WT and *Il1rl1*$^{-/-}$ total CD8$^+$ T cells before infection (left) and virus-specific CD8$^+$ T cells 8 days after LCMV challenge (right). Values represent mean frequency ± SEM of three mice. *N* = 2. (**B**) Control (CD45.1$^+$CD45.2$^-$) and *Il1rl1*$^{-/-}$ (CD45.1$^+$CD45.2$^+$) P14 CD8$^+$ T cells (10^4) were cotransferred into WT and *Il1rl1-Fc* recipient mice (CD45.1$^-$CD45.2$^+$) and were enumerated on day 8 after LCMV. Bars represent the mean ± SEM of four mice per group. $P < 0.0001$ by one-way ANOVA. Results of Bonferroni's posttest are indicated. One representative of three similar experiments is shown. (**C**) Control and *Il1rl1*$^{-/-}$ P14 cells (10^4) were individually transferred into WT recipients (left). Peptide-MHC tetramer–binding cells in WT and *Il1rl1*$^{-/-}$ mice were studied (right). On day 6 after LCMV infection, the indicated cell populations in spleen were analyzed for ST2 expression by flow cytometry. Values represent the mean ± SD of three mice. *N* = 2. (**D**) Flow cytometric analysis of splenic CD62L^{low}CD8$^+$ T cells over time after LCMV infection. Symbols represent the mean ± SEM of three mice (WT days 2 to 8; *Il1rl1*$^{-/-}$ day 6) or the mean of two mice (other symbols). *N* = 2. (**E**) Quantitative reverse-transcription polymerase chain reaction (qRT-PCR) analysis of ST2 mRNA levels in P14 CD8$^+$ T cells. Day 6 and 8 values represent the mean ± SEM of three mice. RNA samples from three donor mice were pooled for combined analysis on days 0 and 4. *N* = 1. (**F** and **G**) Flow cytometric analysis of intracellular phospho-p38 expression in control and *Il1rl1*$^{-/-}$ P14 cells isolated on day 6 (F) or over time after LCMV infection and treated ex vivo with recombinant IL-33. Symbols in (G) represent the mean ± SEM of three mice. Unpaired two-tailed student's *t* test was used for statistical analysis. One representative of two similar experiments is shown. (**H**) Control (CD45.1$^+$CD45.2$^-$) and *Myd88*$^{-/-}$ (CD45.1$^+$CD45.2$^+$) P14 cells

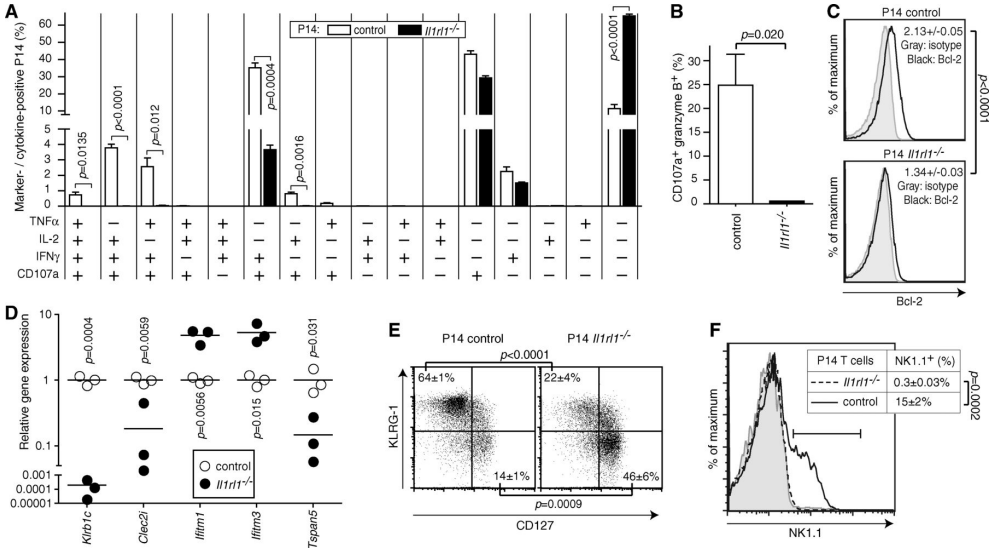

Figure 1.3: Broad and profound influence of ST2 signaling on effector CTL differentiation and functionality.

(A to C) CD45.1+ control and ST2-deficient P14 CD8+ T cells (104) were adoptively transferred into WT recipient mice, which were then challenged with LCMV. Cytokine profile (A), cytolytic phenotype (B), and Bcl-2 expression (C) were assessed on day 8 after LCMV infection. Bars represent mean ± SEM of three mice. Values in (C) represent geometric mean indices (mean ± SD of three mice per group). N = 1 [(A) and (B)] or 2 (C). (D) Gene expression profile of P14 cells from recipients as in (A) to (C). The full set of differentially expressed genes is displayed in fig. 1.S3B (also listed in table S2). We validated select genes by qRT-PCR. Symbols show individual mice. N = 1. (E and F) Phenotypic analysis of splenic Il1rl1–/– and control P14 CD8+ T cells from day 8 LCMV-infected WT recipients as in (A) to (C). Values indicate mean ± SD of three mice. Naïve control P14 T cells are shown as reference in (F) (gray shaded). N = 1. Unpaired two-tailed student's t test was used for statistical analysis.

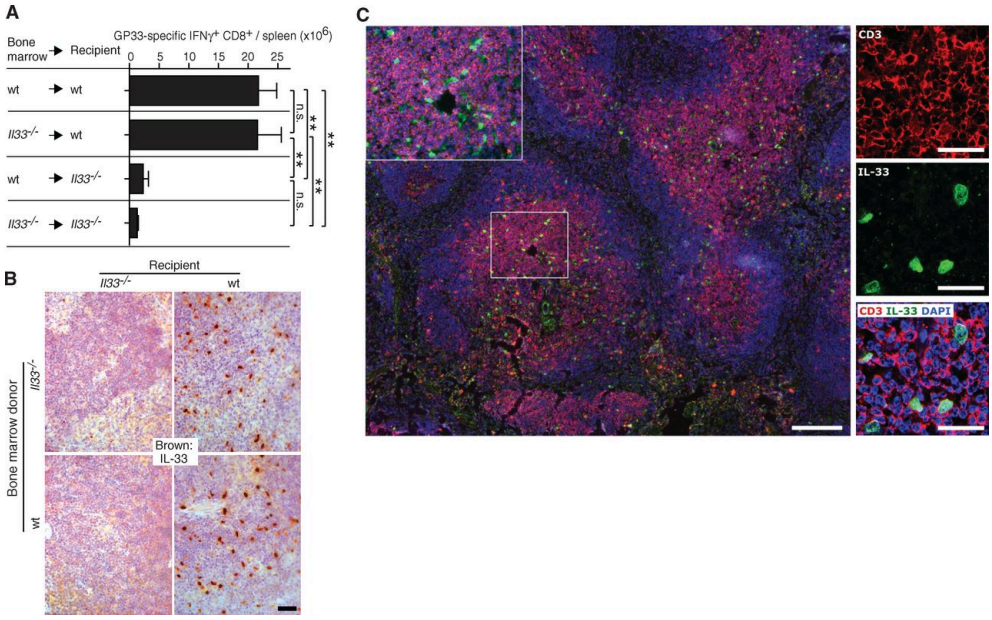

Figure 1.4: Radio-resistant cells of the T cell zone produce IL-33 for efficient CTL induction.

(**A**) Bone marrow chimeras were generated by using *Il33*$^{-/-}$ and WT recipients as indicated. Two months later, the CTL response to LCMV infection was determined (day 8 after infection). Bars represent the mean ± SEM of five mice. $P = 0.0038$ by one-way ANOVA. Results of Bonferroni's posttest are indicated. $N = 2$. (**B**) Spleens from chimeras as in (A) were analyzed for IL-33–expressing cells by immunohistochemistry. The scale bar indicates 50 µm. The image was acquired at 100-fold magnification. Representative pictures from one out of four animals are shown. (**C**) IL-33^{+} cells (green) are predominantly found in the T cell zone (characterized by CD3^{+} T cell clusters, red). DAPI (4′,6′-diamidino-2-phenylindole) was used to stain nuclei (blue). The central white rectangle is displayed at higher magnification in the top left corner of the large image. The small images at right show close vicinity of IL-33^{+} cells and CD3^{+} T cells. Scale bars indicate 200 µm (large image) or 50 µm (small images and inset). Images were acquired at 200-fold magnification by using a slide scanner (large image and inset) and at 400-fold magnification by confocal microscopy (small images). Representative pictures from one out of four mice are shown.

1.6 Supplementary Tables and Figures

Supplementary Table 1.S1. Interleukin and inflammatory cytokine expression in LCMV infection

Gene[1]	Gene abbreviation	Genbank reference sequence	Fold change (infected vs. uninfected)	p-value	stepup (p-value)
Interleukins and inflammatory cytokines					
interferon gamma	Ifng	NM_008337	12.47	0.00	0.02
interleukin 33	IL33	NM_001164724	4.60	0.00	0.05
secreted phosphoprotein 1	Spp1	NM_009263	3.65	0.00	0.06
tumor necrosis factor (ligand)	Tnfsf9	NM_009404	3.25	0.02	0.10
interleukin 6	IL6	NM_031168	2.76	0.01	0.08
interleukin 10	IL10	NM_010548	2.54	0.01	0.10
tumor necrosis factor (ligand)	Tnfsf10	NM_009425	2.54	0.00	0.04
interleukin 1 family, member 9	Il1f9	NM_153511	2.15	0.12	0.30
Fas ligand (TNF superfamily, member 6)	Fasl	NM_010177	2.03	0.00	0.03
interleukin 1 alpha	Il1a	NM_010554	1.92	0.00	0.04
growth differentiation factor 15	Gdf15	NM_011819	1.92	0.00	0.05
tumor necrosis factor	Tnf	NM_013693	1.87	0.00	0.04
macrophage migration inhibitory factor	Mif	NM_010798	1.86	0.01	0.08
inhibin beta-A	Inhba	NM_008380	1.86	0.01	0.10
interleukin 1 beta	Il1b	NM_008361	1.85	0.12	0.30
interleukin 21	Il21	NM_021782	1.82	0.01	0.08
interleukin 15	Il15	NM_008357	1.71	0.00	0.04
kit ligand	Kitl	NM_013598	1.36	0.01	0.08
platelet factor 4	Pf4	NM_019932	1.34	0.02	0.12
colony stimulating factor 1 (macrophage)	Csf1	NM_007778	1.32	0.01	0.08
colony stimulating factor 2 (granulocyte-macrophage)	Csf2	NM_009969	1.32	0.02	0.13
tumor necrosis factor (ligand) superfamily, member 14	Tnfsf14	NM_019418	1.29	0.06	0.20
aminoacyl tRNA synthetase complex-interacting multifunctional protein 1	Aimp1	NM_007926	1.25	0.05	0.18
leukemia inhibitory factor	Lif	NM_008501	1.25	0.14	0.33
interleukin 27	Il27	NM_145636	1.18	0.16	0.35
tumor necrosis factor (ligand) superfamily, member 4	Tnfsf4	NM_009452	1.17	0.06	0.20
CD70 antigen	Cd70	NM_011617	1.15	0.15	0.35
tumor necrosis factor (ligand) superfamily, member 8	Tnfsf8	NM_009403	1.12	0.33	0.54
complement component 3	C3	NM_009778	1.12	0.07	0.23
bone morphogenetic protein 5	Bmp5	NM_007555	1.09	0.20	0.40
interferon alpha 2	Ifna2	NM_010503	1.08	0.31	0.52
interleukin 12b	Il12b	NM_008352	1.07	0.59	0.76
tumor necrosis factor (ligand) superfamily, member 11	Tnfsf11	NM_011613	1.07	0.21	0.42
interleukin 23, alpha subunit p19	Il23a	NM_031252	1.04	0.48	0.67
interleukin 17A	Il17a	NM_010552	1.03	0.59	0.76
interleukin 28B	Il28b	NM_177396	1.03	0.70	0.83
interleukin 11	Il11	NM_008350	1.02	0.86	0.93
interleukin 3	Il3	NM_010556	1.02	0.61	0.77
interleukin 24	Il24	NM_053095	1.02	0.79	0.89
bone morphogenetic protein 1	Bmp1	NR_033241	1.01	0.90	0.95
interferon beta 1	Infb1	NM_010510	1.01	0.95	0.98
interleukin 20	Il20	NM_021380	1.00	0.98	0.99

bone morphogenetic protein 8b	Bmp8b	NM_007559	-1.00	1.00	1.00
interleukin 17C	Il17c	NM_145834	-1.01	0.93	0.96
Tnfsf12-tnfsf13 readthrough transcript	Tnfsf12-Tnfsf13	NM_001034097	-1.01	0.92	0.96
interleukin 1 family, member 6	Il1f6	NM_019450	-1.01	0.84	0.92
interleukin 19	Il19	NM_001009940	-1.01	0.89	0.94
growth differentiation factor 3	Gdf3	NM_008108	-1.01	0.87	0.93
interleukin 4	Il4	NM_021283	-1.01	0.72	0.85
interleukin 1 family, member 8	Il1f8	NM_027163	-1.02	0.93	0.96
myostatin	Mstn	NM_010834	-1.02	0.83	0.91
interferon alpha 4	Ifna4	NM_010504	-1.02	0.72	0.85
interferon alpha 4	Lefty1	NM_010094	-1.03	0.75	0.86
interleukin 34	Il34	NM_029646	-1.03	0.55	0.73
secretoglobin, family 3A, member 1	Scgb3a1	NM_170727	-1.03	0.72	0.85
interleukin 17D	Il17d	NM_145837	-1.03	0.37	0.58
interleukin 5	Il5	NM_010558	-1.03	0.74	0.86
fibroblast growth factor 10	Fgf10	NM_008002	-1.04	0.68	0.82
growth differentiation factor 2	Gdf2	NM_019506	-1.04	0.53	0.72
interleukin 25	Il25	NM_080729	-1.04	0.76	0.87
interleukin 9	Il9	NM_008373	-1.05	0.46	0.66
interleukin 22	Il22	NM_016971	-1.05	0.70	0.83
bone morphogenetic protein 10	Bmp10	NM_009756	-1.06	0.64	0.79
interleukin 17F	Il17f	NM_145856	-1.06	0.65	0.80
tumor necrosis factor (ligand) superfamily, member 18	Tnfsf18	NM_183391	-1.06	0.50	0.69
interferon alpha 1	Ifna1	NM_010502	-1.07	0.14	0.33
interleukin 1 family, member 10	Il1f10	NM_153077	-1.07	0.41	0.61
interleukin 31	Il31	NM_029594	-1.07	0.45	0.65
TNFAIP3 interacting protein 2	Tnip2	NM_139064	-1.07	0.33	0.54
bone morphogenetic protein 7	Bmp7	NM_007557	-1.07	0.23	0.44
interleukin 22	Il22	NM_016971	-1.07	0.61	0.78
interleukin 18	Il18	NM_008360	-1.07	0.63	0.79
interleukin 17B	Il17b	NM_019508	-1.08	0.22	0.43
interleukin 2	Il2	NM_008366	-1.09	0.21	0.42
interleukin 1 family, member 5 (delta)	Il1f5	NM_001146087	-1.09	0.28	0.50
C-reactive protein, pentraxin-related	Crp	NM_007768	-1.09	0.39	0.59
colony stimulating factor 3 (granulocyte)	Csf3	NM_009971	-1.10	0.12	0.30
cardiotrophin 2	Ctf2	NM_198858	-1.10	0.08	0.24
transforming growth factor, beta 1	Tgfb1	NM_011577	-1.10	0.31	0.52
interleukin 13	Il13	NM_008355	-1.12	0.27	0.48
growth differentiation factor 9	Gdf9	NM_008110	-1.13	0.21	0.42
tumor necrosis factor (ligand) superfamily, member 13b	Tnfsf13b	NM_033622	-1.13	0.33	0.54
growth differentiation factor 1	Gdf1	NM_001163282	-1.14	0.20	0.40
bone morphogenetic protein 3	Bmp3	NM_173404	-1.15	0.20	0.41
interleukin 28A	Il28a	NM_001024673	-1.16	0.42	0.63
cardiotrophin 1	Ctf1	NM_007795	-1.17	0.14	0.33
interleukin 12a	Il12a	NM_001159424	-1.19	0.08	0.24
growth differentiation factor 5	Gdf5	NM_008109	-1.22	0.05	0.18
inhibin alpha	Inha	NM_010564	-1.24	0.10	0.27
fibrosin	Fbrs	NM_010183	-1.30	0.01	0.08
interleukin 16	Il16	NM_010551	-1.33	0.00	0.04
bone morphogenetic protein 4	Bmp4	NM_007554	-1.42	0.08	0.24
bone morphogenetic protein 6	Bmp6	NM_007556	-1.46	0.00	0.06

bone morphogenetic protein 2	Bmp2	NM_007553	-1.47	0.02	0.10
growth differentiation factor 11	Gdf11	NM_010272	-1.50	0.01	0.09
lymphotoxin A	Lta	NM_010735	-1.55	0.02	0.10
growth differentiation factor 10	Gdf10	NM_145741	-1.62	0.00	0.06
CD40 ligand	Cd40lg	NM_011616	-1.63	0.01	0.08
FMS-like tyrosine kinase 3 ligand	Flt3l	NM_013520	-1.74	0.00	0.04
interleukin 7	Il7	NM_008371	-1.74	0.00	0.06
lymphotoxin B	Ltb	NM_008518	-1.86	0.01	0.09
Interleukin 33 receptor					
ST2	Il1rl1	NM_001025602	3.07	0.00	0.04

[1] Wt mice were infected with LCMV or were left uninfected (n=3 each), and five days later total spleen RNA was processed for genome-wide cDNA expression analysis. The table displays known interleukins and soluble inflammatory mediators (compiled from the SABiosciences Mouse Inflammatory Cytokines & Receptors PCR Array, SABiosciences Mouse Common Cytokines PCR Array and Lonza Mouse Cytokines and Receptors 96 StellARray qPCR Array) and selectively the IL-33 receptor ST2.

Supplementary Table 1.S2. Differentially expressed genes in wt and *Il1rl1*$^{-/-}$ effector CTLs

Gene[1]	Gene abbreviation	Genbank reference sequence	Fold difference (ST2$^{-/-}$ vs. wt)	p-value	stepup (p-value)
RIKEN cDNA I830127L07 gene	I830127L07Rik	XM_001477102	0.06	0.00	0.00
killer cell lectin-like receptor subfamily B member 1C	Klrb1c	NM_008527	0.11	0.00	0.00
small nucleolar RNA, C/D box 34	Snord34	NR_002455	0.16	0.00	0.00
small nucleolar RNA, C/D box 32A	Snord32a	NR_000002	0.18	0.00	0.00
thymine DNA glycosylase	Tdg	NM_011561	0.23	0.00	0.02
small nucleolar RNA, C/D box 61	Snord61	NR_002903	0.24	0.00	0.01
small nucleolar RNA, C/D box 35A	Snord35a	NR_000003	0.27	0.00	0.00
MRT4, mRNA turnover 4, homolog (S. cerevisiae)	Mrto4	NM_023536	0.31	0.00	0.03
small nucleolar RNA, C/D box 82	Snord82	NR_002851	0.34	0.00	0.00
predicted gene, ENSMUSG00000053178	ENSMUSG00000053178	NM_001042670	0.38	0.00	0.01
tetraspanin 5	Tspan5	NM_019571	0.40	0.00	0.00
killer cell lectin-like receptor subfamily G, member 1	Klrg1	NM_016970	0.40	0.00	0.02
C-type lectin domain family 2, member i	Clec2i	NM_020257	0.41	0.00	0.00
RIKEN cDNA I830127L07 gene	I830127L07Rik	XM_001477102	0.06	0.00	0.00
killer cell lectin-like receptor subfamily B member 1C	Klrb1c	NM_008527	0.11	0.00	0.00
small nucleolar RNA, C/D box 34	Snord34	NR_002455	0.16	0.00	0.00
small nucleolar RNA, C/D box 32A	Snord32a	NR_000002	0.18	0.00	0.00
thymine DNA glycosylase	Tdg	NM_011561	0.23	0.00	0.02
small nucleolar RNA, C/D box 61	Snord61	NR_002903	0.24	0.00	0.01
small nucleolar RNA, C/D box 35A	Snord35a	NR_000003	0.27	0.00	0.00
MRT4, mRNA turnover 4, homolog (S. cerevisiae)	Mrto4	NM_023536	0.31	0.00	0.03
small nucleolar RNA, C/D box 82	Snord82	NR_002851	0.34	0.00	0.00
predicted gene, ENSMUSG00000053178	ENSMUSG00000053178	NM_001042670	0.38	0.00	0.01
tetraspanin 5	Tspan5	NM_019571	0.40	0.00	0.00
killer cell lectin-like receptor subfamily G, member 1	Klrg1	NM_016970	0.40	0.00	0.02
C-type lectin domain family 2, member i	Clec2i	NM_020257	0.41	0.00	0.00
RIKEN cDNA I830127L07 gene	I830127L07Rik	XM_001477102	0.06	0.00	0.00
killer cell lectin-like receptor subfamily B member 1C	Klrb1c	NM_008527	0.11	0.00	0.00
small nucleolar RNA, C/D box 34	Snord34	NR_002455	0.16	0.00	0.00
small nucleolar RNA, C/D box 32A	Snord32a	NR_000002	0.18	0.00	0.00
thymine DNA glycosylase	Tdg	NM_011561	0.23	0.00	0.02
small nucleolar RNA, C/D box 61	Snord61	NR_002903	0.24	0.00	0.01
small nucleolar RNA, C/D box 35A	Snord35a	NR_000003	0.27	0.00	0.00
MRT4, mRNA turnover 4, homolog (S. cerevisiae)	Mrto4	NM_023536	0.31	0.00	0.03
small nucleolar RNA, C/D box 82	Snord82	NR_002851	0.34	0.00	0.00
predicted gene, ENSMUSG00000053178	ENSMUSG00000053178	NM_001042670	0.38	0.00	0.01
tetraspanin 5	Tspan5	NM_019571	0.40	0.00	0.00
killer cell lectin-like receptor subfamily G, member 1	Klrg1	NM_016970	0.40	0.00	0.02
C-type lectin domain family 2, member i	Clec2i	NM_020257	0.41	0.00	0.00
RIKEN cDNA I830127L07 gene	I830127L07Rik	XM_001477102	0.06	0.00	0.00
killer cell lectin-like receptor subfamily B member 1C	Klrb1c	NM_008527	0.11	0.00	0.00
small nucleolar RNA, C/D box 34	Snord34	NR_002455	0.16	0.00	0.00
small nucleolar RNA, C/D box 32A	Snord32a	NR_000002	0.18	0.00	0.00
thymine DNA glycosylase	Tdg	NM_011561	0.23	0.00	0.02
small nucleolar RNA, C/D box 61	Snord61	NR_002903	0.24	0.00	0.01
small nucleolar RNA, C/D box 35A	Snord35a	NR_000003	0.27	0.00	0.00
MRT4, mRNA turnover 4, homolog (S. cerevisiae)	Mrto4	NM_023536	0.31	0.00	0.03
small nucleolar RNA, C/D box 82	Snord82	NR_002851	0.34	0.00	0.00

predicted gene, ENSMUSG00000053178	ENSMUSG00000053178	NM_001042670	0.38	0.00	0.01
tetraspanin 5	Tspan5	NM_019571	0.40	0.00	0.00
killer cell lectin-like receptor subfamily G, member 1	Klrg1	NM_016970	0.40	0.00	0.02
C-type lectin domain family 2, member i	Clec2i	NM_020257	0.41	0.00	0.00
RIKEN cDNA I830127L07 gene	I830127L07Rik	XM_001477102	0.06	0.00	0.00
killer cell lectin-like receptor subfamily B member 1C	Klrb1c	NM_008527	0.11	0.00	0.00
small nucleolar RNA, C/D box 34	Snord34	NR_002455	0.16	0.00	0.00
small nucleolar RNA, C/D box 32A	Snord32a	NR_000002	0.18	0.00	0.00
thymine DNA glycosylase	Tdg	NM_011561	0.23	0.00	0.02
small nucleolar RNA, C/D box 61	Snord61	NR_002903	0.24	0.00	0.01
small nucleolar RNA, C/D box 35A	Snord35a	NR_000003	0.27	0.00	0.00
MRT4, mRNA turnover 4, homolog (S. cerevisiae)	Mrto4	NM_023536	0.31	0.00	0.03
small nucleolar RNA, C/D box 82	Snord82	NR_002851	0.34	0.00	0.00
predicted gene, ENSMUSG00000053178	ENSMUSG00000053178	NM_001042670	0.38	0.00	0.01
tetraspanin 5	Tspan5	NM_019571	0.40	0.00	0.00
killer cell lectin-like receptor subfamily G, member 1	Klrg1	NM_016970	0.40	0.00	0.02

[1] CD45.1$^+$ control and *Il1rl1*$^{-/-}$ P14 indicator CD8 T cells (10^4) were transferred to separate groups of wt recipient mice and were challenged with LCMV. Eight days later, LCMV-specific CD45.1$^+$ CD8$^+$ indicator CTLs were sorted by flow cytometry and were processed for genome-wide cDNA expression analysis (n=3 for each group). Genes are displayed, which were ≥2-fold differentially expressed, with a step-up p-value of <0.05.

fig. S1

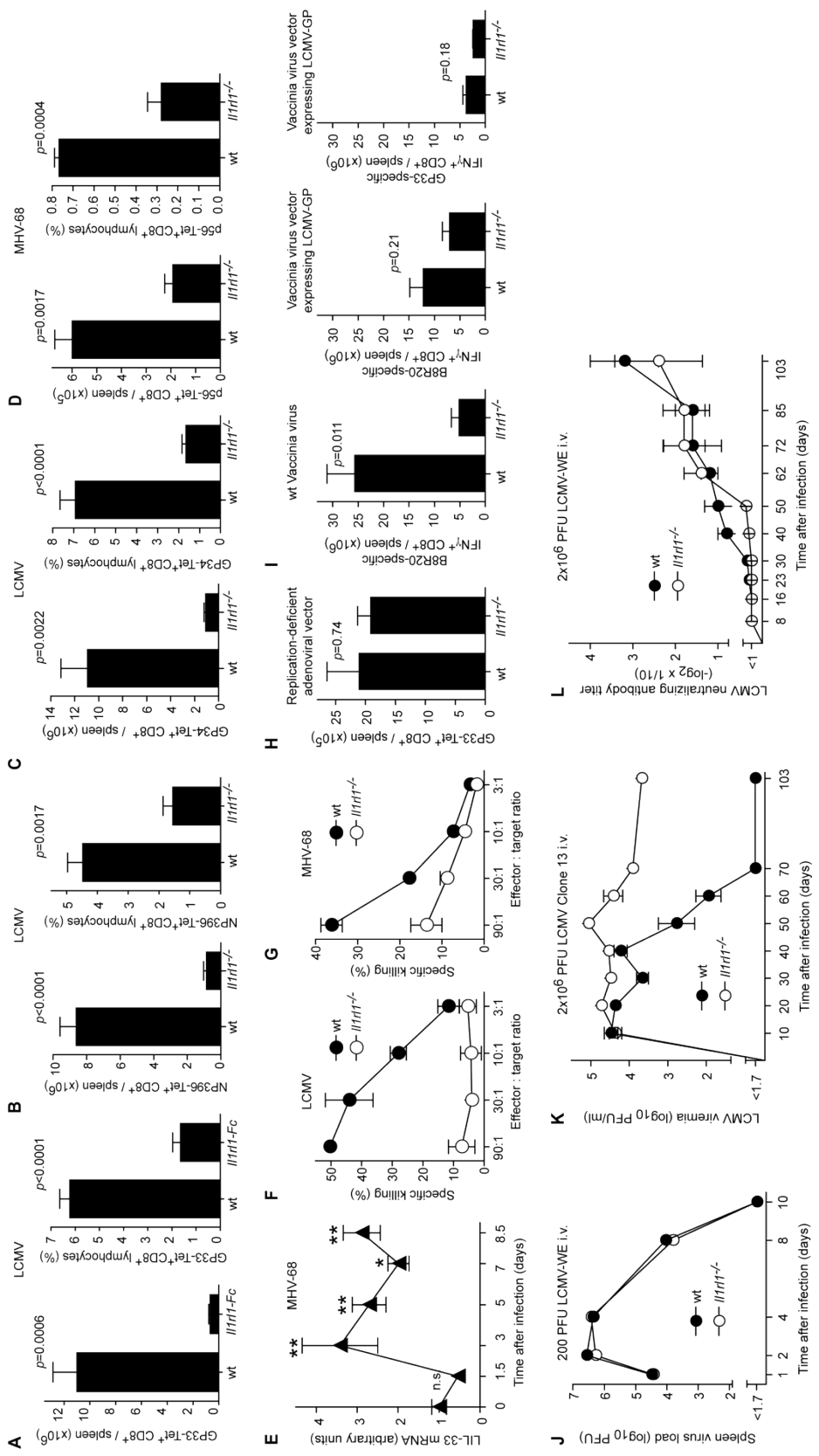
A
LCMV
p=0.0006
GP33-Tet+ CD8+ / spleen (x10^6)
wt
Il1rl1-Fc
B
LCMV
p<0.0001
GP33-Tet+CD8+ lymphocytes (%)
NP396-Tet+ CD8+ / spleen (x10^6)
NP396-Tet+CD8+ lymphocytes (%)
C
LCMV
p=0.0022
GP34-Tet+ CD8+ / spleen (x10^6)
p<0.0001
GP34-Tet+CD8+ lymphocytes (%)
p=0.0017
D
MHV-68
p=0.0017
p56-Tet+ CD8+ / spleen (x10^5)
p=0.0004
p56-Tet+CD8+ lymphocytes (%)
Il1rl1-/-
E
MHV-68
IL1-33 mRNA (arbitrary units)
n.s
Time after infection (days)
F
LCMV
Specific killing (%)
Effector : target ratio
G
MHV-68
H
Replication-deficient adenoviral vector
p=0.74
GP33-Tet+ CD8+ / spleen (x10^5)
I
wt Vaccinia virus
p=0.011
B8R20-specific IFNγ+ CD8+ / spleen (x10^6)
Vaccinia virus vector expressing LCMV-GP
p=0.21
Vaccinia virus vector expressing LCMV-GP
p=0.18
GP33-specific IFNγ+ CD8+ / spleen (x10^6)
J
200 PFU LCMV-WE i.v.
Spleen virus load (log10 PFU)
K
2x10^6 PFU LCMV Clone 13 i.v.
LCMV viremia (log10 PFU/ml)
L
2x10^6 PFU LCMV-WE i.v.
LCMV neutralizing antibody titer (-log2 x 1/10)
Time after infection (days)

Figure 1.S1: IL-33 drives protective CTL responses to replicating viral infection, is induced by MHV-68, and is necessary for control of high dose but not low dose LCMV infection.

A-D: Splenic LCMV-specific CTLs on day 8 (A-C) and MHV-68-specific CTLs (D) on day 10 after infection. Bars represent the mean±SEM of five (A-C) or four (D) mice. One out of two similar experiments is shown in A and B. *N*=1 for C-D. E: Kinetic analysis of IL-33 mRNA expression in the spleen after MHV-68 infection. Symbols represent the mean±SEM of four mice. $P<0.0001$ by 1-way ANOVA. Results of Dunnett's post-test comparing against day 0 values are indicated. n.s.: not significant ; *: $p<0.05$; **: $p<0.01$. *N*=1. F-G: Splenocytes as in A-D were tested in primary ex vivo Cr^{51} release assays. *N*=2 (F) or 1 (G). H-I: CTL response to replication-defective adenoviral vector expressing GP33 (H) and wt vaccinia virus or recombinant vaccinia virus vector expressing LCMV-GP (I). Bars represent the mean±SEM of three to five mice. One representative of two similar experiments is shown. J: LCMV titers in spleen after infection with 200 PFU (standard low dose) of LCMV-WE. Symbols represent the mean of two to six mice per time point. Data are combined from three experiments. K: Viremia after infection with $2x10^6$ PFU of LCMV Clone 13. Symbols represent the mean±SEM of four to six mice per group. *N*=1. L: LCMV-neutralizing antibody in serum after infection with $2x10^6$ PFU of LCMV-WE (high dose, same experiment as in Fig. 1.1G) as determined in plaque reduction assays (Pinschewer, Perez et al. 2004). Bars and symbols represent the mean±SEM of four to five mice. One representative of two similar experiments is shown. The *p*-values displayed in the figures were obtained using unpaired two-tailed student's t test.

fig. S2

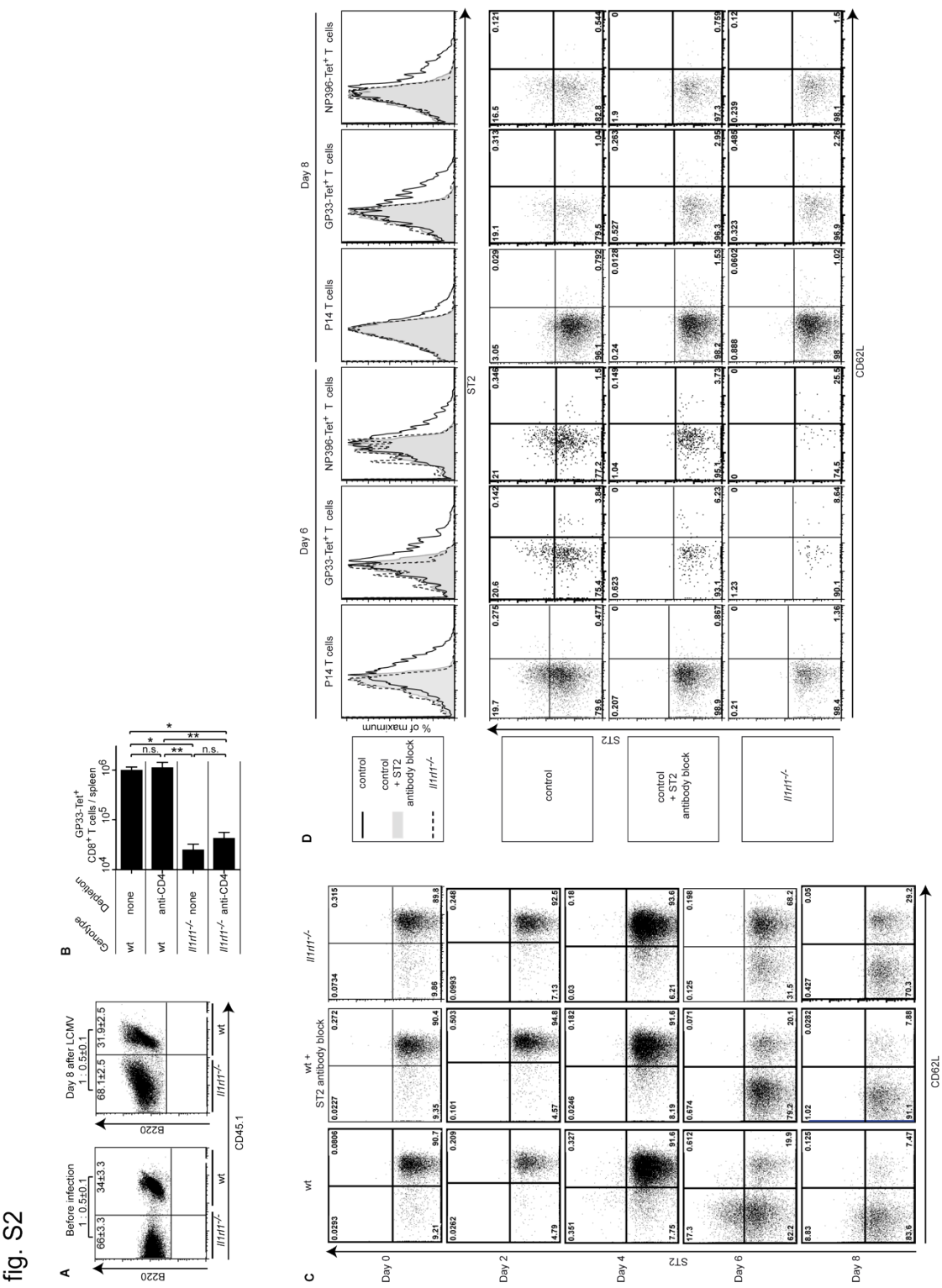
A
Before infection
1 : 0.5±0.1
66±3.3
34±3.3
B220
CD45.1
wt
Il1rl1-/-
Day 8 after LCMV
1 : 0.5±0.1
68.1±2.5
31.9±2.5
B
Genotype
Depletion
wt none
wt anti-CD4
Il1rl1-/- none
Il1rl1-/- anti-CD4
GP33-Tet+ CD8+ T cells / spleen
n.s.
C
wt
wt + ST2 antibody block
Il1rl1-/-
Day 0
Day 2
Day 4
Day 6
Day 8
ST2
CD62L
D
Day 6
Day 8
P14 T cells
GP33-Tet+ T cells
NP396-Tet+ T cells
% of maximum
control
control + ST2 antibody block
Il1rl1-/-
ST2
CD62L

Figure 1.S2: Unaltered repartition of ST2-competent and -deficient B cell compartments after LCMV infection, impaired CTL induction in *Il1rl1*$^{-/-}$ mice irrespective of CD4^{+} T cells, and ST2 expression on antiviral CD8^{+} T cells.

A: Irradiated recipients were reconstituted with wt (CD45.1+) and *Il1rl1*$^{-/-}$ (CD45.1-) bone marrow. Flow cytometric analysis of wt and *Il1rl1*$^{-/-}$ B220+ B cells before (left) and after LCMV challenge (right). Values represent mean frequency±SEM of three mice. *N*=2. B: Wt and *Il1rl1*$^{-/-}$ mice were depleted of CD4^{+} T cells as described (Pinschewer, Perez et al. 2004) or were left untreated. CTL responses were measured on day 8 after LCMV infection. Bars show the mean±SEM of four mice. One representative of two similar experiments is shown. C: ST2 expression of splenic CD8^{+} T cells on the indicated days after LCMV infection (same experiment as displayed in Fig. 1.2D). As a specificity control, ST2-antibody block was performed as described in Methods. One representative mouse out of two to three per group and time point is shown. *N*=2. D: Control and *Il1rl1*$^{-/-}$ P14 cells (10^4) were individually transferred into wt recipients (left panels on day 6 and 8, respectively). Peptide-MHC tetramer-binding cells of wt and *Il1rl1*$^{-/-}$ mice were analyzed on day 6 and 8, and are displayed in the center and right panel, respectively. P14 donor cells (left panels) and endogenous peptide-MHC-binding CTL populations in spleen were analyzed for ST2 expression by flow cytometry. The top row provides comparative histogram charts of representative mice shown in the bottom rows. Representative samples from two to three mice per group and time point are shown. *N*=1.

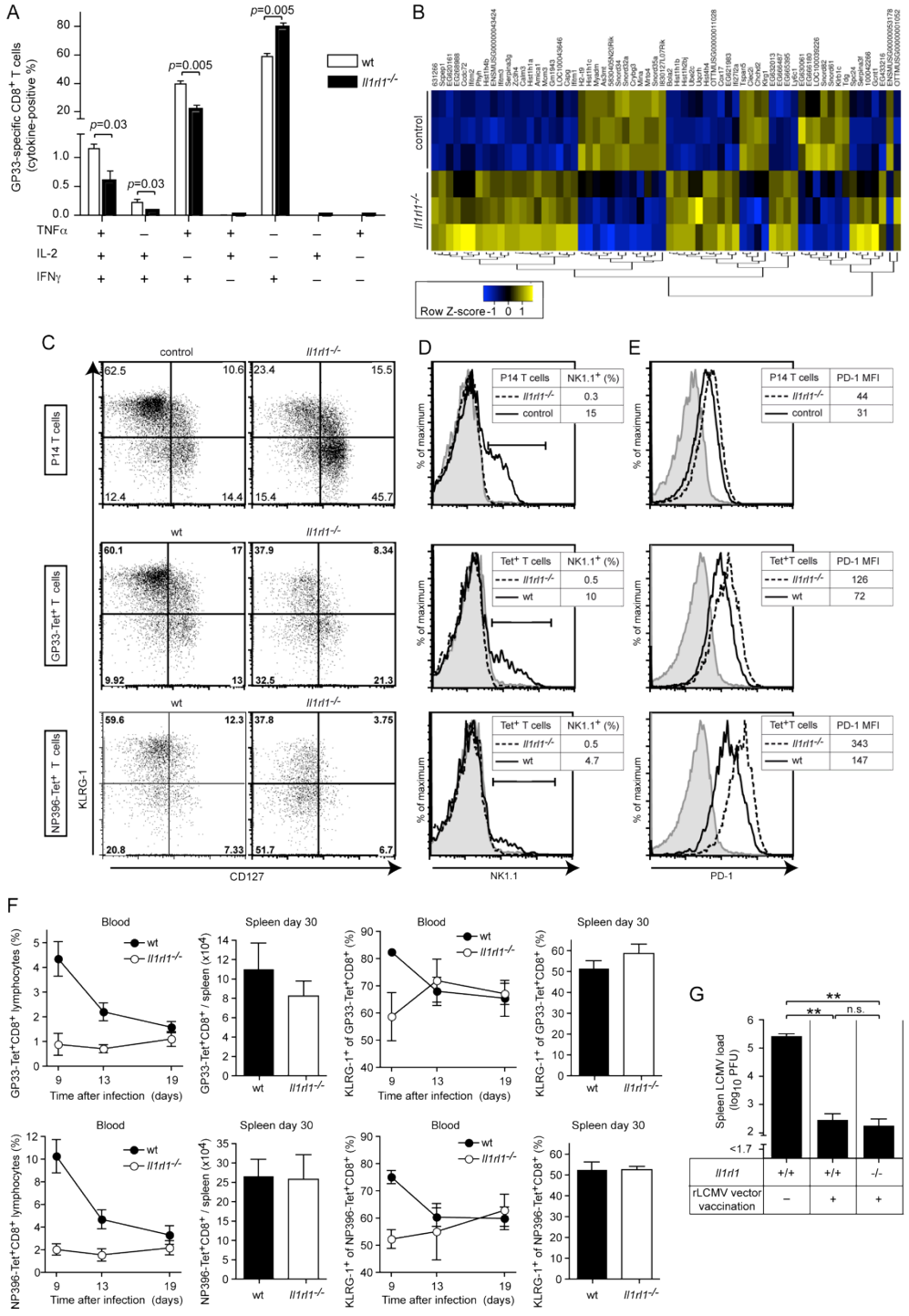

Figure 1.S3: Reduced plurifunctionality, differential gene expression profile and surface marker expression, and defective expansion of *Il1rl1*$^{-/-}$ CTLs in the effector phase.

A: Wt and *Il1rl1*$^{-/-}$ mice were infected with LCMV, and the plurifunctionality of GP33-specific CD8$^+$ T cells was assessed on day 8 after infection by intracellular cytokine stain. Bars display the mean±SEM of four mice. The *p*-values displayed in the figure were obtained by unpaired two-tailed student's t test. *N*=1. B: Gene expression profile of control and *Il1rl1*$^{-/-}$ P14 cells from recipients as in Fig. 1.3A-C. Differentially expressed genes (≥2-fold different, step-up p-value <0.05) are displayed for individual mice (same as in Table S2). *N*=1. C-E: Control and *Il1rl1*$^{-/-}$ P14 cells (10^4) were individually transferred into wt recipients (top row).

Peptide-MHC tetramer-binding cells of wt and *Il1rl1*$^{-/-}$ mice are displayed in the center and bottom rows. On day 8 after LCMV infection the indicated cell populations in spleen (P14, GP33-Tet+ or NP396-Tet+) were phenotypically characterized by flow cytometry. Naïve control P14 T cells (top row) and naïve wt CD8+ T cells (center and bottom row) are shown as reference (gray shaded). Plots are representative for three (P14) or two to three mice (Tet+) per group in one experiment. *N*=1 (P14) or 3 (Tet+ cells). F: Wt and *Il1rl1*$^{-/-}$ mice were infected with 200 PFU of LCMV Armstrong i.v. Virus-specific peptide-MHC tetramer-binding CTLs were monitored in blood over time and enumerated in spleen on day 30, and their KLRG-1 expression was analyzed. Symbols and bars represent the mean±SEM of four mice. One representative of two similar experiments is shown. G: Wt and *Il1rl1*$^{-/-}$ mice were immunized with replication-deficient rLCMV vector (Flatz, Hegazy et al. 2010). On day 206 after immunization these animals and an unvaccinated group of wt mice were challenged with 2x10^{6} PFU LCMV Clone 13 i.v. Viral titers were determined in spleen three days later. Bars show the mean±SEM of five mice. *P*<0.0001 by 1-way ANOVA. Results of Bonferroni's post-test are indicated. n.s.: not significant ; **: p<0.01. One representative of two similar experiments is shown.

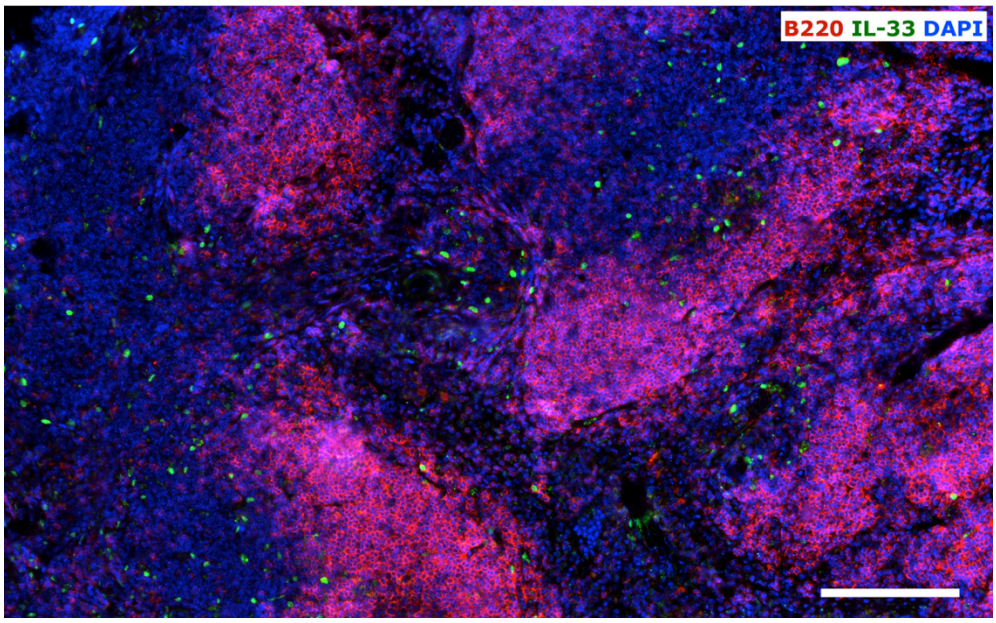

Figure 1.S4: Paucity of IL-33$^+$ cells in the splenic B cell zone.

IL-33$^+$ cells (green) are rarely found in the B cell zone (characterized by dense clusters of B220$^+$ T cells, red). Nuclei are counterstained with DAPI (blue). The scale bar indicates 200 μm. The image was acquired at 200-fold magnification using a slide scanner. Representative pictures from one of four sections are shown.

1.7 Acknowledgments

This work was supported by Bundesministerium für Bildung und Forschung (BMBF)–FORSYS (A.F., M.L.), National Health and Medical Research Council (S.J.), German Research Foundation (GRK1121, A.N.H.), Science Foundation Ireland (P.G.F.), Program for Improvement of Research Environment for Young Researchers, the Special Coordination Funds for Promoting Science and Technology from the Japanese Ministry of Education, Culture, Sports, Science and Technology, Japan Science and Technology Agency, PRESTO (S.N.), BMBF (NGFNplus, FKZ PIM-01GS0802-3; H.A.), Wilhelm Sander-Stiftung (H.A.), German Research Foundation (SFB618 and SFB650, M.L.), Volkswagen Foundation (Lichtenberg Program, M.L.), Fondation Leenaards (D.D.P.), European Community (D.D.P.), and Swiss National Science Foundation (D.M., D.D.P.).

We thank A. Bergthaler, G. R. Burmester, C. Gabay, M. Geuking, A. Kamath, P. H. Lambert, J. Luban, B. Marsland, G. Palmer, A. Radbruch, C. A. Siegrist, and R. M. Zinkernagel for discussions and advice; H. Saito, National Research Institute for Child Health and Development, for $Il33^{-/-}$ mice obtained under a materials transfer agreement (MTA) through the RIKEN Center for Developmental Biology, Laboratory for Animal Resources and Genetic Engineering; A. McKenzie (for $Il1rl1^{-/-}$ mice obtained under MTA); the University of Zurich (for rLCMV technology obtained under MTA) and G. Jennings [Cytos Biotechnology AG, Schlieren, Switzerland, holding patent rights on VLPs provided] for reagents; and J. Weber and B. Steer for technical assistance. The data presented in this paper are tabulated in the main paper and the supporting online material. Microarray data are deposited with National Center for Biotechnology Information Gene Expression Omnibus (GEO, accession number GSE34392) and ArrayExpress (accession number E-MTAB-901). D.D.P. is or has been a shareholder, board member, and consultant to ArenaVax AG, Switzerland, and to Hookipa Biotech GmbH, Austria, commercializing rLCMV vectors (patent application EP 07 025 099.8, coauthored by D.D.P.). The authors declare that they do not have other competing financial interests.

2 Interleukin-33 and Stromal Cells in Chronic Viral Infection

2.1 Summary

In response to viral infection endogenous molecules, called alarmins, are released from necrotic cells serving as a signal of tissue damage. Besides various effects of the alarmin Interleukin-33 (IL-33) on Th2-biased immune responses, we have previously demonstrated its importance for the initiation of a potent CD8+ T cell (CTL) response to acute infection with several prototypic replicating RNA- and DNA-viruses (Bonilla, Frohlich et al. 2012). Whereas CD8+ T cells manage to clear acute LCMV infection independently and even in the absence of CD4+ T cells (Moskophidis, Cobbold et al. 1987, Ahmed, Butler et al. 1988, Rahemtulla, Fung-Leung et al. 1991), an only temporary blockade of CD4+ T cell help abrogates control of chronic LCMV infections and mice become lifelong carriers. LCMV-specific CD8+ T cell responses were completely lost in persistently infected animals upon deletion of CD4+ T cells, underlining the critical role of CD4+ T cell help for maintaining potent antiviral CTL responses during chronic viral infection (Matloubian, Concepcion et al. 1994). Furthermore LCMV-specific antibody responses produced by B cells are essential for control and clearance of persistent LCMV infection, the activation of which also depends on CD4+ T cell help (Bergthaler, Flatz et al. 2009). Thus both CD4+ and CD8+ T cell populations are critical for the outcome of chronic infection (Doherty, Allan et al. 1992, Matloubian, Concepcion et al. 1994).

In this study we investigated whether signaling via the IL-33/ST2 axis is important for CD4 and CD8 T cell responses to chronic LCMV infection. We found that IL-33 plays a crucial role for the expansion and maintenance of both CD8+ and CD4+ T cells as well as for the differentiation of virus-specific CD4+ T cells in chronic viral infection. Using a novel IL-33 reporter mouse we identified fibroblastic reticular cells (FRCs) as the main IL-33 expressing cells in secondary lymphoid organs. By means of GFP-tagged reporter viruses and immunohistochemistry we demonstrate that blood endothelial cells but not FRCs are a main early stromal cell target of systemic LCMV infection. We furthermore present data suggesting that virus-specific CD8+ T cells require a constant ST2-mediated survival signal in order to be maintained in the chronic infection context and that lack of ST2 signaling affects the tissue distribution and differentiation of virus-specific CD4+ T cells towards a T follicular helper cell phenotype.

The present data extends our knowledge on the role of IL-33 as an alarmin in Th1-biased immune responses to the context of chronic viral infections. More detailed knowledge on the factors that influence and shape immune responses to persistent viral infections are

essential to refine immunotherapeutic approaches to chronic viral infections like HIV and HCV, which represent major global health challenges. In the absence of a preventive vaccine, a detailed understanding of the mechanisms underlying chronicity and imperfect immune control should allow for the development of innovative therapies against these diseases.

2.2 Introduction

The immune system has developed mechanisms to sense endogenous damage signals or exogenous danger and trigger activation of signaling cascades to finally initiate or enhance the appropriate immune responses. Upon necrosis, intracellular proteins are released from the dying cell in an uncontrolled fashion. Some of these endogenous molecules, called “alarmins”, can indicate cell damage and warn the immune system of the necrotic event (Oppenheim and Yang 2005, Bianchi 2007). Interleukin-33 (IL-33) is a member of the IL-1 family, which can be released by necrotic cells upon tissue injury (Cayrol and Girard 2009, Luthi, Cullen et al. 2009), classifying it as an alarmin (Moussion, Ortega et al. 2008). Once in the extracellular space, it binds to its cell surface receptor consisting of ST2 in association with the ubiquitous IL-1R accessory protein (IL1RAcP) (Schmitz, Owyang et al. 2005, Ali, Huber et al. 2007) and leads to activation of downstream signaling cascades (Palmer Gabay).

IL-33 has primarily been shown to play a role in the context of Th2-associated immune responses like asthma and allergic responses and in responses against parasitic infections (summarized in (Liew, Pitman et al. 2010, Garlanda, Dinarello et al. 2013)). However, IL-33 has also been shown to be an enhancer of IFN-γ production by iNKT cells, NK cells and CD8+ T cells (Smithgall, Comeau et al. 2008, Bourgeois, Van et al. 2009, Yang, Li et al. 2011). Thus the role of IL-33 is not exclusive to Th2 responses. Indeed, in section 1 we have shown that IL-33 is essential for the establishment of a potent anti-viral immune response and that IL-33 signaling is necessary for the clonal expansion and functionality of cytotoxic CD8+ T cells during viral infection. In case of a lack of IL- 33 signaling on responding CD8+ T cells, they showed impaired cytotoxicity, reduced secretion of cytokines and impaired virus control (Bonilla, Frohlich et al. 2012).

While CD8+ T cells manage to resolve acute viral infections independently of the presence of CD4+ T cells (Moskophidis, Cobbold et al. 1987, Ahmed, Butler et al. 1988, Rahemtulla, Fung-Leung et al. 1991), even a transient depletion or blockade of CD4+ T cells in the course of chronic infection has drastic effects on the immune response and prevents clearance of the virus (Doherty, Allan et al. 1992, Matloubian, Concepcion et al. 1994). As a consequence both CD4+ and CD8+ T cells play an important role in anti-viral immune responses in the chronic infection context and thus for successful clearance of the virus. In the course of chronic infection antiviral CTLs can be deleted or functionally inactivated (Moskophidis, Lechner et al. 1993, Zajac, Blattman et al. 1998),

commonly referred to as “exhaustion” of virus-specific CTLs. The knowledge of factors that are regulating maintenance of T cells in chronic infection is, however, very limited. IL-21 is the only cytokine known to be required for the physical maintenance and functionality of virus-specific CD8+ T cells in chronic viral infections (Elsaesser, Sauer et al. 2009, Frohlich, Kisielow et al. 2009, Yi, Du et al. 2009).

We have demonstrated IL-33 to be vital for expansion of virus-specific cells in acute viral infection and we have shown that radio-resistant cells are the source of IL-33, the release of which finally drives efficient T cell responses (Bonilla, Frohlich et al. 2012), suggesting a prominent role of stromal cells for the outcome of viral infections. Also other reports have investigated the cellular source of IL-33 and found cells in mouse epithelial barrier tissues, lymphoid organs, brain, embryos and inflamed tissues, but not in endothelial vessels to express IL-33 (Pichery, Mirey et al. 2012). Notably the absence of IL-33 in endothelial vessels represents an important species-specific difference between humans and mice (Baekkevold, Roussigne et al. 2003, Carriere, Roussel et al. 2007). Based on immunofluorescence and flow cytometry and the expression of VCAM-1 fibroblastic reticular cells (FRCs) were suggested to be the cellular source of IL-33 (Moussion, Ortega et al. 2008, Pichery, Mirey et al. 2012, Hardman, Panova et al. 2013). FRCs are stromal cells and as such are a part of the non-hematopoietic compartment in secondary lymphoid organs. The non-hematopoietic (CD45-negative) connective tissue compartment of the spleen forms the structural backbone and is made up of three cell types: blood endothelial cells (CD31-positive, gp38-negative), fibroblastic reticular cells (CD31-negative, gp38-positive) and yet poorly characterized so-called double-negative cells. Blood endothelial cells line the interior surface of blood vessels and serve as a barrier between vessel lumen and tissue. Fibroblastic reticular cells form the three-dimensional architecture in splenic T-cell zones. The functions of double-negative cells remain to be investigated (Mebius and Kraal 2005).

We demonstrate that IL-33 released by FRCs is crucial for the expansion, maintenance and differentiation of virus-specific T cells in chronic viral infection, most likely by a continuous low-level signaling via the IL-33/ST2 axis rather than a one time imprinting event. This highlights the importance of IL-33 and the non-hematopoietic cell compartment in immune responses in the chronic infection context.

2.3 Material and Methods

2.3.1 Cells

BHK-21 cells were cultured in high-glucose Dulbecco's Eagle medium (DMEM; Sigma) supplemented with 10 % heat-inactivated fetal calf serum (FCS; Biochrom), 10 mM HEPES (Gibco), 1 mM sodium pyruvate (Gibco) and 1x tryptose phosphate broth (Sigma). MC57 cells were maintained in Minimum Essential Medium (MEM; Sigma) complemented with 5 % heat-inactivated FCS, 2 mM L-glutamine (Gibco) and penicillin-streptomycin (100'000 U/ml penicillin and 50 mg/l streptomycin; Gibco). Both cell lines were cultured at 37 °C in a humidified 5 % CO_2 incubator.

2.3.2 Plasmids

The pol-I L, pC-NP and pC-L plasmids have previously been described (Flatz, Bergthaler et al. 2006). For the generation of the pol-I S plasmid encoding for GFP as a reporter gene and either NP or GP, we used a pol-I Bbs/Bsm cloning plasmid as a basis (pol-I 5'-BsmBI_IGR_BbsI_3'), which enables the insertion of genes at the 5' or 3' UTR with site-specific restriction/ligation using BsmBI or BbsI, respectively. GP was inserted by BbsI digest at the 3' position into the pol-I Bbs/Bsm plasmid and GFP with BsmBI restriction/ligation at the 5' position. pol-I S encoding for GFP and NP (pol-I 5'-GFP_IGR_NP-3') were cloned by inserting NP by BbsI digestion and ligation into the pol-I Bbs/Bsm cloning plasmid and GFP by BsmBI cloning.

2.3.3 DNA transfection of cells and rescue of reporter viruses

BHK-21 cells were seeded into 6-well plates at a density of $4x10^5$ cells/well and transfected 24 hours later with different amounts of DNA using lipofectamine (3 µl/µg DNA; Invitrogen) according to the manufacturer's instructions. For rescue of tri-segmented viruses entirely from plasmid DNA, the two minimal viral trans-acting factors NP and L were delivered from pol-II driven plasmids (0.8 µg pC-NP, 1 µg pC-L) and were co-transfected with 1.4 µg of pol-I L and 0.8 µg of both pol-I driven S segments. 72 hours after transfection the supernatant was harvested and passaged on BHK-21 cells for further amplification of the virus. Viral titers in the supernatant were determined by focus forming assay.

2.3.4 Viruses

Wild-type LCMV strain Clone 13 (Cl13; (Ahmed, Salmi et al. 1984)), originally derived from wild-type LCMV Armstrong, and strain WE (Scott and Rivers 1936) have previously been described. Stocks of wild-type and recombinant viruses were produced by infecting BHK-21 cells at a multiplicity of infection (moi) of 0.01 and supernatant was harvested 48 hours after infection. Viral titers were analyzed by focus forming assay. Mice were infected intravenously with 200, $5x10^5$ or $2x10^6$ plaque forming units (PFU).

2.3.5 Focus forming assay

Titers of LCMV are determined by focus forming assay as previously described (Battegay, Cooper et al. 1991). LCMV is a non-cytolytic virus that does not lyse its host cells and as such does not create plaques. Nevertheless units in this work will be expressed in the more commonly used term plaque forming units (PFU) instead of the correct term focus forming units (FFU). MC57 cells were used for focus forming assay if not stated otherwise. Cells were seeded at a density of $1.6x10^5$ cells per well in a 24-well plate and mixed with 200 µl of 10-fold serial dilutions of virus prepared in MEM/ 2 % FCS. After 2-4 hours of incubation at 37 °C, 200 µl of a viscous medium (2 % Methylcellulose in 2x supplemented DMEM) were added per well to ensure spreading of viral particles only to neighboring cells. After 48 hours at 37 °C the supernatant was flicked off and cells were fixed by adding 200 µl of 4 % paraformaldehyde (PFA; applichem) in PBS for 30 minutes at room temperature (all following steps are performed at room temperature). Cells were permeabilised with 200 µl per well of BSS/ 1 % Triton X-100 (Merck Millipore) for 20 minutes and subsequently blocked for 60 minutes with PBS/ 5 % FCS. For staining of NP-positive foci a rat anti-LCMV-NP monoclonal antibody was used as a primary staining antibody at a dilution of 1:30 in PBS/ 2.5 % FCS for 60 minutes. Plates were washed three times with tap water and the secondary HRP-goat-anti-rat-IgG was added at a dilution of 1:100 in PBS/ 2.5 % FCS and incubated for 1 hour. The plate was again washed three times with tap water. The color reaction (0.5 g/l DAB (Sigma D-5637), 0.5 g/l Ammonium Nickel sulfate in PBS/ 0.015 % H_2O_2) was added and the reaction was stopped after 10 minutes with tap water. Stained foci were counted manually and the final titer calculated according to the dilution.

2.3.6 Mice

IL-33-/- (Oboki, Ohno et al. 2010), ST2-/- (Senn, McCoy et al. 2000), ZP3-Cre (Lewandoski, Wassarman et al. 1997), Smarta1 (SM1) (Oxenius, Bachmann et al. 1998) and P14 (Pircher, Burki et al. 1989) mice have previously been described. ST2-/-SM1 mice and ST2-/-P14 mice were obtained by intercrossing SM1 or P14 mice with ST2-/- mice, respectively. IFNAR-/-P14 mice have previously been reported (Crouse, Bedenikovic et al. 2014) and were kindly provided by Prof. A. Oxenius. C57BL/6J ("B6") mice were either purchased from Charles River or bred in-house. All mice were bred and housed under specific pathogen-free (SPF) conditions. They were bred at the Institut für Labortierkunde of the University of Zurich, Switzerland. All animal experiments were performed at the Universities of Geneva and Basel in accordance with the Swiss law for animal protection and the permission of the respective responsible cantonal authorities of Geneva and Basel. Infection of the mice was done via the intravenous route. Natural killer (NK) cells were depleted by injecting doses of 300 µg anti-NK1.1 antibody (clone PK-136; BioXCell) intraperitonally on day -2, 0, 3 and 6 with day 0 being the day of LCMV injection.

2.3.7 Adoptive cell transfer

LCMV-specific CD8+ P14 cells were purified from the spleen of respective transgenic mice by magnetic cell sorting using the "Naïve CD8a+ T Cell Isolation Kit, mouse" (Miltenyi Biotec) according to the manufacturer's protocol. For purification of LCMV-specific CD4+ SM1 cells from spleens of respective transgenic donors we used the "CD4+ T Cell Isolation Kit II" (Miltenyi Biotec) followed by magnetic cell sorting according to the company's instructions. Purity of the cell suspension was verified by flow cytometry and 500 or 5000 transgenic cells per recipient were transferred intravenously in Balanced Salt Solution (BSS; 0.01 g/l Phenol Red, 0.14 g/l $CaCl_2 \cdot 2\ H_2O$, 8 g/l NaCl, 0.4 g/l KCl, 0.2 g/l $MgSO_4 \cdot 7\ H_2O$, 0.2 g/l $MgCl \cdot 6\ H_2O$, 60 mg/l KH_2PO_4, 0.24 g/l $Na_2HPO_4 \cdot 2\ H_2O$, 1 g/l D-Glucose; KH_2PO_4: Sigma, everything else: Fluka).

2.3.8 Flow cytometry

Blood and single cell suspensions obtained from lymph nodes, spleen and liver were stained with antibodies against CD4 (RM4-5 or GK1.5), CD8 (53-6.7), CD45R/B220 (RA3-6B2), CD45.1 (A20), CD45.2 (104), CD90.1 (OX-7), Ter-119 (TER-119), CD31 (390), gp38 (Podoplanin; 8.1.1), CXCR5 (2G8). Dead cells were excluded with either 7-

AAD or Zombie UV Fixable Viability Kit (Biolegend). CD8+ T cells specific for LCMV-epitopes GP33 or GP276 were analyzed using MHC class I tetramer staining (TC Metrix) as previously described (Gallimore, Glithero et al. 1998). Expression of ST2 on the cell surface was analyzed by staining blood or splenocytes with a digoxigenin-coupled anti-mouse ST2 antibody (DJ8; mdbiosciences) and detecting the signal with a secondary PE-conjugated anti-digoxigenin Fab antibody (Roche). The PE-singal was further amplified with two rounds of amplification using the PE FASER Kit (Miltenyi Biotec) according to the manufacturer's instructions. All stainings were performed in FACS buffer (PBS/ 2 % FCS/ 5 mM EDTA/ 0.05 % sodium azide) if not stated differently.

The cytokine profile of splenocytes was determined by intracellular cytokine staining. For this purpose, spleen cells were restimulated with 1 µg/ml of GP64-80 peptide for 5 hours at 37°C in a humidified 5% CO_2 incubator in presence of 5 µg/ml brefeldin A (added after 1h). Cells were fixed in 2 % paraformaldehyde (PFA; Applichem) and intracellular cytokine staining was performed in FACS buffer containing 0.05 % saponin (Sigma) with antibodies against IFN-γ (XMG1.2), TNF-α (MP6-XT22) and IL-2 (JES6-5H4).

The expression of surface and intracellular molecules as well as GFP expression was analyzed on a Beckman Coulter Gallios or a BD LSR Fortessa flow cytometer using Kaluza (Beckman Coulter) or FlowJo software (Tree Star, Ashland, OR).

2.3.9 Immunofluorescence

Immunofluorescence stainings were performed by collaborators in the groups of Prof. Doron Merkler at University of Geneva and Prof. Sanjiv Luther at University of Lausanne. Briefly, organs from PFA-perfused mice were isolated and fixed in 4% PFA for 1 hour. The tissue was saturated in 30% sucrose and embedded on 100% OCT Tissue-Tek freezing medium. Sections were cut and stained with antibodies specific for CD31, LCMV-NP, Podoplanin (gp38) or IL-33 and with DAPI to stain DNA.

2.3.10 Isolation of cells

Single-cell suspensions for the analysis of lymphocytes from spleen, liver or lymph nodes were obtained by mashing the organs with a piston through a 70 µm cell strainer (BD Biosciences).

Stromal cells from spleens and lymph nodes (inguinal, axillary and brachial) were isolated by cutting the respective organs into small pieces and incubating the tissue in RPMI containing 1 mg/ml Collagenase IV (Worthington), 40 µg/ml DNAseI (Roche) and 2 % (vol/vol) FCS for 30 minutes at 37°C stirring at a speed of 300 rpm. The cell suspension was homogenized by pipetting and incubated for another 30 minutes until no visible pieces were present anymore. The cell suspension was passed through a 70 µm cell strainer and the enzymatic digestion was stopped by addition of FACS buffer (recipe in the flow cytometry section). The proportion of stromal cells was enriched by lysing erythrocytes with ACK Lysis Buffer (0.15 M NH_4Cl, 10 mM $KHCO_3$, 0.1 mM EDTA) for 45 seconds at room temperature and by depleting hematopoietic CD45+ cells by magnetic cell sorting using anti-CD45 beads (Miltenyi Biotec).

Hepatic stromal cells were isolated by chopping the liver into small pieces and incubating the tissue with RPMI containing 2.4 mg/ml collagenase type I (Gibco), 0.2 mg/ml DNAseI (Roche) and 10 % FCS stirring at 300 rpm at 37°C. After 30 minutes the tissue was homogenized with a 18G needle and incubated for another 30 minutes at 37°C. Remaining chunks were homogenized with a 21G needle and the resulting cell suspension filtered through a 70 µm cell strainer. The enzymatic digestion was stopped by adding FACS buffer and the suspension was enriched for stromal cells by lysing erythrocytes and depleting hematopoietic CD45+ cells as described in the previous paragraph.

2.3.11 Statistical Analysis

Statistical significance was determined by 1-way ANOVA followed by Bonferroni's post-test for multiple comparisons using Graphpad Prism software (version 6.0d). p values of $p > 0.5$ were considered not statistically significant (ns), whereas p values of $p < 0.5$ were considered significant (*) with gradations of $p < 0.1$ (**) and $p < 0.01$ (***) being highly significant.

2.4 Results

Generation of a mouse line reporting IL-33 expression by means of GFP.

We have previously reported that the alarmin Interleukin-33 is necessary for eliciting potent CD8+ T cell responses against prototypic RNA- and DNA-viruses, amongst them LCMV (Bonilla, Frohlich et al. 2012). Experiments with bone-marrow chimeric mice, where lethally irradiated wild-type or IL-33 deficient mice were reconstituted with IL-33 competent or IL-33 deficient bone marrow, demonstrated that IL-33 produced by non-hematopoietic stromal cells was essential to drive efficient anti-viral CD8+ T cell responses. Immunofluorescence analysis had confirmed IL-33 expression by radio-resistant cells in the T cell zone of spleens. Following these observations we wanted to further analyze which stromal cell type expresses IL-33. We also aimed at a tool to analyze IL-33 expression by flow cytometry, which thus far has not been possible with antibody-based methods. For a quantitative readout of IL-33 levels on a per cell basis, we aimed at generating a mouse line reporting expression of IL-33 by means of GFP. We took advantage of an IL-33 deficient mouse line that carries a GFP gene and a downstream neomycin resistance gene (neoR) that is flanked by loxP sites ("MT allele"; Fig. 2.1A) (Oboki, Ohno et al. 2010). The entire cassette is inserted in the second exon of the IL-33 open reading frame (ORF), thus its expression is controlled by the IL-33 promoter. However, the knock-in as such did not provide any detectable reporter activity (data not shown). We hypothesized that expression of the neomycin resistance gene, which is controlled by a strong promoter, interferes with and suppresses upstream expression of GFP to undetectable levels. By intercrossing these mice with ZP3-Cre mice that express the loxP site-specific DNA recombinase Cre in oocytes (Lewandoski, Wassarman et al. 1997), the loxP-flanked neoR downstream of GFP was excised (→ "IL-33 reporting allele"; Fig. 2.1A). Indeed, upon excision of neoR, IL-33 promoter-driven GFP expression was not suppressed anymore and could readily be detected by flow cytometry.

Fibroblastic reticular and lymphatic endothelial cells are the main producers of interleukin-33 in secondary lymphoid organs.

In order to test whether our breeding strategy led to detectable GFP expression in IL-33 producing cells, we isolated stromal cells from the spleens of uninfected IL-33 reporter mice. The regulatory mechanisms of IL-33 expression are not well understood yet and it

has not been conclusively analyzed so far whether positive or negative feedback loops play a role for regulation of IL-33 expression. Taking this into consideration, we used our IL-33 reporter mice in a hemizygous background, so that they were IL-33 competent. This enabled us to reduce the risk for artifacts due to the lack of IL-33 in the system. We established an optimized protocol for the isolation of splenic stroma by collagenase digestion of the tissue followed by depletion of hematopoietic CD45+ cells. When analyzing the resulting single-cell suspension by flow cytometry (Fig. 2.1B-D), we excluded erythrocytes and all remaining CD45+ hematopoietic cells. The expression pattern of the endothelial cell marker CD31 and the fibroblast marker gp38 (Podoplanin) allowed us to distinguish fibroblastic reticular cells (FRC; gp38+CD31-) from blood endothelial cells (BEC; gp38-CD31+) and double-negative stromal cells (DN; gp38-CD31-) (Fig. 2.1B). Each of the three stromal cell populations was further analyzed for their GFP expression and the percentage of GFP+ cells within the respective compartment was quantified (Fig. 2.1C-D). Whereas DNs and BECs only had a very small population of GFP+ cells (DN: 0.13 %; BEC: 0.15 %), 45 % of FRCs showed a pronounced population of GFP+ and thus IL-33 producing cells (Fig. 2.1D; one respresentative histogram of the GFP profile of FRCs is shown in Fig. 2.1C). The same held true when analyzing the total amount of GFP+ cells per spleen, in that we also found most of the GFP+ cells to be FRCs (Fig 2.1D). In parallel we isolated the stroma of lymph nodes from uninfected IL-33 reporter mice by collagenase digestion and analyzed it by flow cytometry. The stroma compartment in lymph nodes consists of four populations, which also can be distinguished by expression of CD31 and gp38. Expression patterns of FRC, BEC and DN were the same as in spleen but unlike in spleen, a fourth stromal cell population, the lymphatic endothelial cells (LEC) can be identified by expression of both markers CD31 and gp38 (Fig. 2.1E). Analysis of the percentage of GFP+ cells confirmed FRCs as the main GFP+ expressing cell type but also more than 10 % of LECs were found positive for GFP under naïve conditions (Fig. 2.1F), whereas BECs and DNs only showed a very low percentage of GFP+ cells (0.06 % and 0.38 %, respectively). However, since LECs are comparatively rare in lymph nodes, FRCs quantitatively made up for the majority of GFP+ cells in that organ. Importantly, we also analyzed the hematopoietic compartment of the organs of IL-33 reporter mice. However, GFP+ cells were virtually absent within this compartment (< 0.01 % of the analyzed population; data not shown).

We tested whether the IL-33 reporting mouse line was a faithful reflection of IL-33 expression patterns. Spleens and lymph nodes of hemizygous IL-33 reporter mice were

co-stained with anti-IL33 specific antibodies and analyzed by immunofluorescence (Fig. 2.2A+C; done by H-Y. Huang and S. Favre in the Luther lab at UNIL). We found that virtually all cells that were stained by the anti-IL-33 antibody were also positive for GFP. In addition we found GFP single-positive cells, which probably can be explained by the higher sensitivity of the GFP signal as compared to immunofluorescence staining with an IL-33 specific antibody. We also validated our homozygous IL-33 deficient mice, which did not show any immunofluorescence staining with the IL-33 specific antibody, neither in spleen nor in lymph nodes (Fig. 2.2B+D; done by H-Y. Huang and S. Favre in the Luther lab at UNIL). Consequently we can conclude that our IL-33 reporting mice reliably detect IL-33 promoter activity and that fibroblastic reticular cells and lymphatic endothelial cells are the main producers of IL-33 in resting secondary lymphoid organs. By validating our IL-33 reporter mouse line we also confirmed our earlier findings that the IL-33 signal originates from the non-hematopoietic compartment of SLOs (Bonilla, Frohlich et al. 2012).

Blood endothelial cells rather than IL-33 producing fibroblastic reticular cells are the primary stromal cell target of LCMV in spleen.

We have shown that IL-33 is important for an anti-viral immune response against LCMV. The mechanism, however, that triggers release of IL-33, remains to be elucidated. In order to investigate whether release of IL-33 could be a consequence of infection of the IL-33 expressing cells we generated recombinant reporter viruses, which allow us to track infected cells by expression of GFP. It has been shown that it is possible to introduce foreign genes of interest into the genome of normally bi-segmented wild-type LCMV. Following a published strategy (Emonet, Garidou et al. 2009) we introduced two copies of the green-fluorescent protein (GFP) into the genome of wild-type LCMV. This resulted in recombinant viral particles with three RNA segments (1L + 2S) instead of one L and one S segment in wild-type LCMV (Fig. 2.3A+B). We rescued the tri-segmented reporter virus (r3LCMV-GFP) in cell culture by reverse genetic systems (Flatz, Bergthaler et al. 2006, Flatz, Hegazy et al. 2010). r3LCMV-GFP-infected cells express GFP allowing their identification by flow cytometry. We infected C57BL/6 mice with $5x10^5$ PFU of either r3LCMV-GFP or wild-type LCMV and isolated splenic stromal cells three days after infection. Stromal cell subpopulations were identified by their expression of gp38 and CD31 (Fig. 2.3C) and analyzed for GFP expression (Fig. 2.3D-E). The percentage and absolute number of GFP+ i.e. r3LCMV-GFP-infected cells within each stromal cell population was quantified (Figure 2.3F). As expected, wild-type LCMV-

infected animals showed only background levels of GFP (Fig. 2.3D and "ctrl" in Fig. 2.3F). In r3LCMV-GFP infected animals, GFP+ cells were undetectable in the double-negative population and only 1.13 % of FRCs showed detectable GFP signal. We found comparably more (7.4 %) reporter virus-infected BECs. Also when expressed as absolute numbers of GFP+ cells per spleen, infected BECs were at least 50 times more abundant than infected FRCs or DNs (Fig. 2.3F). This finding was further corroborated by immunofluorescence analysis on tissue sections. We infected mice i.v. with wild-type LCMV and stained spleen sections for the endothelial cell marker CD31 and LCMV nucleoprotein (NP) to identify infected BECs. Indeed we found a considerable number of cells costained for both CD31 and NP in all our spleen sections (Fig. 2.3G; stains performed by I. Wagner in the Merkler lab at UNIGE). This validated our findings obtained by flow cytometry and at the same time demonstrated that recombinant r3LCMV shows the same tropism as wild-type LCMV. An analogous pattern of r3LCMV-GFP distribution was found in hepatic stromal cells on day three after infection (Figure 2.3H). CD31+ gp38-negative BECs can be distinguished from other populations of CD31-negative stromal cells. Again, wild-type LCMV infected animals served as negative controls (ctrl). Whereas no infected cells could be detected in the CD31- liver stromal cells, 4 % of the BECs were found to be GFP+. Thus we concluded that BECs rather than FRCs are the predominant stromal target cell population in early LCMV infection.

Lack of ST2 leads to depletion of virus-specific CD8+ T cells during chronic LCMV infection.

To test whether signaling via IL-33/ST2 is necessary for the maintenance of virus-specific CTLs during chronic viral infection, we infected either ST2-deficient or wild-type C57BL/6 mice with a high-dose of LCMV Clone 13 to establish chronic infection. We tracked frequencies of LCMV-specific CD8+ T cells over time by flow cytometry (Fig. 2.4A-B). GP276-specific CD8+ T cells, which are the dominant population of anti-viral CD8+ T cells in chronic infection, were depleted within 44 days after infection in ST2-deficient mice, whereas GP276-specific CTLs in wild-type mice were stably maintained (Fig. 2.4C). GP33-specific CD8+ T cells showed the same trend even though a lot less pronounced (Fig. 2.4C). Consequently, this suggests that signaling via the IL-33/ST2 pathway is important for the maintenance of virus-specific CTL responses during chronic infection.

T cell-intrinsic signaling via IL-33/ST2 is essential for stable maintenance of virus-specific CTLs during chronic infection.

We have shown that the induction of a potent virus-specific CD8+ T cell response and more precisely the clonal expansion of these CTLs is reliant on CTL-intrinsic IL-33/ST2 signaling in acute infection (Bonilla, Frohlich et al. 2012). In the previous figure we demonstrated that lack of the ST2 receptor leads to the disappearance of virus-specific CTLs during chronic infection. We now aimed to investigate whether this observation is, analogously to our data published for acute viral infections, also mediated by T cell-intrinsic signaling. We adoptively transferred (adTf) a physiological number of transgenic LCMV-specific CD8+ T cells (P14) into C57BL/6 recipient mice. P14 cells were specific for the LCMV epitope GP33-41 (GP33) but were either ST2-competent (wt P14) or ST2-deficient (ST2ko P14). One day after adTf we infected the recipients with high-dose Clone 13 or low-dose LCMV strain WE. Infection with a high dose ($2x10^6$ PFU) of Clone 13 leads to the establishment of a chronic infection, whereas low dose of LCMV WE results in an acute infection. Blood was taken on different time points after infection and the expansion and maintenance of the adoptively transferred virus-specific indicator CD8+ T cells was analyzed by flow cytometry (Fig. 2.5A-B). Expansion and survival of the transferred P14 cell population was analyzed in the context of chronic (Fig. 2.5C) or acute infection (Fig. 2.5D) and results were graphed as percentage of transferred P14 cells of the total CD8+ T cell pool in blood (upper panels). Additionally we calculated the "maintenance" of these cell populations by expressing these values as percentage of the peak of population expansion on day 9 after infection (lower panels). Thereby we normalized for the defective expansion in the early phase after infection. Whereas ST2-competent virus-specific CD8+ T cells showed stable frequencies over time both under chronic and acute infection conditions, a marked difference was noted when comparing the maintenance of ST2-deficient P14 cells in acute and chronic infection. In acute infection ST2ko P14 cells showed defective expansion, reflected by the lower numbers on day 9 after infection, but thereafter were stably maintained, parallel to wild-type P14 cells (Fig. 2.5D). This contrasted sharply with the outcome in chronic infection. ST2ko P14 cells were not maintained, showed continuously decreasing frequencies in blood, and in most animals reached technical detection limits around 44 days after infection (Fig. 2.5C). Therefore signaling via the IL-33/ST2 pathway seemed to be critical both for the expansion and the maintenance of virus-specific CD8+ T cells by CTL-intrinsic signaling in chronic viral infection. Besides the frequency of the transferred cells in the blood, we also investigated the distribution of the transferred cells in lymphoid organs by analyzing

spleen and lymph nodes 24 days after chronic (Fig. 2.5E) or acute infection (Fig. 2.5F). In all tissues analyzed and in both infection settings we consistently found less ST2ko P14 cells than wild-type cells, due to the defective expansion of ST2-deficient cells. However, there were no marked differences in the overall distribution of the respective cell-types in the organs analyzed. Thus the tissue distribution of virus-specific CD8+ T cells does not seem to be affected by the presence or absence of ST2/IL-33 signaling. Since expansion of ST2-deficient P14 cells is impaired in the early phase after both acute and chronic infection, a concern could have been that this uneven starting point might have affected our conclusion regarding the maintenance of these cells in a chronic setting. To even-up for the defective expansion, we transferred the usual number of wt P14 cells and in parallel into a separate group of recipients a 10-fold higher number of ST2ko cells, followed by infection of the recipients one day later. We tracked the frequency of the transferred cells in the blood throughout the course of acute or chronic infection (Fig. 2.5G-H). The higher input of ST2ko P14 cells was reflected in comparably higher frequencies in blood on day 6, both in chronic and acute infection settings. This was expected since CD8+ T cell expansion had not yet reached its peak and the influence of the IL-33/ST2 axis plays mostly at later time points (Bonilla, Frohlich et al. 2012). In acute infection, comparably stronger expansion of the wild-type P14 cells between day 6 and day 9 eliminated the 10-fold differences to ST2ko P14 cells, such that equal levels were reached. Thereafter both populations were stably maintained until at least day 27 (Fig. 2.5H). Also in chronic infection the differences in transferred cell numbers were detectable until day 6 after infection. Between day 6 and 15, wt P14 cells expanded further and were stably maintained thereafter. Conversely, ST2ko P14 cells did not expand further after day 6 but exhibited continuously declining frequencies (Fig. 2.5G). In summary this figure showed that virus-specific CD8+ T cells that cannot sense IL-33 are defective both in expansion and maintenance in chronic viral infection, confirming that the depletion of ST2-deficient CTLs during chronic viral infection is due to T cell-intrinsic signaling.

A subset of virus-specific CTLs in chronic infection continuously expresses surface ST2.

Our previous experiments had shown that virus-specific CD8+ T cells depended on IL-33/ST2 signals to expand and be maintained in chronic viral infection. However, it remained unclear whether they retained the ability to sense IL-33-mediated expansion and survival signals throughout chronic infection or whether their differential behavior

reflected a phenotypic "imprinting" mechanism due to a one-time signal early during infection. Expression levels of the cellular receptor ST2 can be detected by ST2-specific antibody staining and flow cytometry. We reasoned that continuous or transient receptor expression on virus-specific CTLs would give important hints on the possibilities for continuous ST2 signaling. We adoptively transferred wild-type or ST2ko P14 cells into wild-type hosts and infected them one day later with LCMV to establish either acute or chronic infection. We measured ST2 expression on the surface of transferred P14 cells throughout infection (Fig. 2.6A-B). We quantified labeling intensity in flow cytometry to assess expression levels (Fig. 2.6C) and determined the percentage of ST2+ cells within the transferred population over time (Fig. 2.6D). In order to control for potential inter-experimental variability of staining intensity at different time points, we normalized both readouts on every time point to the background values represented by the ST2ko P14 cells. Both, fluorescence intensity and the percentage of ST2+ cells showed that ST2 expression is highest on day 6 after infection with decreasing levels thereafter. Similar kinetics were detected for both infection settings. Even though the levels of ST2-expression and the percentage of ST2+ cells were declining over time, ST2 was detectable on a subset of cells for at least 27 days after infection (representative histograms of day 23 shown in Figure 2.6E). Consequently, ST2 expression seemed higher in the early phase of infection but a subset of virus-specific cells apparently retained the receptor throughout the chronic phase.

Up-regulation of ST2 on activated LCMV-specific CD8+ T cells is independent of IFNAR signaling.

It is well established that signaling through the type I interferon receptor (IFNAR) is essential for clonal expansion of adoptively transferred LCMV-specific CD8+ T cell populations (Kolumam, Thomas et al. 2005). Even in the absence of NK cells, which were found to be largely accountable for this phenotype, a more modest but still clearly defective expansion of IFNAR-deficient P14 cells was suggestive for T cell-intrinsic proliferative defects in the context of IFNAR deficiency (Crouse, Bedenikovic et al. 2014). In order to elucidate whether IFNAR signaling was necessary for up-regulation of ST2 on the surface of LCMV-specific CTLs, we adoptively transferred wild-type or IFNAR-deficient P14 cells into NK cell-depleted C57BL/6 recipients, infected them one day later with LCMV and analyzed the frequency of transferred cells on different time points by flow cytometry (Fig. 2.7A). As expected and in agreement with the mentioned publication, IFNAR-deficient cells were considerably impaired in clonal expansion upon

LCMV infection (Fig. 2.7C). However, levels of ST2 on the surface of transferred cells were indistinguishable on wild-type and IFNAR-deficient cells, no matter whether ST2 expression was analyzed at the level of protein (fluorescence intensity) or as percentage receptor-bearing cells (Fig 2.7D). Therefore signaling via IFNAR did not seem to account for the induction of ST2 and the deficient clonal expansion of ST2-deficient virus-specific CD8+ T cells.

Early up-regulation and subsequent reduction in IL-33-expressing cell numbers and IL-33 protein levels in the LCMV-infected spleen.

In our previous report we have shown by quantitative PCR that IL-33 mRNA levels are up-regulated after acute infection, with kinetics paralleling viral genome copy numbers in the spleen. Additionally, we observed an increase in IL-33 expression when analyzing IL-33 levels of FRCs in secondary lymphoid organs of acutely LCMV-infected GFP reporter mice (data not shown). Here we wanted to investigate whether chronic LCMV infection led to an increase in cellular IL-33 levels or in the number of IL-33-expressing cells. We established chronic LCMV infection in hemizygous IL-33 reporter mice and analyzed splenic stroma on different time points after infection (Fig. 2.8A). The non-hematopoietic compartment of the spleen was analyzed by flow cytometry (Fig. 2.8B) and analogously to uninfected mice (Fig. 2.1 and 2.2), FRCs were found to be the dominant cell type producing IL-33 under infection conditions. We analyzed IL-33 reporter levels as reflected in GFP mean fluorescence intensity of GFP+ FRCs and detected a rise in IL-33 expression on a per cell level. We also counted the total number of GFP+ FRCs per spleen (Fig. 2.8C) and found it to increase. By both readouts the initial slight increase of IL-33 levels and IL-33-expressing cells up until day 8 after infection was followed by a decline in the subsequent chronic phase of infection. However, even though this tendency was detected both on a per-cell level as well as in the percentage of IL-33 expressing FRCs, we acknowledge the effect to be more modest than suggested by earlier reports on FRC kinetics in acute LCMV infection (Scandella, Bolinger et al. 2008).

The functionality of LCMV-specific CD4+ T cells does not depend on ST2/IL-33 signaling.

We have shown that ST2-deficient virus-specific CD8+ T cells have a defect in expansion and maintenance during chronic infection. Furthermore, we have demonstrated in our previous publication that ST2 signaling has a profound impact on ex vivo

functionality of anti-viral CTLs in acute infection, which is widely thought to correlate with the protective capacity of CD8+ T cells (Appay, van Lier et al. 2008). Whereas CD4+ T cells are not necessary for the resolution of an acute LCMV infection, it has been shown that CD4+ T cells play a critical role for the outcome of chronic infections (Matloubian, Concepcion et al. 1994). In order to investigate whether ST2-signaling also has an impact on anti-viral CD4+ T cell effector function in chronic LCMV infection, we adoptively transferred 500 wild-type or ST2-deficient LCMV-specific CD4+ T cells (wt SM1 or ST2ko SM1) into C57BL/6 mice and infected the recipients one day later with LCMV to establish acute or chronic infection. Fourteen days later we analyzed the capacity of transferred SM1 cells to produce the prototypic inflammatory Th1 cytokines IFN-γ, TNF-α and IL-2 after peptide stimulation (Fig. 2.9A). We quantified the single, double- or triple-producers of these cytokines for both, SM1 cells originating from chronically (Fig. 2.9B) or acutely infected mice (Fig. 2.9C). In both cases ST2-deficient SM1 cells were at least as functional as wild-type SM1 cells. During chronic infection there even seemed to be somewhat higher numbers of IFN-γ/TNF-α double-producers and IFN-γ/TNF-α/IL-2 multifunctional CD4+ T cells. In the light of these findings, ST2ko CD4+ T cells seemed to form fully functional Th1 cells in chronic viral infection.

Lack of ST2-signaling impacts the tissue distribution of CD4+ T cells in chronic infection.

The experiments in Figure 2.9 have demonstrated that signaling via IL-33/ST2 is not essential for the Th1 cytokine profile of antiviral CD4+ T cells. However, since we had previously shown that IL-33 signaling is critical for expansion and maintenance of virus-specific CD8+ T cells, we performed analogous adoptive transfer experiments with virus-specific CD4+ T cells in order to investigate whether ST2-deficient SM1 cells showed defective population expansion analogously to ST2ko P14 cells. We transferred 500 wild-type or ST2ko SM1 cells into C57BL/6 recipients and infected the mice one day later with LCMV to establish acute or chronic infection. The frequency of the transferred cells was analyzed on several time points after infection (Fig. 2.10A-B). In acute infection we detected an impaired expansion of ST2ko SM1 cells as compared to wild-type SM1 cells. But cells that had expanded until day 9 after infection were thereafter maintained similarly to wild-type cells (Fig. 2.10D). In chronic infection, virus-specific wt SM1 cells expanded as expected and after a peak around day 6-9 exhibited detectable albeit modest population contraction when progressing towards the chronic phase (Fig. 2.10C). In contrast, we could barely detect any transferred ST2ko SM1 cells in the blood and

populations were too small to calculate reliable "maintenance" values (n.d. in Figure 2.10C). Thus we investigated whether the transferred CD4+ T cells were differentially distributed in different organs. Wild-type SM1 cells showed an equal distribution in blood, spleen and lymph nodes of chronically LCMV-infected recipients. Conversely, the distribution of ST2ko CD4+ T cells was severely distorted (Fig. 2.10E). In striking contrast to their virtual absence from blood, adoptively transferred ST2ko SM1 were found both in spleen and lymph nodes in numbers quite similar to wild-type cells. This suggested that the tissue distribution of ST2ko SM1 cells was affected by the lack of ST2 signaling and that these cells were retained in lymphoid organs and did not efficiently recirculate through the bloodstream. This phenotype was not detected in acute infection, and ST2ko cells were found at comparable frequencies in all three tissues analyzed (Fig. 2.10F).

Absence of ST2 favors the differentiation of virus-specific CD4+ T cells into a T follicular helper cell phenotype.

Given that ST2-deficient CD4+ T cells are retained in lymphoid organs and don't efficiently recirculate in the bloodstream, we hypothesized that the lack of ST2-signaling might influence the differentiation program of these cells which in turn might be at the root of an altered tissue distribution. T follicular helper cells (Tfh) are specialized providers of B cell help in germinal centers and as such are located mostly in lymphoid organs. Homing chemokine receptors such as CXCR5 represent a hallmark of the Tfh phenotype and we hypothesized that such a differentiation might retain them in secondary lymphoid organs and provide help to B cells. We transferred 500 wild-type or ST2ko SM1 cells into C57BL/6 recipients and infected the mice one day later with LCMV Clone 13 to establish chronic infection. Fifteen days later we analyzed the transferred SM1 cells in the spleen for CXCR5 expression (Fig. 2.11A-B). We found that CXCR5+ cells were significantly overrepresented within the ST2ko SM1 population as compared to wt SM1 cells (Fig. 2.11C). Thus ST2-deficiency promoted the differentiation of virus-specific CD4+ T cells towards a T follicular helper phenotype.

2.5 Discussion

We present data that extends our knowledge on the essential role of IL-33/ST2 signaling in efficient T cell responses during acute viral infection to the context of chronic infections. Viral replication is commonly referred to as "danger" for the host's immune system (Gallucci and Matzinger 2001) and our previous report has provided evidence that also damage due to viral replication can directly enhance antiviral CTL responses via the alarmin IL-33 (Bonilla, Frohlich et al. 2012). As shown here, virus-specific CTLs that cannot sense the Interleukin-33 during chronic infection fail to be maintained over time and are continuously depleted. This implies a constant necessity for damage signals like IL-33 in the extracellular space in persistent viral infections like LCMV in mice or HIV and HBV in humans in order to enhance effector functions and ensure maintenance of potent CTL responses.

Our flow cytometry and immunofluorescence-based findings of IL-33 expression by FRCs is in line with the expression pattern of this cytokine found in other recently published reporter systems (Moussion, Ortega et al. 2008, Pichery, Mirey et al. 2012, Hardman, Panova et al. 2013). This validates our IL-33 reporter mouse as a faithful tool to further investigate IL-33 expression in various conditions and in an at least semi-quantitative fashion without the need for prior processing of cells or tissues. Our approach and the citrine reporter mouse (Hardman, Panova et al. 2013) are the first live cell reporters that enable investigation of IL-33 expression in mice directly in vivo and under various inflammatory or pathological conditions, whereas previous studies were limited to quantification of mRNA levels in tissues or immunohistochemical analyses of a lacZ-based reporter offering little quantitative insights. We have detected only a slight trend towards up-regulation of IL-33 protein in the early phase of chronic infection, both in terms of fluorescence intensity and total numbers of GFP+ FRCs per spleen. This was somewhat unexpected, since we had previously reported an increase in IL-33 mRNA detected by qPCR (Bonilla, Frohlich et al. 2012), and GFP fluorescence intensity in our IL-33 reporter mice after acute LCMV infection also was found to be augmented (data not shown). Conversely, we found a significant decrease of IL-33 expressing FRCs in later phases of the infection (day 15-23). It is known that chronic LCMV infection results in reduced cellularity and altered splenic architecture (Odermatt, Eppler et al. 1991), especially a loss of FRCs during Clone 13 infection has previously been reported (Mueller, Matloubian et al. 2007). In our hands total numbers of FRCs remained normal

upon Clone 13 infection, whereas a slight but significant reduction in total number of IL-33 expressing FRCs was apparent in later phases of the infection. This discrepancy could be explained by the differential methodology applied (immunohistochemistry with tracer localization by Mueller et al. vs. flow cytometry by us). The decrease in IL-33 expressing FRCs in chronic infection might be a result of the disruption of the splenic architecture, which would be in line with the mentioned publications. Alternatively and mechanistically more attractive, a selective loss as a result of cell death of IL-33 expressing FRCs could represent a sophisticated albeit unknown biological mechanism to release IL-33 into the extra-cellular space leading to activation of and rendering it bioavailable for signaling to immune cells. This in turn requires the FRCs in SLOs to have a massive turn over rate in order to provide constant supply of the danger signal but at the same time to replace dying cells and ensure an intact lymphoid organ structure in persistent infection.

It has been postulated that FRCs were a main target of LCMV Clone 13 and that high numbers of FRCs both in spleen and lymph nodes were directly infected by LCMV (Mueller, Matloubian et al. 2007). This contrasts with results obtained in our study. Our flow cytometric analyses of mice infected with reporter viruses could not confirm such a tropism of LCMV. We found a pronounced population of infected BECs of murine spleen and liver, but total numbers of infected FRCs per spleen were negligible in our hands, which may be due, at least in parts, to their comparatively rare occurrence in lymphoid organs. This discrepancy could be explained by different technical readouts. We used flow cytometry with the endothelial cell marker CD31 and the fibroblast marker gp38 (Podoplanin) to differentiate stromal cell subsets, whereas Mueller et al. based their findings on the immunohistochemical analysis of ER-TR7 stained spleen and lymph node sections. Doubts have cast over the specificity of the ER-TR7 antibody and its utility for the identification of FRCs in tissues, owing to the antibody's propensity for staining extracellular matrix. Another technical difference between our study and the one by Mueller consists in our use of tri-segmented reporter viruses. However, all available evidence suggests that these reporter viruses faithfully recreate the natural virus' tropism (Emonet, Garidou et al. 2009). Additionally, we have confirmed our findings by immunohistochemistry using wild-type virus. Conversely, our finding of LCMV tropism for BECs is in agreement with data published by Frebel et al. in 2012 (Frebel, Nindl et al. 2012). They used a flow cytometric approach to analyze liver and lung tissue upon LCMV infection by staining for LCMV nucleoprotein NP and the endothelial cell marker CD31 and identified endothelial cells as a major viral target.

There are two potential explanations for differential maintenance of wild-type and ST2-deficient CD8+ T cells. A continuous survival and/or differentiation signal via the IL-33/ST2 pathway might be required for the maintenance of virus-specific T cells or a one-time "imprint" type of signal via the IL-33/ST2 pathway could program cells for survival. We favor the explanation of a continuous survival and/or differentiation signal over the imprinting signal, which would have to be obtained during the early phase of the response. This hypothesis is supported by our finding that a considerable level of ST2 remains on at least a subset of LCMV-specific CD8+ T cells throughout chronic infection and late after acute infection. The mechanisms and signaling cascades leading to ST2 up-regulation and maintenance remain unclear. We can exclude, however, that up-regulation of ST2 on the surface of virus-specific CD8+ T cells depends on IFNAR.

Our data on the altered recirculation behavior of ST2-deficient CD4+ T cells and the ST2-inhibited Th1 differentiation of SM1 cells seem surprising at first glance because ST2 on CD4+ T cells is commonly thought of as a marker of Th2 differentiation (Lohning, Stroehmann et al. 1998) and would not be expected to influence Th1-biased responses at all. However, a recent study showing impaired IFN-γ production of ST2ko CD4+ T cells in Salmonella infection and LPS stimulation is in line with our findings (O'Donnell, Pham et al. 2014). Our analyses of CD4+ T cells in the LCMV context were, however, restricted to the first 9-14 days after infection, and we cannot rule out at present that the observed phenotypic differences vanish later on. It is known that levels of antigen and the cytokine milieu can drive CD4+ T cells into a variety of different T helper phenotypes. This enables a certain degree of flexibility and plasticity of the immune responses. However, whereas Brooks et al. have shown that exhaustion of CD4+ T cells is the result of continuous exposure to viral antigens, the mechanisms that govern CD4+ T cell differentiation in persistent viral infection are only incompletely understood (Brooks, McGavern et al. 2006). Interleukin-21 has been characterized as one of the main players for potent CD4+ T cell help in chronic viral infection and it was also found essential for maintaining not only the help to CD8+ T cells (Elsaesser, Sauer et al. 2009, Frohlich, Kisielow et al. 2009, Yi, Du et al. 2009) but also for stimulation of germinal center B cells and antibody production in the late phase of infection (Ozaki, Spolski et al. 2002, Linterman, Beaton et al. 2010, Zotos, Coquet et al. 2010). Fahey et al. have furthermore shown that viral persistence directly influences differentiation of CD4+ T cells to preferentially develop into Tfh cells rather than Th1 helper cells (Fahey, Wilson et al. 2011). A very recent publication suggests that de novo Th1 generation is suppressed during viral persistence by a type-I IFN-mediated mechanism, which in turn favors

almost exclusive differentiation of CD4+ T cells into Tfh cells instead of Th1 cells (Osokine, Snell et al. 2014). Indeed, ST2 seems to have an impact on CD4+ T cell differentiation since ST2-deficient mice expressed significantly more CXCR5 on their surface, a receptor required for localization of T cells into the B cell follicles where they drive germinal center formation and provide B cell help through direct cell-cell interactions and secretion of cytokines like IL-21 (reviewed in (Crotty 2011)). This might be indicative for a preferential differentiation of ST2-deficient cells into Tfh cells.

In summary, we present evidence that damage signals represent an important molecular signature for the hosts' continuous efforts at clearing chronic viral infections. Gaining a more detailed knowledge of the events that shape immune responses in the chronic infection context is important to improve existing or develop new therapeutic interventions against infectious diseases and cancer.

2.6 Figures

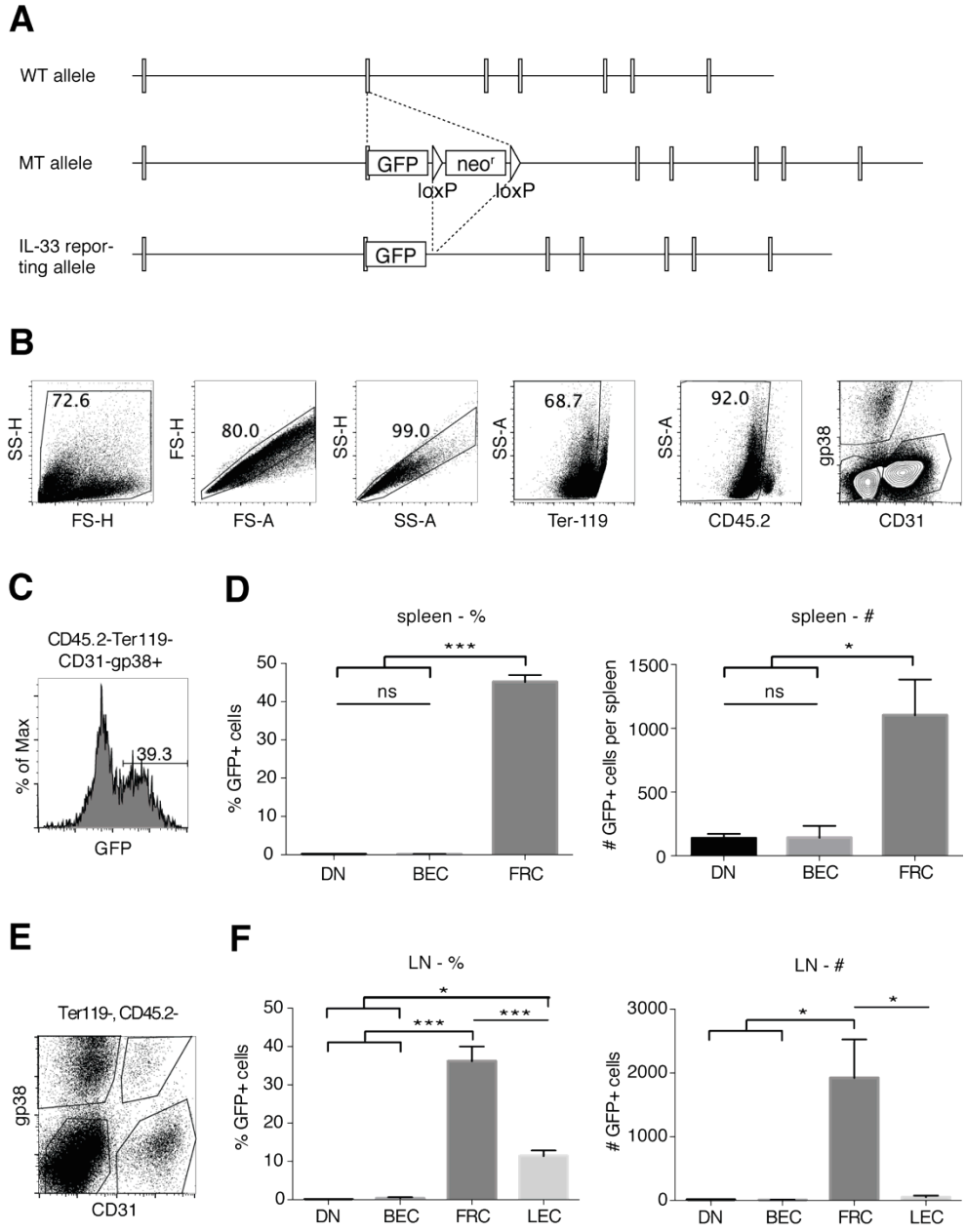

Figure 2.1: Fibroblastic reticular cells and lymphatic endothelial cells are the main IL-33 producing cell populations in uninfected lymphatic organs.

(A) A mouse strain that reports expression of IL-33 by means of GFP was generated by removing a loxP-flanked neomycin resistance gene (neo^R) downstream of the GFP open reading frame of an IL-33 deficient line (Oboki, Ohno et al. 2010). IL-33 deficient mice carrying the mutant allele ("MT allele"; obtained from S. Nakae) were intercrossed with ZP3-Cre mice encoding the loxP site-specific DNA recombinase Cre in oocytes resulting in the excision of the neo^r cassette (→ "IL33 reporting allele") and expression of the reporter gene GFP under the control of the IL-33 reporter. (B-D) Single-cell suspensions of spleens from uninfected IL-33 reporter mice were prepared by collagenase digestion, stained with CD45.2, Ter-119, gp38 and CD31-specific antibodies and analyzed by flow cytometry. (B) Gating

strategy and identification of three splenic stromal cell populations by expression of gp38 and CD31 (gated on single Ter119-CD45.2- cells): fibroblastic reticular cells (FRCs; gp38+CD31-), blood endothelial cells (BECs; gp38-CD31+) and double negative stromal cells (DN; gp38-CD31-). (C) Representative histogram of the GFP profile of gp38+CD31- FRCs (gated on CD45.2-, Ter119-, CD31-, gp38+). (D) Quantification of the GFP+ populations within the three stromal cell types FRC, BEC and DN as percentage (left panel) or total cell numbers per spleen (right panel). Symbols and bars represent the mean±SEM of three mice per group. Representative data from one out of at least three independent experiments are shown. ns, not statistically significant ($p \geq 0.05$); ***: $p < 0.001$ (1-way ANOVA followed by Bonferroni's post-test for multiple comparisons). (E) Lymph nodes of uninfected IL-33 reporter mice were digested with collagenase. The resulting single cell suspension was stained with CD45.2, Ter119, gp38 and CD31-specific antibodies and analyzed by flow cytometry. (E) Identification of the four stromal cell populations in lymph nodes by expression of gp38 and CD31 (gated on single Ter119- CD45.2- cells): FRCs (gp38+CD31-), BECs (gp38-CD31+), lymphatic endothelial cells (LECs; gp38+CD31+) and double negative stromal cells (DN; gp38-CD31-). (F) Percentage (left panel) and total amount (right panel) of GFP+ cells of the four stromal cell populations in lymph nodes: FRCs, DNs, BECs and LECs. Bars represent the mean±SEM of three mice per group. Representative data from one out of at least three independent experiments are shown. ns, not statistically significant ($p \geq 0.05$); *: $p < 0.05$; **: $p < 0.01$; ***: $p < 0.001$ (1-way ANOVA followed by Bonferroni's post-test for multiple comparisons).

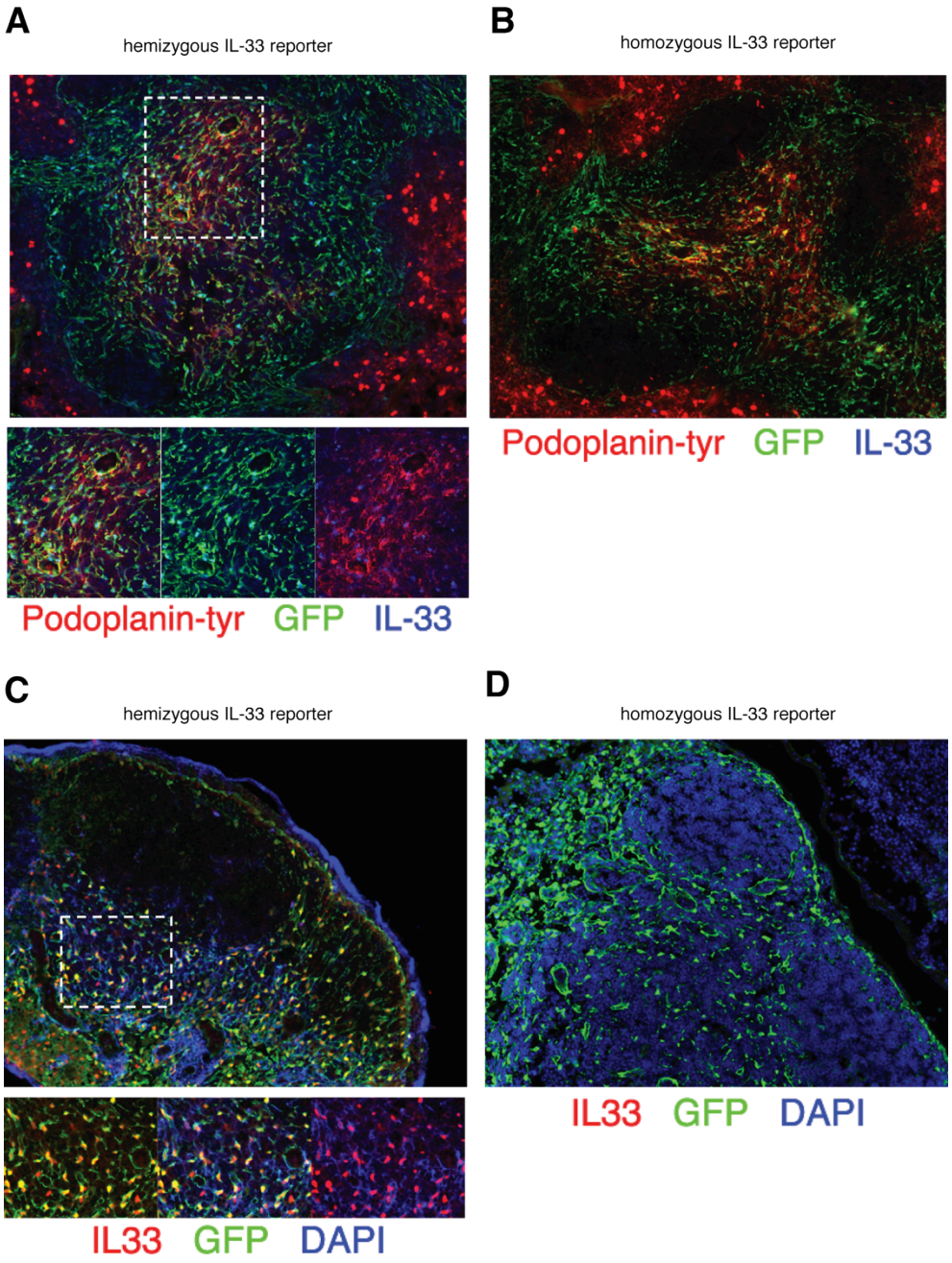

Figure 2.2: Validation of the IL-33 reporter mouse line by immunofluorescence.

Spleens of hemi- (A) or homozygous (B) IL-33 reporter mice were cut and stained for Podoplanin (gp38) and IL-33 and co-staining of the IL-33 specific stain with the IL-33 reporting GFP signal of the reporter mice was analyzed by immunohistochemistry. Analogously sections of lymph nodes of hemi- (C) and homozygous (D) IL-33 reporter mice were stained with DAPI and an IL-33 specific antibody and analyzed by immunofluorescence. The sections shown are representative of at least three animals.

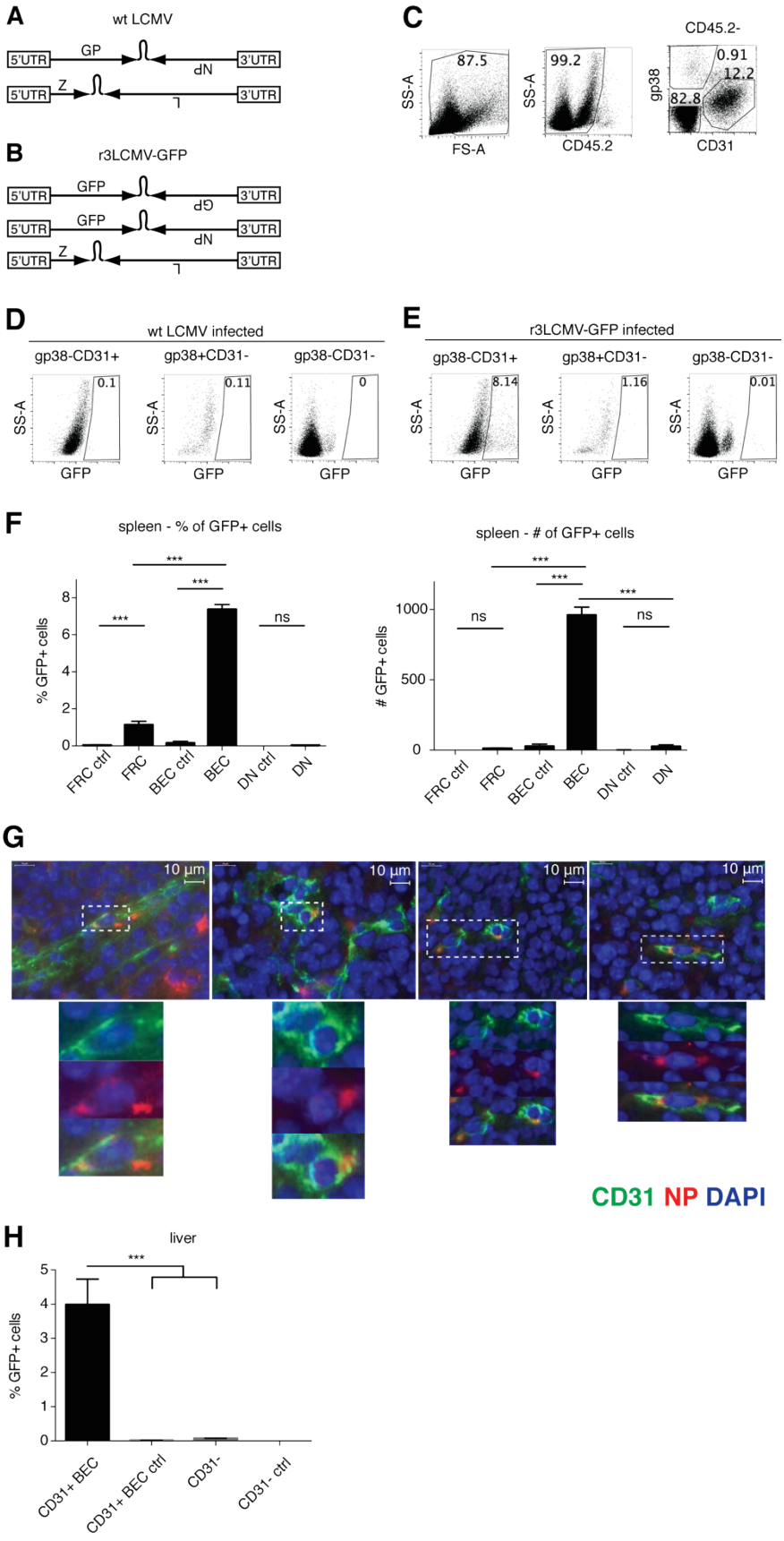

Figure 2.3: Blood endothelial cells are the primary stromal cell type infected by LCMV.

(A-B) Schematic representation of the genomic organization of wild-type LCMV (wt LCMV; A) and tri-segmented GFP-encoding LCMV (r3LCMV-GFP; B). The bi-segmented genome of wild-type LCMV consists of one S segment encoding for the glycoprotein GP and nucleoprotein NP and one L segment encoding for the matrix protein Z and the viral polymerase L (A). The genome of tri-segmented LCMV (r3LCMV) consists of one L and two S segments with two copies of GFP inserted into each one of the S segments (B). (C-F) We infected C57BL/6 mice i.v. with $5x10^5$ PFU of wild-type LCMV (D) or r3LCMV-GFP (E), isolated splenic stromal cells by collagenase digestion three days after infection and analyzed them by flow cytometry. The gating strategy for the identification of the three splenic stromal cell subsets (FRC: gp38+CD31-; BEC: gp38-CD31+; DN: gp38-CD31-) is depicted in (C). (D-E) Representative FACS plots of the GFP expression profile of each stromal cell population for one wild-type LCMV infected mouse (D) and one r3LCMV-GFP infected mouse (E). (F) Quantification of the percentage (left panel) and the total amount of GFP+ cells per spleen (right panel) within each stromal cell type in the spleen of r3LCMV-GFP-infected mice (wt LCMV infected mice as ctrl). (G) Spleens of mice infected with $5x10^5$ PFU of wild-type LCMV were stained for CD31 (green) and the LCMV nucleoprotein (NP; red) and sections were analyzed by immunofluorescence. Representative sections are shown in (G). Uninfected organs were used as negative control (data not shown). (H) Liver stromal cells were obtained by collagenase digestion of the organ and the resulting single cell suspension was analyzed by flow cytometry. Stromal cells were classified as CD31+gp38- BECs or CD31- stromal cells and the percentage of GFP+ cells was quantified. Mice infected with wild-type LCMV served as negative controls. Bars represent the mean±SEM of four mice per group. Representative data from one out of at least two independent experiments are shown. ns, not statistically significant ($p \geq 0.05$); ***: $p < 0.001$ (1-way ANOVA followed by Bonferroni's post-test for multiple comparisons).

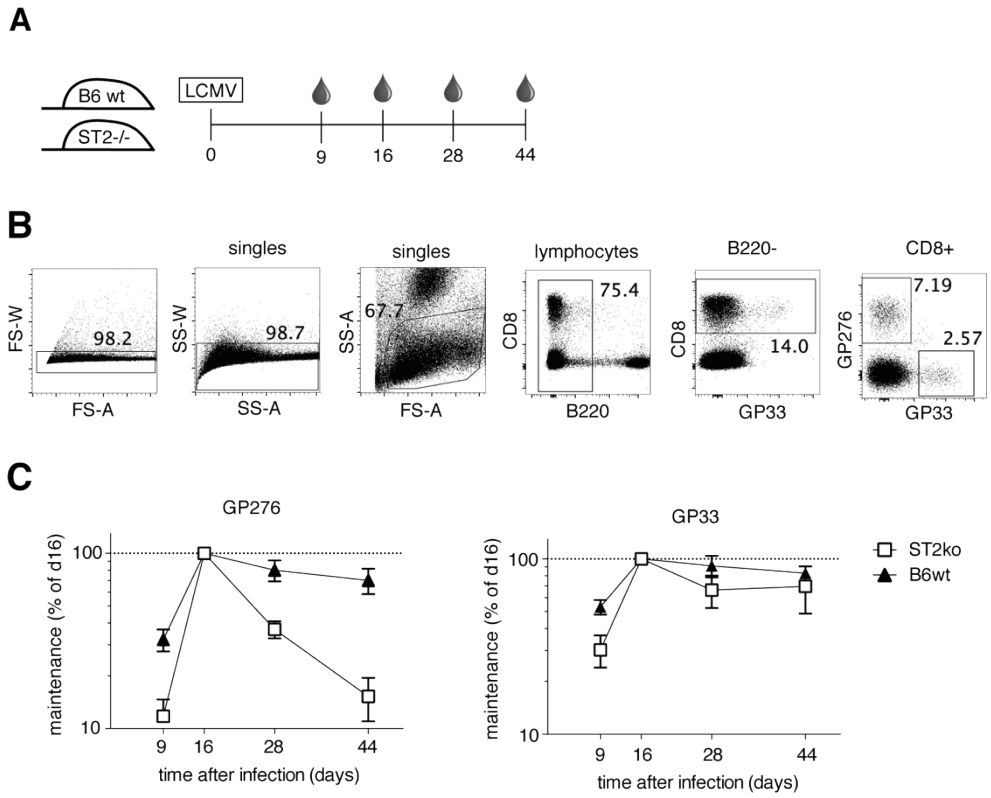

Figure 2.4: Virus-specific CD8+ T cells are depleted during chronic LCMV infection in ST2-deficient mice.

(A-C) We infected C57BL/6 wt (black triangles) or ST2-/- (white squares) mice i.v. with $2x10^6$ PFU LCMV Clone 13 and took blood on the indicated time points after infection (A). Blood was stained for virus-specific CD8+ T cells by specific tetramer-staining for the LCMV epitopes GP276 and GP33 and the frequency of LCMV-specific CD8+ T cells was analyzed according to the gating strategy outlined in (B). (C) The frequency of virus-specific CD8+ T cells was analyzed by calculating the percentage of GP276+ or GP33+ T cells within the CD8+ T cell pool and is expressed as maintenance (% of d16), by normalizing the respective Tetramer+ percentages to the value obtained on day 16. Symbols and bars represent the mean±SEM of 4-5 mice per group. Representative data from one out of two independent experiments are shown.

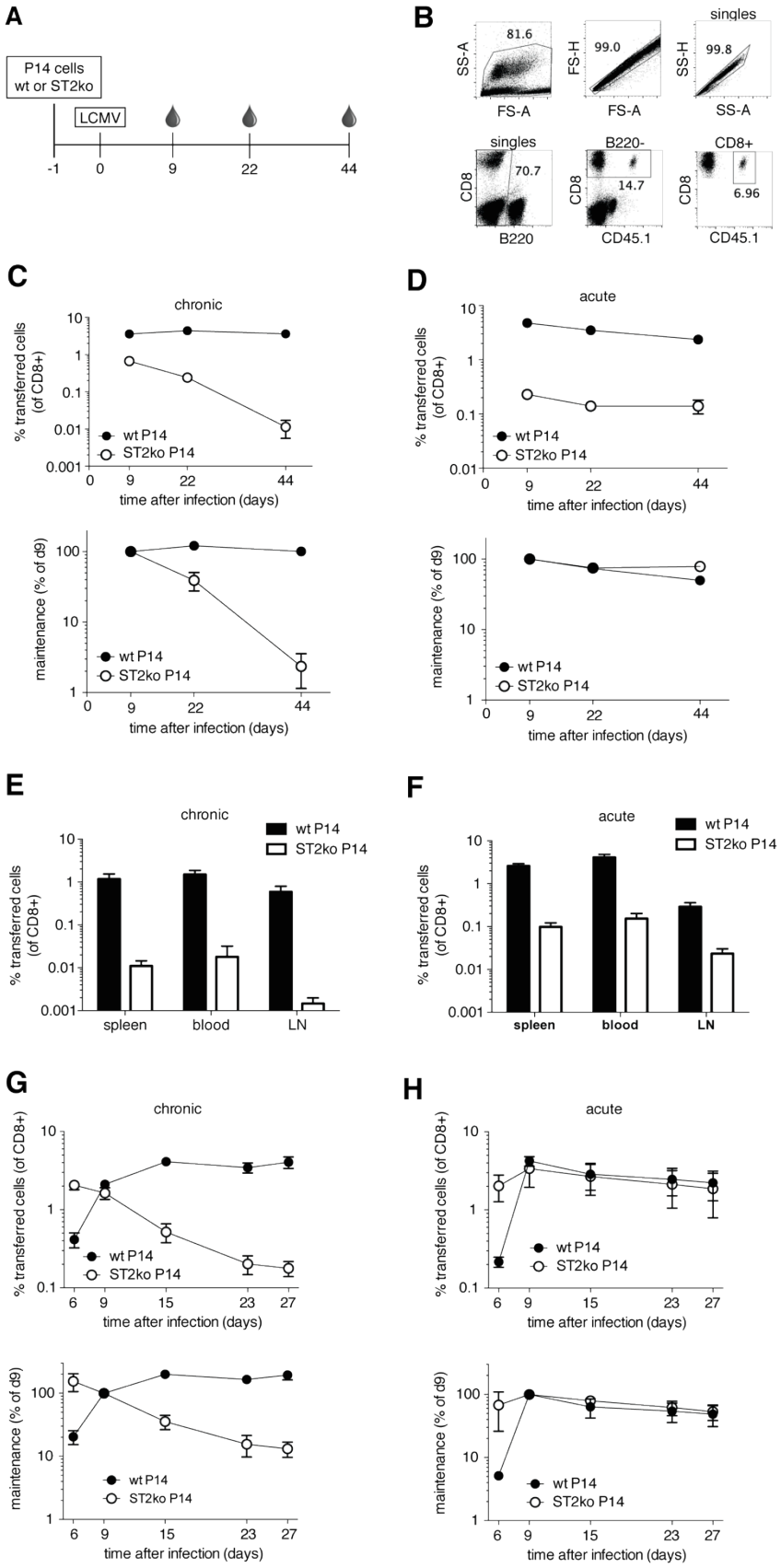

Figure 2.5: CTL-intrinsic signaling via ST2 is crucial for the maintenance of virus-specific CD8+ T cells during chronic viral infection.

(A) Adoptive transfer of 500 wild-type (wt) or ST2-deficient (ST2ko) P14 cells into C57BL/6 mice was followed by i.v. infection with either $2x10^6$ PFU LCMV Clone 13 (chronic) or 200 PFU LCMV WE (acute) one day later. Blood was taken at indicated time points and analyzed by flow cytometry. Transferred P14 cells were identified by CD45.1 expression following the gating strategy displayed in (B). Quantification of wild-type P14 cells (black circles) or ST2ko P14 cells (white circles) after chronic (C) or acute (D) infection are displayed either as percentage of transferred cells of the total CD8+ T cell pool (gated on single B220-CD8+ cells, upper panels) or as "maintenance" after normalization to values obtained on day 9 after infection (lower panels). Symbols and bars represent the mean±SEM of four mice per group. Representative data from one out of three independent experiments are shown. (E-F) Blood, spleen and lymph nodes were taken 23 days after infection with LCMV and frequencies of transferred cells in the organs after chronic (E) or acute (F) infection were analyzed by flow cytometry with gating as outlined in (B). The percentage of transferred cells within the CD8+ cell population was analyzed for each organ. Bars represent the mean±SEM of five mice per group. Representative data from one out of two independent experiments are shown. (G-H) To compensate for the defective expansion of ST2ko P14 cells in the early phase of infection, we transferred 500 wt (black circles) or 5000 ST2ko P14 cells (white circles) and infected the mice one day later with either $2x10^6$ PFU LCMV Clone 13 (chronic; G) or 200 PFU LCMV WE (acute; H). Blood samples were taken at indicated time points after infection and analyzed by flow cytometry with gating analogous to (B). Expansion and maintenance of transferred cells is displayed as percentage of transferred cells within the total CD8+ T cell pool (gated on B220-CD8+ cells; upper panels) or as maintenance as of day 9 by normalizing the percentage of transferred cells within the CD8+ cells to the value obtained on day 9 after infection (lower panels). Symbols and bars represent the mean±SEM of five mice per group.

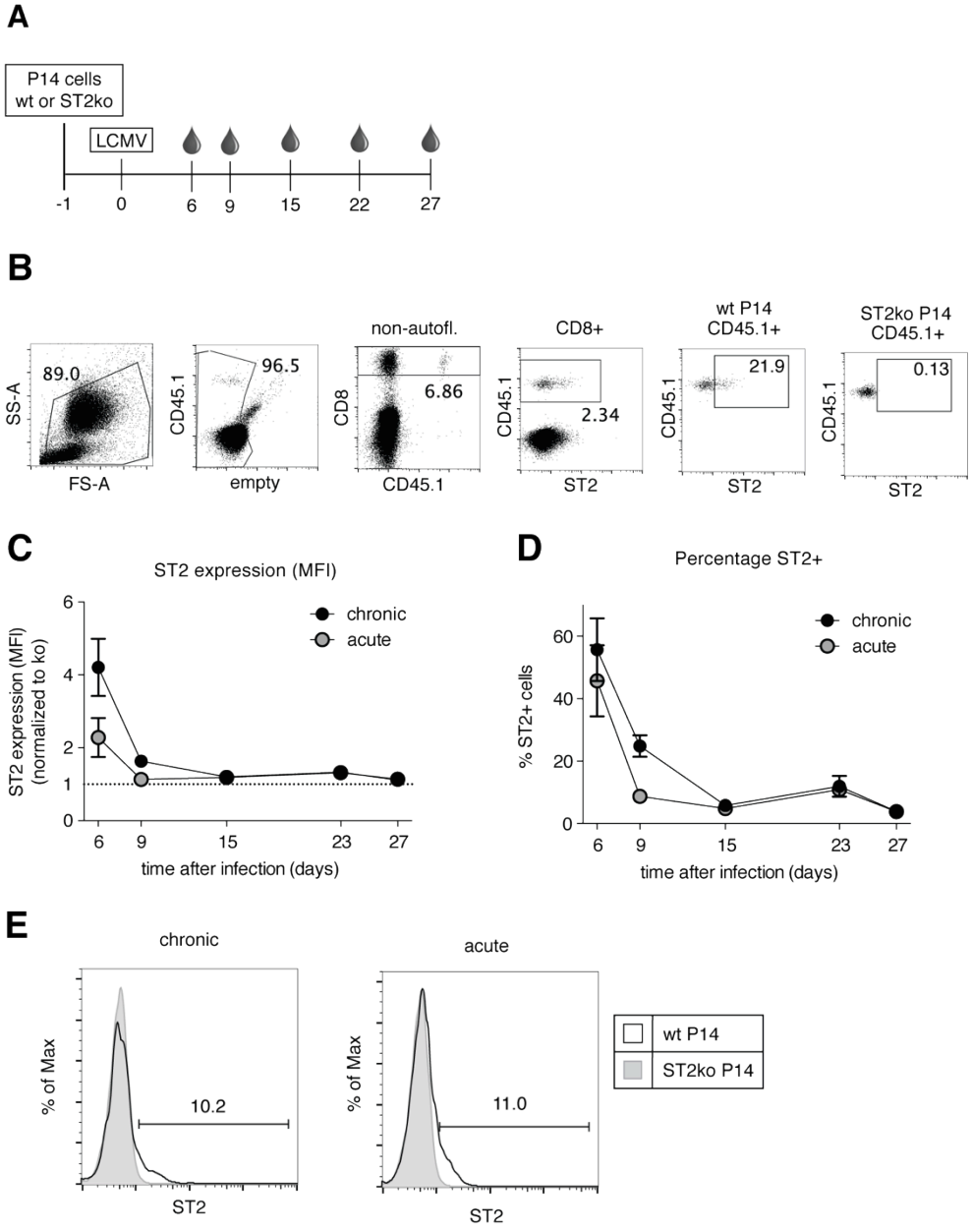

Figure 2.6: Expression of ST2 on the surface of virus-specific CD8+ T cells is continuously detectable until at least day 27 after infection on a subset of cells.

We transferred 500 wt or ST2-deficient (ST2ko) P14 cells into C57BL/6 recipients and infected them one day later i.v. with $2x10^6$ PFU LCMV Clone 13 (chronic) or 200 PFU LCMV WE (acute). Blood was taken at indicated time points after infection (A) and the expression of ST2 on the surface of transferred cells was analyzed by flow cytometry according to the gating strategy outlined in (B). Expression of ST2 on the surface of wild-type P14 cells was analyzed both as mean fluorescence intensity ("MFI"; C) and as percentage of transferred cells positive for ST2 (D) after chronic (black circles) or acute infection (grey circles). (C) The MFI of ST2 was normalized to the background intensity of ST2ko P14 cells, which was arbitrarily set to 1 on the respective time points after infection. Symbols and bars represent the mean±SEM of five mice per group. Two representative histograms of ST2 expression on the surface of wt P14 (black line) or ST2ko P14 (grey shade) on day 23 after chronic or acute infection are shown in (E).

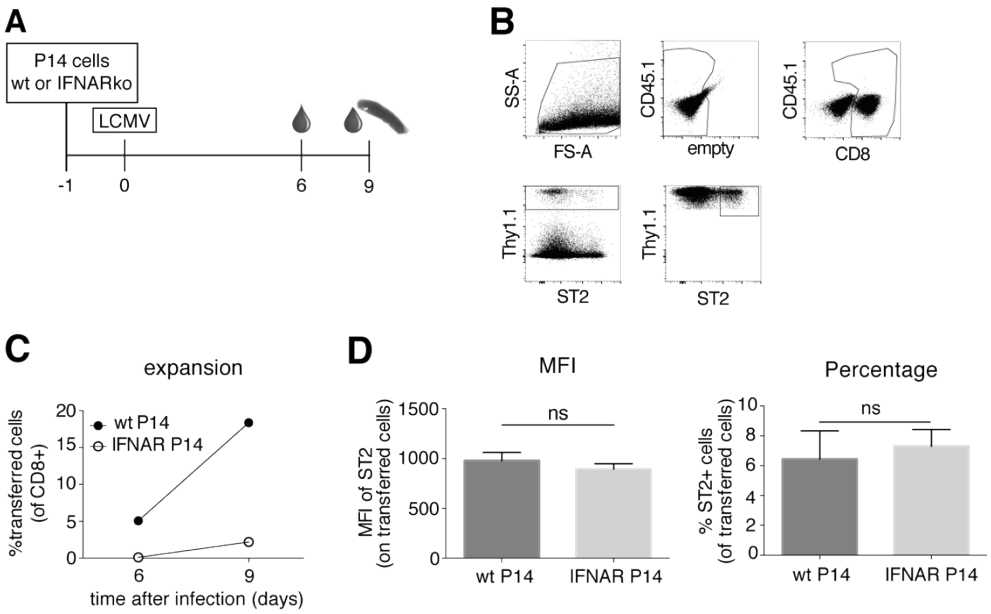

Figure 2.7: Signaling via IFNAR does not account for for the up-regulation of ST2 on the surface of virus-specific CD8+ T cells after LCMV infection.

(A) We transferred $1.5x10^3$ wt or IFNAR-/- P14 cells into C57BL/6 recipients and infected them one day later with 200 PFU LCMV-WE. Blood was taken at indicated time points after infection and the spleen was isolated 9 days after infection. The frequency of transferred cells in the blood and the expression of ST2 on the surface of transferred cells in the spleen was analyzed by flow cytometry according to the gating strategy outlined in (B). (C) The expansion of wt (black circles) or IFNAR-/- P14 cells (empty circles) in the blood was analyzed as percentage of transferred cells of the total CD8+ T cell pool. (D) ST2 expression on the surface of virus-specific CD8+ T cells in the spleen was quantified as mean fluorescence intensity of the ST2 signal on transferred cells (left panel) or the percentage of ST2+ cells within the transferred cells (right panel).

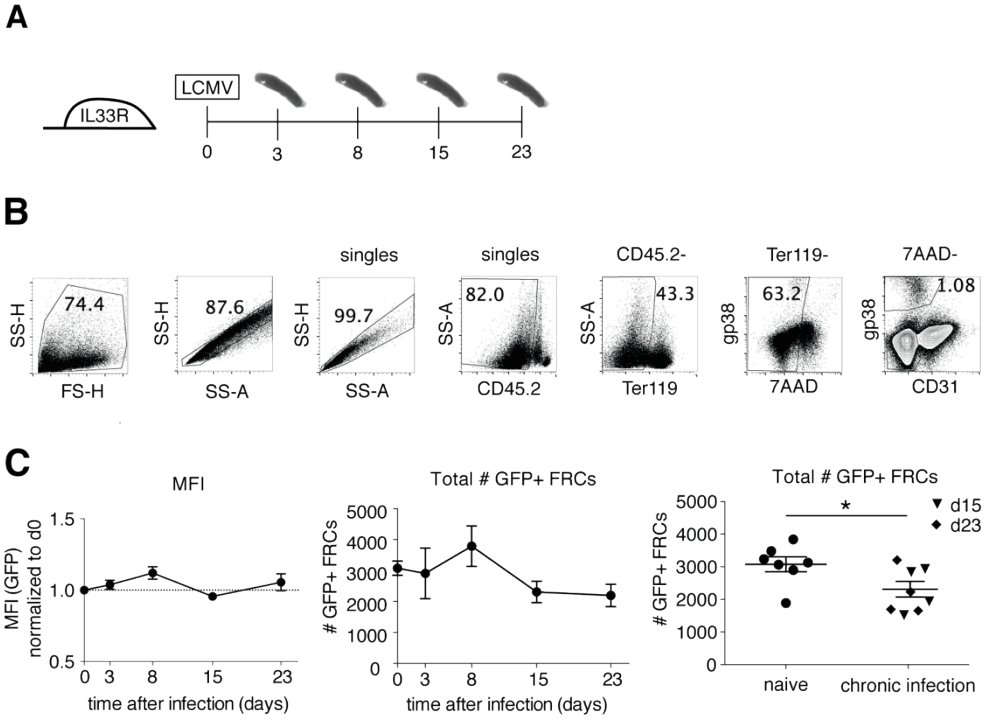

Figure 2.8: IL-33 reporter mice show a slight increase of IL-33 expressing FRCs early after chronic LCMV infection and a reduction thereafter.

(A) We infected hemizygous IL-33 reporter mice i.v. with $2x10^6$ PFU LCMV Clone 13 and isolated splenic stromal cells on different times after infection. Spleen stroma was isolated by collagenase-digestion and was further analyzed by flow cytometry. The three stromal cell populations FRCs (gp38+CD31-), BECs (gp38-CD31+) and DN (gp38-CD31-) were identified by gating out doublets and CD45.2+Ter119+7AAD+ cells as outlined in (B). FRCs were the only cell population showing detectable GFP signals and MFI of GFP+ FRCs as well as the total number of GFP+ FRCs per spleen on different time points after chronic infection are shown in (C). Symbols and bars represent the mean±SEM of three mice per group. *: $p < 0.05$ (unpaired student's t test).

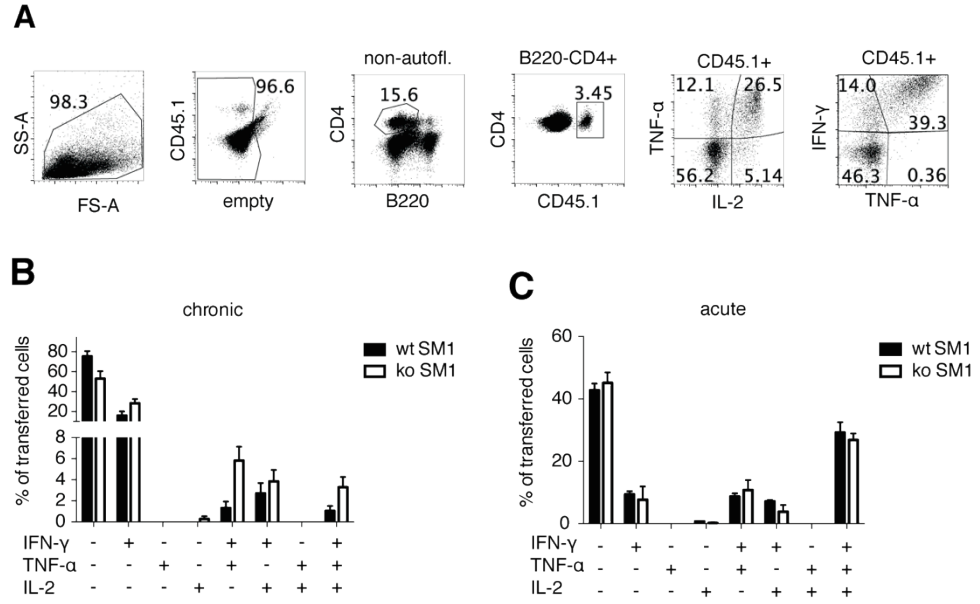

Figure 2.9: Virus-specific CD4+ T cells deficient of ST2 are fully functional during viral infection.

We adoptively transferred 500 wt or ST2-deficient (ST2ko) SM1 cells into C57BL/6 recipients and infected them i.v. with $2x10^6$ PFU LCMV Clone 13 (chronic) or 200 PFU LCMV WE (acute) on the day after. Spleens were taken 14 days after infection and the functionality of the transferred LCMV-specific CD4+ T cells was analyzed by flow cytometry. The gating strategy is outlined in (A). (B) and (C) show the cytokine profile (IFN-γ, TNF-α and IL-2) of the transferred wt (black bars) or ST2ko (white bars) SM1 cells after chronic (B) or acute (C) infection. Symbols and bars represent the mean±SEM of five mice per group.

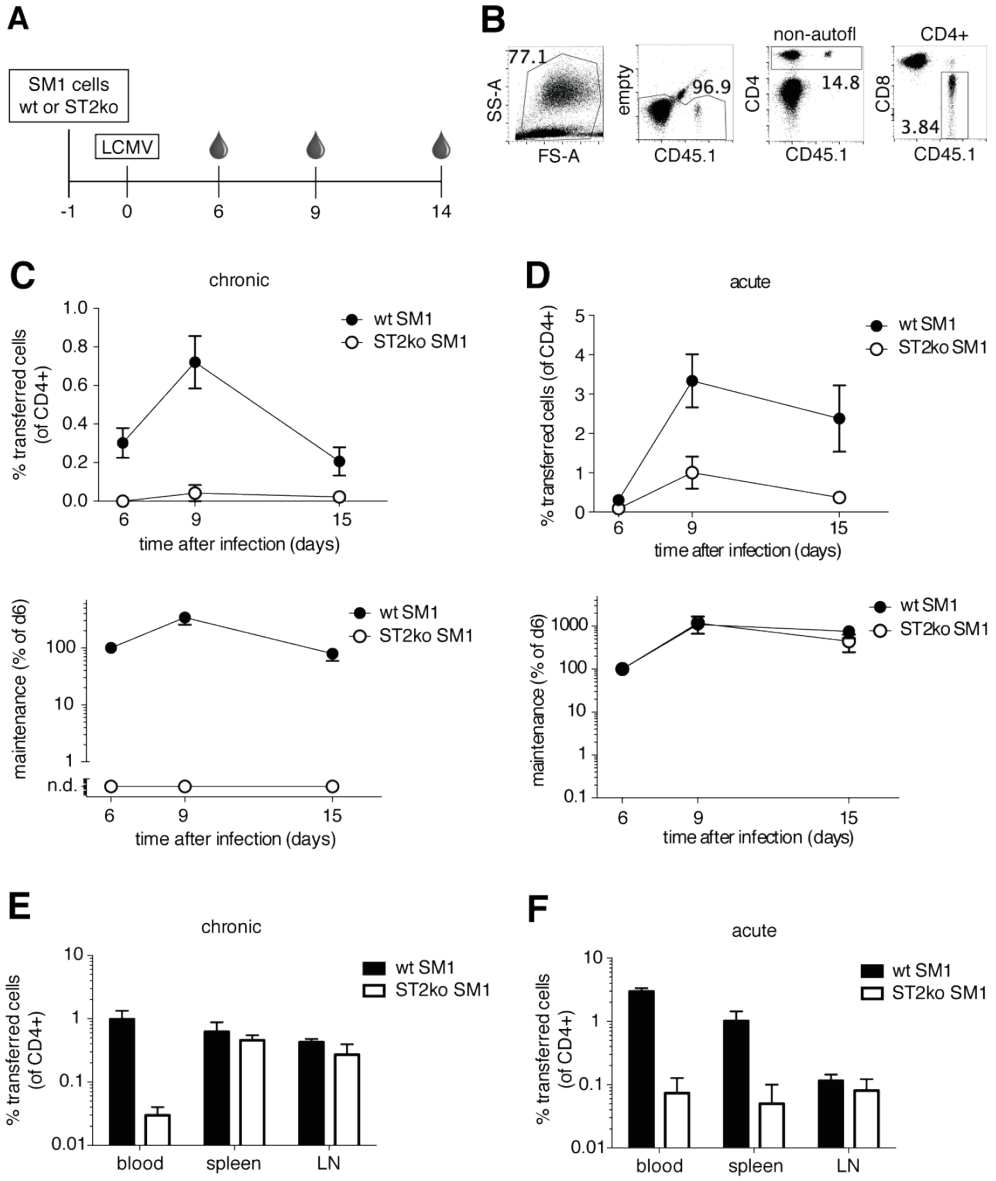

Figure 2.10: ST2-deficiency in virus-specific CD4+ T cells alters the tissue distribution and impairs recirculation of cells in the bloodstream.

(A) 500 wt or ST2ko SM1 cells were adoptively transferred into C57BL/6 mice followed by i.v. infection with $2x10^6$ PFU LCMV Clone 13 (chronic) or 200 PFU LCMV WE (acute) one day later. Blood was taken at the indicated time points after infection and the frequency of transferred cells was analyzed by flow cytometry following the gating strategy outlined in (B). Frequency of wt (black circles) and ST2ko (white circles) SM1 cells after chronic (C) and acute (D) infection is expressed as percentage of CD4+ T cells (upper panels) or maintenance normalized to values obtained 6 days after infection (in percent; lower panels). Symbols and bars represent the mean±SEM of 3-5 mice per group. Representative data from one out of at least three independent experiments are shown. (E-F) Blood, spleen and lymph nodes of the mice were taken 16 days after chronic (E) or acute (F) infection and frequencies of transferred wt (black bars) or ST2ko SM1 cells (white bars) were analyzed by flow cytometry (gating analogous to (B); n.d. not determined). Symbols and bars represent the mean±SEM of 3-5 mice per group. Representative data from one out of at least three independent experiments are shown.

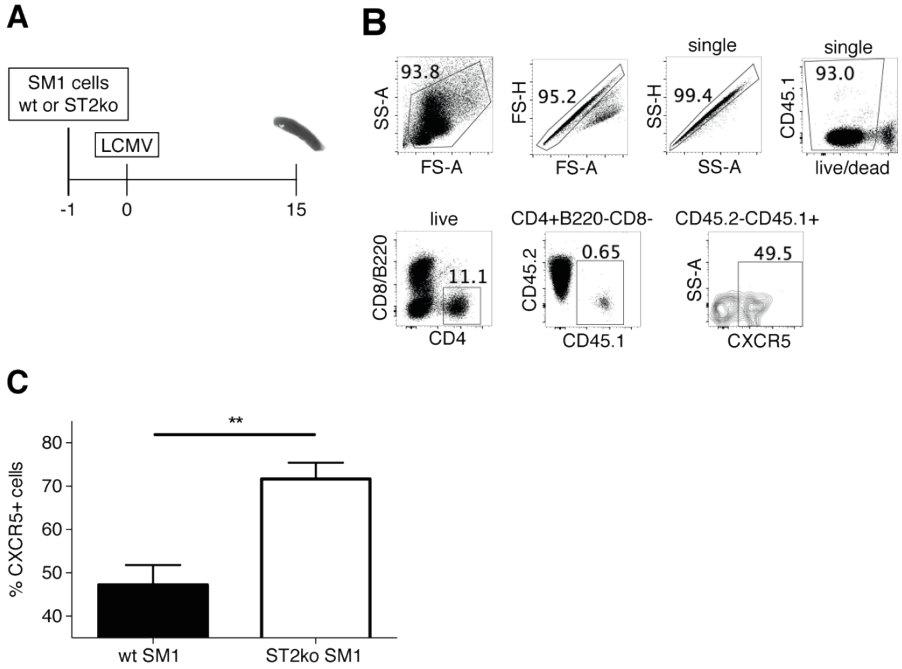

Figure 2.11: ST2-deficient virus-specific CD4+ T cells show higher expression of a typical marker for T follicular helper cells.

(A) We adoptively transferred 500 wt or ST2ko SM1 cells i.v. into C57BL/6 recipients and infected them one day later with $2x10^6$ PFU LCMV Clone 13. 15 days after infection the Tfh phenotype of transferred cells in the spleen was analyzed by flow cytometry with staining for CXCR5 (gating strategy shown in (B)). The percentage of CXCR5+ cells within the transferred cell population was quantified (C). Bars represent the mean±SEM of five mice per group. Representative data from one out of two independent experiments are shown. **: $p < 0.01$ (unpaired student's t test).

3 Engineering of Genetically and Phenotypically Stable Transgene Expressing tri-segmented LCMV

3.1 Summary

Several members of the family arenaviridae can cause viral hemorrhagic fever when transmitted to humans. Except for Junin virus, preventive vaccines are not available and strategies to stably attenuate arenaviruses remain to be refined. Using lymphocytic choriomeningitis virus (LCMV), the prototypic arenavirus, several key concepts of arenavirus molecular biology have been unraveled. The virus' utility for studies on antiviral immunity, notably in persistent infection, but also its potential as vaccine delivery system has created considerable interest in strategies how to stably accommodate transgenes in the bi-segmented viral RNA genome. The large (L) segment expresses the viral RNA-dependent RNA polymerase (RdRp) L and the matrix protein Z in an ambisense coding strategy. Analogously, the short (S) segment encodes for the nucleoprotein NP and the glycoprotein GP. It had previously been shown that foreign genes of interest can be introduced in the genome of replication-competent LCMV by generating tri-segmented viruses with one L and two S segments. According to this strategy, each of the two S segments carries only either NP or GP in their respective natural positions and one gene of interest in each of the resulting free spaces (r3LCMV^{nat}). Here we demonstrate that such tri-segmented viruses show impaired growth both in vitro and in vivo owing to preferential packaging of only one instead of two S segments, thus producing replication-deficient bi-segmented viral particles in excess. The selection pressure created by this attenuation favors the selection of emerging variants that have recombined their two S segments, resulting in phenotypic reversion to wild-type virus and transgene loss. Sequence analysis of such recombined RNA species revealed a pattern consistent with a copy-choice mechanism of the RdRp, putatively after pausing at an RNA hairpin structure, which facilitates template-switch. Accordingly, we demonstrate that transposition of the GP ORF, artificially positioning it under transcriptional control of the NP promoter (r3LCMV^{art}), prevented the emergence of recombined genomes. r3LCMV^{art} exhibited stable transgene expression and reduced viremia for >100 days of systemic persistent infection in immune-deficient mice.

This work provides experimental evidence for inter-segmental recombination as a previously postulated mechanism of arenavirus evolution. The resulting r3LCMV^{art} re-engineering strategy offers reliable transgene expression and stable attenuation, thus critically augmenting its utility for basic research as well as for clinical use in vaccination and immunotherapy of infectious disease and cancer.

3.2 Introduction

When accidentally transmitted to humans, several members of the Arenaviridae family can cause viral hemorrhagic fever associated with significant mortality (Geisbert and Jahrling 2004), representing a serious concern for public health in the concerned areas. Numerous arenaviruses can be found in rodent populations around the world. In addition to the Old World arenavirus Lassa virus (LASV), which can be found in Africa, several New World arenaviruses like Junin or Machupo are prevalent in rodents in South America (Johnson, Kuns et al. 1966, Tesh, Wilson et al. 1993, Mills, Ellis et al. 1994). Except for Junin virus, preventive vaccines remain unavailable for clinical use and anti-viral therapy is limited to the nucleoside analog ribavirin. Thus there is considerable interest in developing new vaccines and treatments for arenaviral infections. This in turn requires a better understanding of the molecular biology of the virus and of the viral determinants that are shaping viral pathogenesis.

In order to shed light on these questions, transgenic arenaviruses are extensively used and hold great promise for basic research and the vaccine field. Recombinant arenaviruses encoding additional genes of interest serve as reporter viruses or as a tool to study the function of select viral proteins in the viral life cycle. In the vaccine field transgenic arenaviruses could be used as live-attenuated viruses analogously to a Mopeia/LASV reassortant in the fight against LASV (Lukashevich, Patterson et al. 2005). Similarly, by exchanging the glycoprotein (GP) for an unrelated GP, as reported for vesicular stomatitis virus (VSV) (Bergthaler, Gerber et al. 2006), arenaviruses can be attenuated in a directed fashion. Recombinant arenaviruses also allow for the generation of replication-deficient vaccine vectors by replacing GP with a vaccine antigen. The resulting vector elicits T cell responses and protective neutralizing antibodies to the vaccine antigen but not against the vector itself, enabling efficient homologous boosts (Flatz, Hegazy et al. 2010).

Since its recovery entirely from plasmid (Flatz, Bergthaler et al. 2006, Sanchez and de la Torre 2006), LCMV, the prototypic model virus in arenavirus research, became a very interesting candidate for vaccine development. Many of its characteristics make it a promising vector for vaccine design. Firstly, LCMV elicits a broad and long-lived T cell response (Homann, Teyton et al. 2001), which is a prerequisite for the induction of potent cellular immunity. Secondly, LCMV has a strong tropism for DCs and activates them upon infection, thus enabling presentation of the antigen by professional antigen-presenting cells. Infection and activation of DCs has been shown to be crucial for potent

CD8+ T cell responses (Probst, Lagnel et al. 2003, Steinman 2007). Thirdly, LCMV induces low neutralizing antibodies against LCMV GP but high protective neutralizing antibody responses to foreign transgenes, which is suitable with homologous boost strategies and supports its potential as a vaccine vector in humans (Pinschewer, Perez et al. 2004).

LCMV is an enveloped non-cytolytic virus with a cytoplasmic life cycle. Upon entry into the host cell subgenomic mRNAs are transcribed from the genome and replicative intermediates by the viral polymerase. The LCMV genome consists of two segments of single-stranded RNA of negative strand (L: 7.2 kb, S: 3.4 kb). Each segment encodes for two viral genes in opposite orientations. The short segment (S segment) encodes the GP precursor (GP-C; 75 kDa) and the nucleoprotein (NP; 63 kDa) (Salvato, Shimomaye et al. 1988). The long segment (L segment) expresses the RNA-dependent RNA polymerase (RdRp; L; approx. 200 kDa) and the matrix protein Z (11 kDa) (Fig. 3.1A) (Salvato, Shimomaye et al. 1989, Salvato and Shimomaye 1989). GP-C is post-translationally cleaved into GP-1 and GP-2 (Buchmeier and Oldstone 1979). Trimers of GP-1 and GP-2 are assembled as spikes on the surface of virions and mediate entry into host cells. NP binds to the viral RNA, forming the nucleocapsid (NC), which serves as a template for the viral RdRp. The nucleocapsid associated with the viral polymerase L forms the so-called ribonucleoprotein (RNP) complex, which is active both in replication and transcription and represents the minimum unit of viral infectivity. It has been shown that NP and L are the minimal trans-acting factors necessary for viral RNA transcription and replication (Lee, Novella et al. 2000). The two genes on each segment are separated by a non-coding intergenic region (IGR) and are flanked by 5' and 3' untranslated regions (UTR). The IGR forms a stable hairpin structure and is involved in structure-dependent termination of viral mRNA transcription (Pinschewer, Perez et al. 2005). The terminal nucleotides of the UTR show a high degree of complementarity and form secondary structures. These panhandles serve as the viral promoter for transcription and replication and their analysis by site-directed mutagenesis has revealed sequence- and structure-dependence, tolerating not even minor sequence changes (Perez and de la Torre 2003).

The generation of recombinant negative-stranded RNA viruses expressing foreign genes has been pursued for a long time. Several strategies have been published for other viruses (Garcia-Sastre, Muster et al. 1994, Percy, Barclay et al. 1994, Flick and Hobom 1999, Machado, Naffakh et al. 2003), but only one approach, namely the generation of a tri-segmented genome, has proven successful for LCMV (Emonet, Garidou et al. 2009). Two

foreign genes were inserted into the bi-segmented genome of LCMV, resulting in tri-segmented LCMV particles (r3LCMV) with two S and one L segment. Each of the S segments was reengineered and one of the foreign genes inserted at the GP position of one S segment and the second foreign gene inserted at the NP position of the other S segment (Fig. 3.1B). Recombinant tri-segmented LCMVs have been rescued and are viable both in vitro and in vivo (Emonet, Garidou et al. 2009, Popkin, Teijaro et al. 2011).

The polymerase of RNA viruses lacks proofreading activity and thus introduces mutations during replication (Holland, Spindler et al. 1982, Duffy, Shackelton et al. 2008). However, RNA viruses increase their evolutionary potential not only through mutations but also through exchange of genetic material amongst each other, called recombination (Worobey and Holmes 1999). Recombination is a fairly common event in positive-sense (PS) RNA viruses (Cooper, Purchase et al. 1974, Hahn, Lustig et al. 1988, Lai 1992, Holmes, Worobey et al. 1999, Mikkelsen and Pedersen 2000). Negative-sense (NS) RNA viruses are generally thought not to recombine at all or only sporadically (Chare, Gould et al. 2003), but several events have been documented in recent years, notably for hantavirus (Sibold, Meisel et al. 1999, Sironen, Vaheri et al. 2001, Klempa, Schmidt et al. 2003) and for the arenavirus Whitewater Arroyo Virus (Charrel, de Lamballerie et al. 2001, Archer and Rico-Hesse 2002). More evidence for recombination in NS RNA viruses was found by artificial generation of recombined variants in vitro (Plyusnin, Kukkonen et al. 2002, Spann, Collins et al. 2003). Recombination between two lineages of NS RNA viruses was furthermore confirmed by phylogenetic analysis of the filovirus Zaire ebolavirus (Wittmann, Biek et al. 2007). Taken together, this shows that intersegmental exchange of genetic information between RNA strands is a rare but occurring event in PS as well as segmented and non-segmented NS RNA viruses, increasing the evolutionary flexibility of these viruses. Especially in the light of potential application in vaccination recombination of recombinant LCMV has to be excluded at best before use of recombinant viruses for research and notably clinical application.

We developed a novel molecular design of tri-segmented transgenic r3LCMV (r3LCMV^{art}) in which reshuffling of the GP-encoding S segment with expression of the GP from the 3'UTR prevented the emergence of recombined bi-segmented genomes during persistent infection. The newly developed r3LCMV^{art} exhibited stable transgene expression and attenuated viremia for more than 100 days of persistent infection. Both features are critical for human clinical use and recommend r3LCMV^{art} for safe vaccine delivery in infectious disease and cancer.

3.3 Material and Methods

3.3.1 Cells

BHK-21 cells were cultured in high-glucose Dulbecco's Eagle medium (DMEM; Sigma) supplemented with 10 % heat-inactivated fetal calf serum (FCS; Biochrom), 10 mM HEPES (Gibco), 1 mM sodium pyruvate (Gibco) and 1x tryptose phosphate broth (Sigma). MC57 cells were maintained in Minimum Essential Medium (MEM; Sigma) complemented with 5 % heat-inactivated FCS, 2 mM L-glutamine (Gibco) and penicillin-streptomycin (100'000 U/ml penicillin and 50 mg/l streptomycin; Gibco). Both cell lines were cultured at 37 °C in a humidified 5 % CO_2 incubator.

NP-expressing BHK-21 cells were generated by transfecting BHK-21 cells with a plasmid expressing NP under the control of the eukaryotic EF1-alpha promoter and encoding the puromycin resistance gene according to the manufacturer's protocol. 48 hours after transfection, 4 µg/ml puromycin was added to the medium. Another 48 hours later, cells were passaged into T150 flasks. Once separate clones became visible, cells were harvested and serially diluted into a 96-well plate to obtain single clones. Wells were checked optically for the growth of cell populations from single clones and respective cells were passaged into 6-well plates once they formed a confluent monolayer. NP-expressing BHK-21 cells were cultured in BHK-21 medium in the presence of 4 µg/ml puromycin.

GP-expressing BHK-21 cells have previously been described (Flatz, Hegazy et al. 2010). Briefly, BHK-21 cells were stably transfected with a plasmid that expresses a codon-optimized LCMV-GP cDNA and the puromycin resistance cassette (Matter, Pavelic et al. 2007). GP-expressing clones were selected by the addition of 4 µg/ml puromycin to the medium and single clones were obtained by serial dilutions as described for the NP-expressing BHK-21 cells.

3.3.2 Plasmids

The pol-I L, pC-NP and pC-L plasmids have previously been described (Flatz, Bergthaler et al. 2006). For the generation of pol-I S plasmids encoding for GFP or RFP as reporter genes and either NP or GP, we used a pol-I Bbs/Bsm cloning plasmid as a basis (pol-I 5'-BsmBI_IGR_BbsI_3'). This plasmid encodes for the 5' untranslated region (5' UTR) of the viral S segment followed by two BsmBI restriction sites, the intergenic region (IGR),

an NP rest and CAT open reading frame (ORF) flanked by BbsI restriction sites and the 3' UTR of the S segment. The pol-I S plasmids encoding for GP in its natural 5' and GFP in antisense orientation at the 3' position (pol-I 5'-GFP_IGR_GP-3') were cloned by inserting GP by BsmBI site-specific restriction and ligation into the pol-I Bbs/Bsm plasmid. In a second step GFP was inserted by BbsI digestion and ligation. In order to obtain pol-I S plasmids encoding for GP in the artificial 3' orientation (pol-I 5'-GFP_IGR_GP-3'), GP was inserted by BbsI digest at the 3' position into the pol-I Bbs/Bsm plasmid and GFP with BsmBI restriction/ligation at the 5' position. pol-I S encoding for GFP or RFP and NP (pol-I 5'-GFP_IGR_NP-3' or pol-I 5'RFP_IGR_NP-3') were cloned by inserting NP instead of GP by BbsI digestion and ligation into the pol-I Bbs/Bsm cloning plasmid and GFP or RFP by BsmI cloning. The pol-I plasmid with GP of LCMV strain WE and NP of LCMV strain Clone 13 (Cl13) were cloned by inserting the respective genes by Bbs and Bsm site-specific restriction/ligation at the respective sites in the pol-I Bbs/Bsm cloning plasmid.

The S segment encoding for the WE/WET fusion GP was obtained by replacing the last 255 base pairs of the WE ORF with a codon-optimized sequence named "WET". This was achieved by PCR amplifying in a first step a fragment of WE GP with one WE specific primer (5'-AATCGTCTCTAAGGATGGGTCAGATTGTGACAATG-3') and a WE specific fusion-primer carrying an overhang complementary to the WET sequence (5'-AATCGTCTCTAAGGATGGGTCAGATTGTGACAATG-3'). In parallel the WET sequence was amplified by PCR using a WET-specific primer (5'-CTCGGTGATCATGTTATCTGCTTCTTGTTCGATTTGA-3') and a WET-specific fusion-primer complementary to the WE sequence (5'-AATCGTCTCTTTCTTTATCTCCTCTTCCAGATGG-3'). In a third PCR reaction the two PCR products were fused by PCR fusion using the two mentioned fusion-primers. The resulting WE/WET fusion fragment was digested with BsmBI and ligated into a pol-I BsmBI_IGR_GFP-3' plasmid that had been digested with the same restriction enzyme.

The pol-I plasmid encoding for the recombined S segment of the in vivo recombined virus r3LCMV-GFP^{nat} #3 was cloned by inserting the synthesized DNA fragment (done by Genscript) by site-specific restriction/ligation with SacI and XmaI into a plasmid encoding a wild-type S-segment under the control of a pol-I promoter (pol-I GP_IGR_NP) resulting in pol-I GP_IGR_GFP_IGR_NP.

3.3.3 DNA transfection of cells and rescue of recombinant viruses

BHK-21 cells were seeded into 6-well plates at a density of $4x10^5$ cells/well and transfected 24 hours later with different amounts of DNA using either lipofectamine (3 µl/µg DNA; Invitrogen) or jetPRIME (2 µl/µg DNA; Polyplus) according to the manufacturer's instructions. For rescue of recombinant bi-segmented viruses entirely from plasmid DNA, the two minimal viral trans-acting factors NP and L were delivered from pol-II driven plasmids (0.8 µg pC-NP, 1 µg pC-L) and were co-transfected with 1.4 µg of pol-I L and 0.8 µg of pol-I S. In case of rescue of tri-segmented r3LCMV consisting of one L and two S segments, 0.8 µg of both pol-I driven S segments were included in the transfection mix. 72 hours after transfection the supernatant was harvested and passaged on BHK-21 cells for further amplification of the virus. Viral titers in the supernatant were determined by focus forming assay.

3.3.4 Viruses and growth kinetics of viruses

Wild-type Cl13 LCMV, originally derived from wild-type LCMV Armstrong, has previously been described (Ahmed, Salmi et al. 1984). Stocks of wild-type and recombinant viruses were produced by infecting BHK-21 cells at a multiplicity of infection (moi) of 0.01 and supernatant was harvested 48 hours after infection. Growth curves of viruses were done in vitro in a 6-well format. BHK-21 cells were seeded at a density of 6×10^5 cells/well and infected 24 hours later by incubating the cells together with 500 µl of the virus inoculum at a moi of 0.01 for 90 minutes on a rocker plate at 37°C and 5% CO_2. Fresh medium was added and cells incubated at 37 °C/ 5 % CO_2 for 72 to 96 hours. Supernatant was taken at given time points (normally 18, 24, 48, 72 hours) and viral titers analyzed by focus forming assay.

3.3.5 Focus forming assay

Titers of LCMV are determined by focus forming assay. LCMV is a non-cytolytic virus that does not lyse its host cells and as such does not create plaques. Nevertheless units in this work will be expressed in the more commonly used term plaque forming units (PFU) instead of the correct term focus forming units (FFU). MC57 cells were used for focus forming assay if not stated otherwise. Cells were seeded at a density of $1.6x10^5$ cells per well in a 24-well plate and mixed with 200 µl of 10-fold serial dilutions of virus prepared in MEM/ 2 % FCS. After 2-4 hours of incubation at 37 °C, 200 µl of a viscous medium

(2 % Methylcellulose in 2x supplemented DMEM) were added per well to ensure spreading of viral particles only to neighboring cells. After 48 hours at 37 °C the supernatant was flicked off and cells were fixed by adding 200 µl of 4 % paraformaldehyde (PFA) in PBS for 30 minutes at room temperature (all following steps are performed at room temperature). Cells were permeabilised with 200 µl per well of BSS/ 1 % Triton X-100 (Merck Millipore) for 20 minutes and subsequently blocked for 60 minutes with PBS/ 5 % FCS. For anti-NP staining a rat anti-LCMV-NP monoclonal antibody was used as a primary staining antibody at a dilution of 1:30 in PBS/ 2.5 % FCS for 60 minutes. For anti-GFP staining purified rat-anti-GFP antibody (Biolegend 338002) was used at a dilution of 1:2000 in PBS/ 2.5 % FCS. Plates were washed three times with tap water and the secondary HRP-goat-anti-rat-IgG was added at a dilution of 1:100 in PBS/ 2.5 % FCS and incubated for 1 hour. The plate was again washed three times with tap water. The color reaction (0.5 g/l DAB (Sigma D-5637), 0.5 g/l Ammonium Nickel sulfate in PBS/ 0.015 % H_2O_2) was added and the reaction was stopped after 10 minutes with tap water. Stained foci were counted manually and the final titer calculated according to the dilution.

For anti-GP staining of cells, plates were fixed with 50 % MeOH/ 50 % Acetone for 5 minutes and washed with PBS. Blocking was done as described. As primary antibody anti-GP GP83.4 (produced from hybridomas) was diluted 1:10 in PBS/ 2.5 % FCS and incubated for 60 minutes. After three washes with tap water, the secondary HRP-rabbit-anti-mouse IgG antibody was added at a dilution of 1:50 in PBS/ 2.5 % FCS and incubated for 60 minutes. After another three washes with tap water the color reaction was added as described above.

In order to determine the viremia of mice in blood, one drop of blood (corresponding to 50 µl volume) was collected in 950 µl of BSS-heparin (Na-heparin, Braun, 1 IE/ml final), mixed by inverting and stored at -80 °C until further use.

3.3.6 Mice

AGRAG mice (IFNα/β$R^{-/-}$, IFNγ$R^{-/-}$, $RAG^{-/-}$) have previously been described (Pinschewer, Flatz et al. 2010) and were bred and housed under specific pathogen-free (SPF) conditions. They were bred at the Institut für Labortierkunde of the University of Zurich, Switzerland. All animal experiments were performed at the Universities of Geneva and Basel in accordance with the Swiss law for animal protection and the permission of the

respective responsible cantonal authorities of Geneva and Basel. Infection of the mice was done intravenously at a dose of 1×10^4 PFU per mouse.

3.3.7 Preparation of viral RNA and Sequencing

Viral RNA was extracted from cell culture supernatant or the serum of infected mice using the QIAamp Viral RNA Mini Kit (QIAGEN) according to the manufacturer's instructions. The reverse-transcription reaction was done with ThermoScript RT-PCR System (Invitrogen) and a primer specific for LCMV NP (5'-GGCTCCCAGATCTGAAAACTGTT-3') following the manufacturer's protocol. Amplification by PCR was done by using 2 µl of the cDNA from the RT step and NP- and GP-specific primers (NP-specific: same as in RT reaction, GP- specific: 5'-GCTGGCTTGTCACTAATGGCTC-3'). The PCR reaction was done using Phusion High-Fidelity DNA Polymerase (NEB). Amplified products were analyzed on and excised from a 2 % agarose gel, purified using QIAquick Gel Extraction Kit (QIAGEN) and sent for DNA Sanger Sequencing (Microsynth) using the NP- and GP-specific primers.

3.3.8 Flow cytometry

Blood was stained with antibodies against CD11c (N418), CD11b (M1/70), CD19 (6D5), NK1.1 (PK136), CD90.2 (30-H12) and GR-1 (RB6-8C5). The expression of surface molecules stained with specific antibodies as well as GFP and RFP expression was analyzed on a BD LSR Fortessa flow cytometer using FlowJo software (Tree Star, Ashland, OR).

3.3.9 Statistical analysis

Statistical significance was determined by two-tailed unpaired t test or 1-way ANOVA followed by Dunnett's or Bonferroni's post-test for multiple comparisons using Graphpad Prism software (version 6.0d). p values of $p > 0.5$ were considered not statistically significant (ns), whereas p values of $p < 0.5$ were considered significant (*) with gradations of $p < 0.1$ (**) and $p < 0.01$ (***) being highly significant.

3.4 Results

Recombinant tri-segmented viruses grow to lower titers than wild-type LCMV.

The genome of wild-type LCMV consists of two single-stranded RNA segments of negative polarity (1L, 1S) (Fig. 3.1A). In recent years it has been shown that it is possible to introduce additional foreign genes into the genome of bi-segmented LCMV particles (Emonet, Garidou et al. 2009). Genes of interest are inserted into the S segment of LCMV resulting in viral particles with three RNA segments (2S + 1L). The only currently published strategy keeps both NP and GP in their natural position in the S segment, thus placing GFP or other transgenes in the respective free sites (r3LCMV-GFP^{nat}) (Fig. 3.1B). This was the intuitive approach aimed at minimizing the likely risk that genetic reshuffling of the S segment abrogates the resulting genome's viability. However, we hypothesized that it should also be possible to juxtapose GP to the 3'UTR, expressing it from the promoter element that normally drives NP (r3LCMV-GFP^{art}; Fig. 3.1C). We generated the respective expression plasmids by recombinant cDNA cloning and rescued all three viral constructs entirely from plasmid DNA (for details see Materials and Methods, (Flatz, Bergthaler et al. 2006) and (Emonet, Garidou et al. 2009). We performed comparative growth curves with the three viruses (Fig. 3.1D). All three viruses showed highest titers 48 hours after infection, with peak titers of tri-segmented viruses 10-100 fold lower than wild-type virus. Wild-type LCMV reached 3.4×10^6 PFU/ml, r3LCMV-GFP^{nat} peaked at 2.7×10^4 PFU/ml and r3LCMV-GFP^{art} at 2.2×10^5 PFU/ml. Irrespective of its similarly reduced peak titers, r3LCMV-GFP^{nat} exhibited somewhat higher cell-free infectivity during early time points than r3LCMV-GFP^{art}.

Packaging of tri-segmented viral particles is less efficient than of bi-segmented virus.

These observations suggested that the addition of a second S segment impaired and delayed viral growth. We hypothesized that this reduction in viral fitness might be due to inefficient packaging of all three RNA segments into viral particles, and that an excess of bi-segmented particles were formed, which failed to productively replicate when infecting fresh cells. For these experiments we used r3LCMVs with two different reporter genes i.e. GFP together with GP on one S segment and NP next to red fluorescent protein (RFP) on the second S segment. This resulted in two viruses named r3LCMV-GFP/RFP^{nat} and r3LCMV-GFP/RFP^{art}, which differed only in the arrangement of GFP and GP on the respective S segment. We infected BHK-21 cells with r3LCMV-GFP/RFP^{nat}, r3LCMV-

GFP/RFP^{art} or bi-segmented r2LCMV and performed focus forming assays on normal BHK-21 cells or, in parallel, with stably transfected BHK-21 cells expressing either GP (BHK-GP) or NP (BHK-NP) (Flatz, Hegazy et al. 2010) as cell substrate. Wild-type and GP-complementing cells were stained for nucleoprotein-expressing viral foci, whereas NP-complementing cells were stained for GP-positive foci. Thereby, immunofocus formation on wild-type BHK-21 cells detected only tri-segmented virions. BHK-GP cells replicated tri-segmented virions as well as bi-segmented ones containing the L segment in combination with the NP-expressing S segment (but devoid of the GP-expressing S). Conversely, BHK-NP cells replicated tri-segmented LCMV and additionally NP-deficient virions consisting of the L and the GP-expressing S segment (but devoid of the NP-expressing S segment). We found that infectious titers of both r3LCMV-GFP/RFP^{nat} and r3LCMV-GFP/RFP^{art} were consistently higher when assessed on BHK-GP or BHK-NP cells than when infectivity was tested on wild-type BHK-21 cells. Conversely, titers of r2LCMV were similar, irrespective of the cell substrate used to assess its infectivity. In order to correct for potential intrinsic differences in permissiveness of each cell line to LCMV, each virus' titer on BHK-21 cells was normalized to one for display, and BHK-GP as well as BHK-NP titers were expressed as a multiple thereof thus reflecting cell substrate-related titer differences (Fig. 3.2A). On either one of the complementing cells, an approximately five to ten-fold titer difference was observed for r3LCMV-GFP/RFP^{nat} and r3LCMV-GFP/RFP^{art}, which was significantly higher than for r2LCMV. This suggested that a majority of the viral particles, which were formed by the two tri-segmented viruses contained only one of the two S segments encoding either only the NP- (NP-only particles) or the GP-expressing S segment (GP-only particles), respectively. The 5-fold or greater difference in titer suggested that both, NP-only and also GP-only particles outnumbered tri-segmented particles approximately five-fold each, and that tri-segmented particles made up for less than 10 percent of virions only, which was compatible with the reduction in viral peak titers when grown on non-complementing cells (Fig. 3.1D). We also validated these findings by flow cytometry. Non-complementing BHK-21 cells or BHK-NP cells were infected with r3LCMV-GFP/RFP^{art} or r2LCMV as gating control and fluorescence intensities of GFP and RFP were assessed with a flow cytometer (Fig. 3.2B). Since the minimal transacting factors are not provided by wild-type BHK-21 cells, only virions containing at least an L segment together with the NP-expressing S segment can initiate an infectious cycle after cell entry, resulting in fluorescence signal (RFP). Accordingly, a population of RFP+GFP- cells was observed upon infection of BHK-21 cells, reflecting NP-only particles. RFP+GFP+ double-positive

cells were evidence of bona fide tri-segmented particles. According to our gating RFP-GFP+ cells were also observed, yet had a higher RFP MFI than RFP-GFP- cells, suggesting that they represented early stages of infection by tri-segmented particles, an interpretation that is also supported by the continuity of this population and the RFP+GFP+ double positive one. However, when growing tri-segmented r3LCMV-GFP/RFP^{art} on BHK-NP cells, thus substituting for this minimal transacting factor, we observed a 5-fold higher number of RFP-GFP+ cells as compared to infection of non-complementing BHK-21 cells. Conversely, RFP+GFP- (NP-only particles) and GFP+RFP+ double-positive cells (tri-segmented particles) were detected in comparable abundance (Fig. 3.2C). These results confirmed at the single-cell level the findings obtained by focus forming assay corroborating that tri-segmented virus preparations contain a majority of bi-segmented replication-deficient particles. These findings offered a likely explanation for attenuated growth of r3LCMV-GFP/RFP^{nat} and r3LCMV-GFP/RFP^{art}, providing insight into an apparently quite inefficient random packaging of tri-segmented viruses.

Cloning and rescue of recombinant viruses to track recombination in vivo.

Since tri-segmented viruses show impaired growth kinetics as seen in figure 3.1, we hypothesized that there should be high selection pressure on such viruses to recombine their genetic information for NP and GP on only one S segment. Inter-segmental recombination of arenaviruses is postulated to have led to the phylogenetic evolution of the North American clade (Charrel, Feldmann et al. 2002) and thus seemed a likely mechanism whereby tri-segmented viruses could re-establish a functional bi-segmented genome. Looking at the genomic organization of the two tri-segmented viruses we postulated that the selection pressure on r3LCMV-GFP^{nat} might favor recombination events in the area of the IGR, to bring GP and NP together on the same segment, while getting rid of GFP. In the population of r3LCMV-GFP^{art} selection pressure should be equally high, however, the reshuffling of GP and its positioning next to the 3'UTR should render it very difficult if not impossible for this virus to combine its two S segments into one functional segment (see Fig. 3.7 below). In account of the caveats for the identification of RNA recombination and to firmly discriminate it from potential cDNA contamination (Boni, de Jong et al. 2010), we cloned an S segment carrying GFP together with a recombinant GP ORF in which the terminal 255 nucleotides were codon-optimized. The resulting GP had a different nucleotide sequence but identical translation product as the wild-type WE strain GP (WE/WET-GP, Fig. 3.3A). This recombinant WE/WET GP

ORF did not, however, exist as an infectious bi-segmented virus nor did our laboratory possess a cDNA construct where it was associated with NP. Any potential bi-segmented virus containing WE/WET on the same segment as NP was therefore deemed clear evidence of intersegmental recombination, differentiating such viruses from potentially contaminating cDNA or RNA in the respective assays. To test whether the chimeric glycoprotein had an effect on viral fitness, we performed cell culture growth curves of the recombinant tri-segmented virus carrying the WE/WET fusion GP (r3LCMV-WEWET/GFP^{nat}) in comparison with a tri-segmented virus carrying the wild-type WE-GP (r3LCMV-WE/GFP^{nat}) (Fig. 3.3B). Growth kinetics and peak titers of the two viruses were comparable (r3LCMV-WE/GFP^{nat}: 1.7x10^6 PFU/ml, r3LCMV-WEWET/GFP^{nat}: 2.3x10^6 PFU/ml). Thus the chimeric WEWET glycoprotein did not detectably impact viral growth.

We expected that potential recombination events should happen between the NP and GP genes of the S segment, and thus would likely involve the IGR in some way. Hence we introduced a single nucleotide deletion in the intergenic region of the NP-encoding S segment, to serve as a genetic tag. The choice of this nucleotide deletion was made because it is situated in a stretch that unlike most of the S segment IGR is not conserved between strains, neither in sequence nor in length. We reasoned that in case of a recombination event this "tagged" (marked as * throughout) intergenic region should allow us to identify the genetic origin of S segment IGR sequences. The position of the deleted cytosine (marked with an arrow) and a schematic of the resulting NP carrying S segment is depicted in Figure 3.3C. In order to test whether the introduced deletion in the IGR had an impact on viral growth, we rescued recombinant r3LCMV-GFP^{nat} with or without the single nucleotide deletion. Growth curve experiments were performed on BHK-21 cells (moi = 0.01). A tri-segmented virus with a wild-type IGR (r3LCMV-GFP^{nat}) and its comparator with the mutated IGR (r3LCMV-GFP^{nat} IGR*) grew at a similar rate and reached indistinguishable peak titers (Figure 3.3D). Consequently the tag of the IGR on the NP-carrying S segment did not have a detectable impact on viral fitness, thus validating its use for subsequent experimentation in vivo.

r3LCMV-GFP^{nat} but not r3LCMV-GFP^{art} persistent infection in mice reaches viremia levels equivalent to bi-segmented wild-type virus and results in loss of GFP expression.

Upon rescue of the recombinant r3LCMV-GFP^{nat} we aimed at investigating whether tri-segmented viruses recombined in vivo. For this purpose we infected AGRAG mice with

r3LCMV-GFP^{nat}, r3LCMV-GFP^{art} or a bi-segmented r2LCMV as control. AGRAG mice carry deficient genes for the Interferon-α/β receptor, the Interferon-γ receptor and a mutation of the RAG1 gene leading to an immuno-deficient phenotype and establishment of chronic viremia after infection with tri-segmented LCMV. Blood samples were taken over time and viral titers were assessed by focus forming assay (Fig. 3.4A). Carriers of bi-segmented LCMV showed high titer viremia in the range of 5×10^5 PFU/ml blood within 5 days after infection, with subsequently stable viremia in the 10^4 - 10^5 PFU/ml range until at least day 50 post infection. Mice infected with tri-segmented LCMV showed viral loads of about 5×10^3 PFU/ml blood until day 20, in line with attenuated growth in cell culture (compare Fig. 3.1D). From day 30 onwards, carriers of r3LCMV-GFP^{nat} displayed a rise in viral titers, which was not observed in animals infected with r3LCMV-GFP^{art}, resulting in a more than 10-fold difference in viremia on day 50. To determine whether the dominating virus population still carried the GFP reporter gene, thus resulting in GFP expression in infected cells, we performed viral focus formation assays with blood samples of r3LCMV-GFP^{nat} and r3LCMV-GFP^{art} carriers taken on day 127 after infection. We stained for the nucleoprotein or the reporter gene GFP (Fig. 3.4B). Whereas staining of blood isolated from r3LCMV-GFP^{art} carriers resulted in equal amounts of foci with anti-NP and anti-GFP antibody detection (both assessments independently indicating viral titers in the 10^3 PFU/ml range), we observed at least 100-fold higher numbers of total (NP+) r3LCMV-GFP^{nat} foci than foci staining for GFP. Viral titers of at least 10^4 PFU/ml were measured based on anti-NP detection, whereas two out of three mice failed to show any detectable GFP-positive infectivity and one mouse had a residual fraction of GFP-positive foci in the 100 PFU/ml range, corresponding to the lower limit of detection of our assays. GFP expression of infected cells was also assessed by fluorescence microscopy. GFP-fluorescent foci were virtually undetectable when assaying blood from r3LCMV-GFP^{nat} carriers whereas manual counts of GFP-positive foci from r3LCMV-GFP^{art} carrier blood matched the titer results obtained with anti-NP focus forming assay (data not shown). We further verified reporter gene expression by flow cytometric analysis of PBMCs of infected mice on day 120 after infection. We found that more than 10 % of CD11b+GR1- monocytes/macrophages were positive for GFP in r3LCMV-GFP^{art} infected animals whereas blood from r3LCMV-GFP^{nat} evidenced only background levels of GFP, which was comparable to animals infected with non-fluorescent r2LCMV (Fig. 3.4C-E). This finding further supported the hypothesis that tri-segmented viruses with GP in their natural position lose reporter gene expression over

time whereas transposition of the GP in the artificial 3'UTR juxtaposition prevented transgene loss.

Tri-segmented viruses with GP in the natural position can recombine their two S segments resulting in a single S segment with two IGRs and transgene sequence rudiments.

Figure 3.4 had shown elevated viremia and loss of reporter gene expression in mice infected with r3LCMV-GFP^{nat}. We hypothesized that a recombination event could account for this experimental outcome. Intersegmental recombination should combine GP and NP on the same S segment, obviating the need for a second S segment in the viral replication cycle. Such an event could then have explained viremia at the level of wild-type virus in combination with loss of reporter gene expression. To test this possibility we isolated viral RNA from the serum of infected mice and used a pair of primers binding to NP and GP sequences, respectively, to selectively amplify by RT-PCR only putatively recombined RNA molecules, carrying both NP and GP ORFs in ambisense orientation on one RNA segment. The resulting PCR fragments were analyzed by gel electrophoresis (Fig. 3.5A). The sera of all r3LCMV-GFP^{nat} carriers gave rise to RT-dependent PCR products, whereas r3LCMV-GFP^{art} carriers and naïve controls did not show any specific bands. Control PCR reactions were performed on mock-RT-treated RNA samples to rule out cDNA contaminations as a source of PCR product. Sequencing results of three individual r3LCMV-GFP^{nat} carriers are schematically represented in Figure 3.5C. We observed that the three mice contained viral RNA segments of distinct sequence yet with a similar pattern: C-terminal portions of GP and NP were found in ambisense orientation on one RNA segment. Between them both intergenic regions, i.e. the one of the NP-expressing and the one of the original GP-expressing segment were at least partially retained, separated by a fragment of either one or both GFP reporter genes. The direction and length of the GFP fragment varied between the three RNA species recovered from individual mice, which was indicative of independent recombination events. In further support of this notion, the exact same recombined RNA sequence was recovered from two consecutive samples taken from the same mouse with more than three weeks interval between sampling.

Recombinant r2LCMV with two IGRs on the S segment is viable and grows to similar titers as bi-segmented LCMV with only one IGR in the S segment.

The above sequencing data revealed a consistent pattern of viral genetic elements in recombined S segments amongst which the dual IGR was particularly noteworthy and characteristic. We were unaware of arenaviruses with repeats of intergenic regions on one S segment. A dual stem loop is, however, naturally found in the Old World arenavirus Mopeia (Wilson and Clegg 1991). Hence we cloned the rearranged S segment of r3LCMV-GFP^{nat} carrier #3 with the two IGRs and the remnant of GFP into a pol-I driven S segment expression plasmid and rescued the respective virus. Growth kinetics of this virus (r2LCMV_2IGRs) on BHK-21 cells were compared to tri-segmented r3LCMV-GFP^{nat} and bi-segmented r2LCMV (Fig. 3.6). Infectious cell-free titers of r2LCMV_2IGRs exceeded those of r3LCMV-GFP^{nat} already at early time points and reached identical peak titers as r2LCMV (1.7×10^7 PFU/ml vs. 1.6×10^7 PFU/ml, respectively). Importantly, r2LCMV_2IGRs grew to considerably higher peak titers than its parental tri-segmented r3LCMV-GFP^{nat} attesting to the selective advantage of intersegmental recombination despite duplication of the IGR during this process.

Proposed model of recombination events

Based on our sequencing results we postulate that tri-segmented LCMV particles can recombine their two S segments thus reuniting GP and NP on the same segment. The model in Figure 3.7 and its legend summarize the likely molecular steps in RNA synthesis. The observation that the GFP remnant between the two IGRs had either one of two possible orientations or a combination of both suggested that recombination is based on a copy-choice mechanism, which can take place both during genome or antigenome synthesis. Copy-choice, a well-known mechanism of RNA recombination, is the result of a switch of the RdRp from one template to another one during RNA synthesis, where polymerization of the nascent strand continues (Lazzarini, Keene et al. 1981, Kirkegaard and Baltimore 1986, King 1988, Cascone, Haydar et al. 1993). This was first suggested by Cooper et al. (Cooper, Steiner-Pryor et al. 1974) and later on confirmed as the dominant mechanism of recombination in RNA viruses (Kirkegaard and Baltimore 1986, Lai 1992, Nagy, Dzianott et al. 1995). Even though copy-choice as a mechanism for RNA recombination has only formally been proven for positive-sense RNA viruses, negative-sense RNA viruses have been shown to exchange genetic information between different RNA segments and they fulfill all requirements for copy-choice. The three steps involved

in RNA recombination and the physical requirements for a template-switch have been dissected and involve the generation of a primer on the donor RNA, strand transfer and binding of the RdRp to the acceptor RNA and primer elongation on the acceptor RNA (Jarvis and Kirkegaard 1991, Lai 1992, Nagy and Simon 1997).

During antigenome synthesis the RdRp reads in 5'→3' direction through the NP ORF and the IGR (Fig. 3.7A). At the end of the IGR it supposedly pauses, as suggested by the observation that the 3' end of viral mRNAs projects into this sequence stretch (Meyer and Southern 1993) and that the IGR is necessary for transcription termination (Pinschewer, Perez et al. 2005). This pausing due to a strong secondary structure is called structure-dependent polymerase pausing (Auperin, Galinski et al. 1984). Stalling of the polymerase enables copy-choice resulting in strand-switch (Kirkegaard and Baltimore 1986) and it has been shown that the presence of a secondary structure in the acceptor strand is necessary for recombination between virus-associated RNAs (Cascone, Haydar et al. 1993). Stalling of RNA synthesis has been shown to provide an opportunity for the RdRp and/or the nascent strand to interact with the acceptor RNA, thus enabling and initiating a recombination event (reviewed in (Nagy and Simon 1997)).

Since the RdRp can only read in 5'→3' direction, it can only produce a functional and complete S segment when it continues the read somewhere upstream of GP, thus either inside the GFP ORF or even in the IGR itself, from where it can subsequently read through the complete GP ORF with the 5'UTR attached. Recombination can probably also take place during genome synthesis where the polymerase starts reading from the 5'UTR of the GP-encoding S segment. After replicating the GP ORF and the IGR, the secondary structure of the IGR again makes the polymerase to pause, thus enabling copy-choice and strand-switch to the NP-encoding S segment where it continues the read in 5'→3' direction from somewhere randomly within the GFP ORF or inside the IGR, to subsequently read through the entire NP ORF with the 3'UTR (Fig. 3.7B). In the RNA species analyzed, copy-choice has seemingly favored continuation inside the GFP ORF and a direct template switch into an IGR was apparently disfavored. Hence, both of the above copy-choice events resulted in viral RNA segments with GP, a first at least partially intact IGR, a fragment of GFP in either sense- or anti-sense orientation, a second full-length IGR and the NP ORF. The whole RNA segments were flanked by the 5' and 3'UTR, which could form a panhandle structure, a known requirement for a functional viral promoter (Perez and de la Torre 2003). One should assume that analogous stalling and subsequent copy-choice events of the RdRp could also take place during genome or

antigenome synthesis of the r3LCMV-GFP^{art} virus. However, as summarized in Figure 3.7C-D, due to the re-positioning of the GP, the resulting viral segment would carry two 3'UTRs which would fail to form a functional viral promoter for the RdRp and the resulting molecule would not be amplified by the viral polymerase complex. According to this model, reshuffling of the GP with the resulting juxtaposition to and expression under control of the 3'UTR prevents the tri-segmented virus from recombining its two S segments, its reversion to wild-type growth and loss of its transgenes.

3.5 Discussion

Here we have shown that r3LCMV-GP^{nat} can recombine its two S segments resulting in wild-type growth and loss of transgene expression. This can be avoided by repositioning GP under control of the 3'UTR. The resulting r3LCMV-GP^{art} shows consistently attenuated growth in immune-deficient mice with stable transgene expression over at least 150 days.

These results contrast with two studies published by Emonet et al. and Popkin et al. (Emonet, Garidou et al. 2009, Popkin, Teijaro et al. 2011). Both groups of investigators report that r3LCMV particles have wild-type growth kinetics in cell culture, whereas viral loads in mice were dramatically reduced. In our hands, however, tri-segmented LCMV consistently showed drastically impaired growth both in vitro and in vivo (Fig. 3.1D). The reason for this apparent discrepancy of in vitro kinetics is unclear. One explanation could be the use of different cell types for titrating the cell culture supernatants and assess viral titers. Whereas Emonet et al. used non-complementing Vero cells for titration of viral supernatants, we use MC57G cells. Popkin. et al. did not specify, which cells were used for immunofocus assays. Complementing cells would allow the propagation of replication-competent tri- but also replication-deficient bi-segmented particles (carrying e.g. only the NP-encoding S segment in case of GP-complementing cell lines). In this case, titers of tri-segmented viruses would be overestimated. Another important discrepancy between our results and the two above reports is the difference in stability of transgene expression. We analyzed transgene expression by flow cytometry of circulating blood cells. Additionally, we performed focus forming assay from blood and serum looking both at GFP-staining and actual fluorescence by immunofluorescence at regular intervals up until 150 days after infection. In contrast, Emonet et al. investigated stability of the transgene in vitro in ten serial passages of the virus in cell culture, looking at the activity of the CAT transgene in infected cells by CAT assay. Popkin et al. assessed GFP expression by flow cytometry on day 56 after r3LCMV-GP^{nat} infection in spleen cells of IFNAR1-/- mice and found GFP+ cells. However, recombination and subsequent selection of recombined viral genomes comprise random events. Hence, the replacement of r3LCMV by a newly emerging r2LCMV requires a certain size of the viral pool and enough time for the recombined r2LCMV virus to outgrow r3LCMV. We trust that infection of immune-deficient mice and transgene expression analysis over 5 months represents a demanding setting, whereas passage in vitro drastically limits the pool as

well as burst size of the virus, and less than two months of replication in a partially immune-competent organism might not have allowed the recombinants enough time to outgrow the r3LCMV population. Moreover, the percentage of transgene-positive virions was not systematically assessed. Hence the stability of transgene expression as postulated by Emonet et al. and Popkin et al. may have been based on both, less stringent test settings and assessment.

The slightly higher cell culture titers of r3LCMV-GP^{art} compared to r3LCMV-GP^{nat} might be explained by the stronger viral promoter in the 3'UTR, which leads to significantly (~5x) higher mRNA levels as compared to mRNA controlled by the promoter in the 5'UTR (Fuller-Pace and Southern 1988). r3LCMV-GP^{art} replication leads to higher GP levels, which might lead to enhanced viral growth. We also observed, that cells infected with r3LCMV-GFP^{nat} showed higher GFP signals compared to r3LCMV-GFP^{art} infected cells, both in vitro and in vivo (data not shown). Also this finding is consistent with the higher levels of NP mRNA reported by Fuller-Pace et al. (Fuller-Pace and Southern 1988).

We observed that tri-segmented viruses kept their natural tropism since a substantial population of monocytes/macrophages in the blood of r3LCMV-GFP^{art} carriers was found infected (Fig. 3.4D) and this cell type is a known target of LCMV (Walker and Murphy 1987). This finding is in agreement with observations published by Emonet et al. who analyzed tropism of r3LCMV after intracranial infection and found it to be comparable to wild-type LCMV (Emonet, Garidou et al. 2009).

Upon isolation of viral RNA from r3LCMV-GFP^{nat} and r3LCMV-GFP^{art} carriers, we found the exact same nucleotide sequence in the serum of the same animal on time points lying 80 days apart from each other. This is in further support of the hypothesis that recombined viral genomes with a single S segment encoding for both NP and GP gain in fitness and thus outcompete and displace all other tri-segmented variants (Popkin, Teijaro et al. 2011). In addition this observation argues against an artifact of our RT-PCR-based analysis. The additional IGR surprisingly does not impair viral growth of recombined viruses, which was rather unexpected since the IGR forms a strong secondary hairpin structure, which can lead to stalling of the polymerase (Auperin, Galinski et al. 1984).

In summary, we demonstrate that tri-segmented LCMV can be re-engineered to improve genetic stability and ensure constant transgene expression. In addition we provide experimental data to confirm intersegmental recombination as a mechanism of

arenaviruses to enhance their evolutionary potential, which has already previously been postulated to be accountable for a new evolutionary lineage of New World Arenaviruses by recombination between two Tacaribe complex viruses by phylogenetic analyses (Charrel, de Lamballerie et al. 2001, Charrel, Feldmann et al. 2002). Recombinant LCMV expressing additional foreign genes are a promising tool for multiple applications. It can be used to assess gene functions in the context of productive viral infection in vivo and in research on the mechanisms of viral persistence. Furthermore r3LCMV is gaining interest as a tool for vaccination and in vivo antibody production. Administration of r3LCMV not only induces a potent cellular immune response but also stimulates antibodies against transgenes, using the viral infection as a natural adjuvant (Popkin, Teijaro et al. 2011). The natural tropism of LCMV for macrophages and dendritic cells (Sevilla, Kunz et al. 2000, Sevilla, Kunz et al. 2003, Sevilla, McGavern et al. 2004) enables efficient transport of the immunogen to and presentation of the antigen by antigen-presenting cells, ensuring induction of efficient immune responses (Popkin, Teijaro et al. 2011).

This work presents new evidence on how to ensure long-term attenuation of r3LCMV and warranting constant expression of transgenes. Both are critical features for use of r3LCMV in basic research as well as for potential clinical applications as vaccination platform and a tool for immunotherapy of infectious diseases and cancer.

3.6 Figures

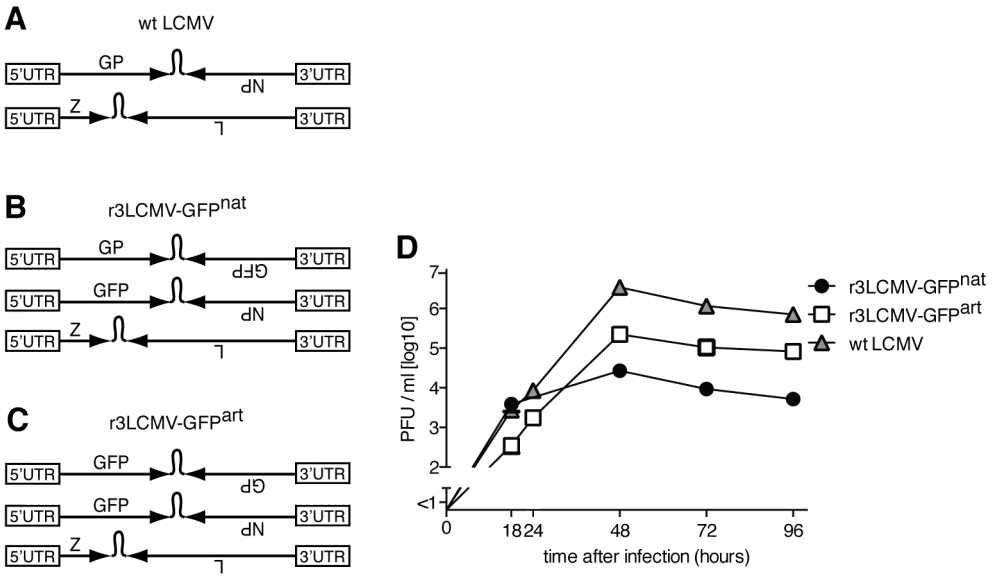

Figure 3.1: Recombinant tri-segmented viruses show impaired growth compared to wild-type LCMV indepenently of the position of the glycoprotein ORF in the genome.

(A-C) Schematic representation of the genomic organization of bi- and tri-segmented LCMV. The bi-segmented genome of wild-type LCMV consists of one S segment encoding for the glycoprotein GP and nucleoprotein NP and one L segment encoding for the matrix protein Z and the viral polymerase L (A). Both segments are flanked by the respective 5' and 3' untranslated regions (UTRs). The genome of recombinant tri-segmented LCMV (r3LCMV) consists of one L and two S segments with one position where to insert a gene of interest (here: green fluorescent protein GFP) into each one of the S segments. (B) r3LCMV-GFP^{nat} has all viral genes in their natural position whereas the GP ORF in r3LCMV-GFP^{art} is artificially iuxtaposed and expressed under control of the 3' UTR (C). (D) Growth kinetics of the indicated viruses in BHK-21 cells, infected at a multiplicity of infection (moi) of 0.01 (wild-type LCMV: grey triangles; r3LCMV-GFP^{nat}: black circles; r3LCMV-GFP^{art}: white squares). Supernatant was taken at the indicated time points after infection and viral titers were determined by focus forming assay. Symbols and bars represent the mean±SEM of three replicates per group and are hidden in the symbol size. Data represent one representative of three independent experiments.

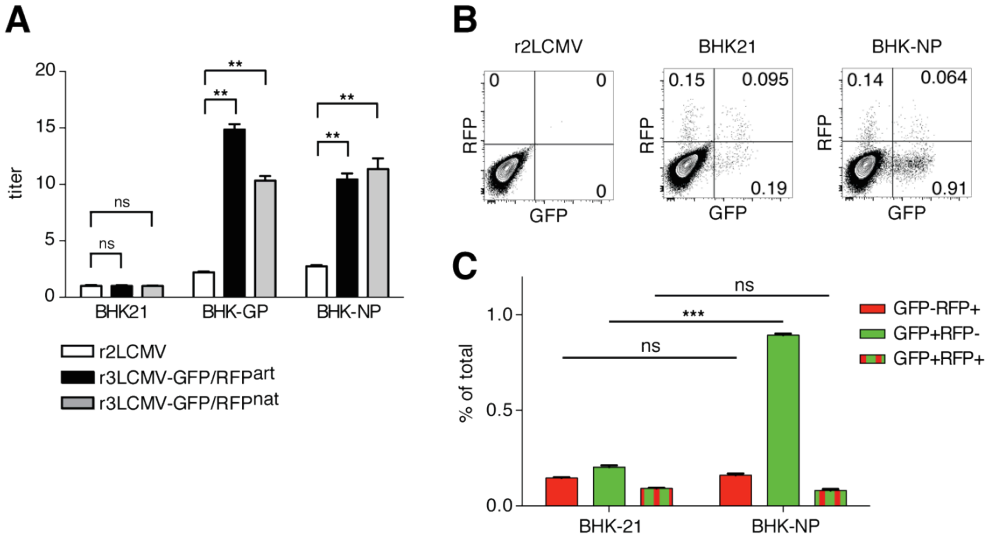

Figure 3.2: Tri-segmented virus preparations contain a majority of bi-segmented replication-deficient particles.

(A) r2LCMV (white bars), r3LCMV-GFP/RFP^{art} (black bars, GFP-GP, RFP-NP) and r3LCMV-GFP/RFP^{nat} (grey bars, GP-GFP, RFP-NP) were grown on wild-type BHK-21 cells and the infectivity of supernatant was determined on wild-type non-complementing BHK-21 cells (BHK21), GP-expressing (BHK-GP) or NP-expressing (BHK-NP) BHK-21 cells. Titers on BHK-21 and BHK-GP cells were determined by staining NP-positive viral foci. Titers on NP-complementing BHK-21 cells were determined by counting GP-positive foci. Titers were normalized to the average titer obtained when assessed on BHK-21 cells and thus are expressed as a multiple thereof. Bars represent the mean±SEM of six replicates per group. One representative of at least three independent experiments is shown. ns, not statistically significant ($p \geq 0.05$); **: $p < 0.01$ by 1-way ANOVA followed by Dunnett's post-test using r2LCMV as a reference. (B) r2LCMV (left plot) or r3LCMV-GFP/RFP^{art} (middle and right plot) were grown on wild-type BHK-21 cells (BHK21) or NP-expressing BHK-21 cells (BHK-NP) and fluorescence was assessed 12 hours after infection by flow cytometry. r2LCMV infected cells were used as gating control. One representative plot per condition is shown. (C) Quantification of GFP+, RFP+ or GFP+RFP+ double positive cells 12 hours after infection with r3LCMV-GFP/RFP^{art} on BHK-21 or BHK-NP cells. Bars represent the mean±SEM of three replicates per group. One representative of at least three independent experiments is shown. ns, not statistically significant ($p \geq 0.05$); ***: $p < 0.001$ by unpaired two-tailed student's *t* test.

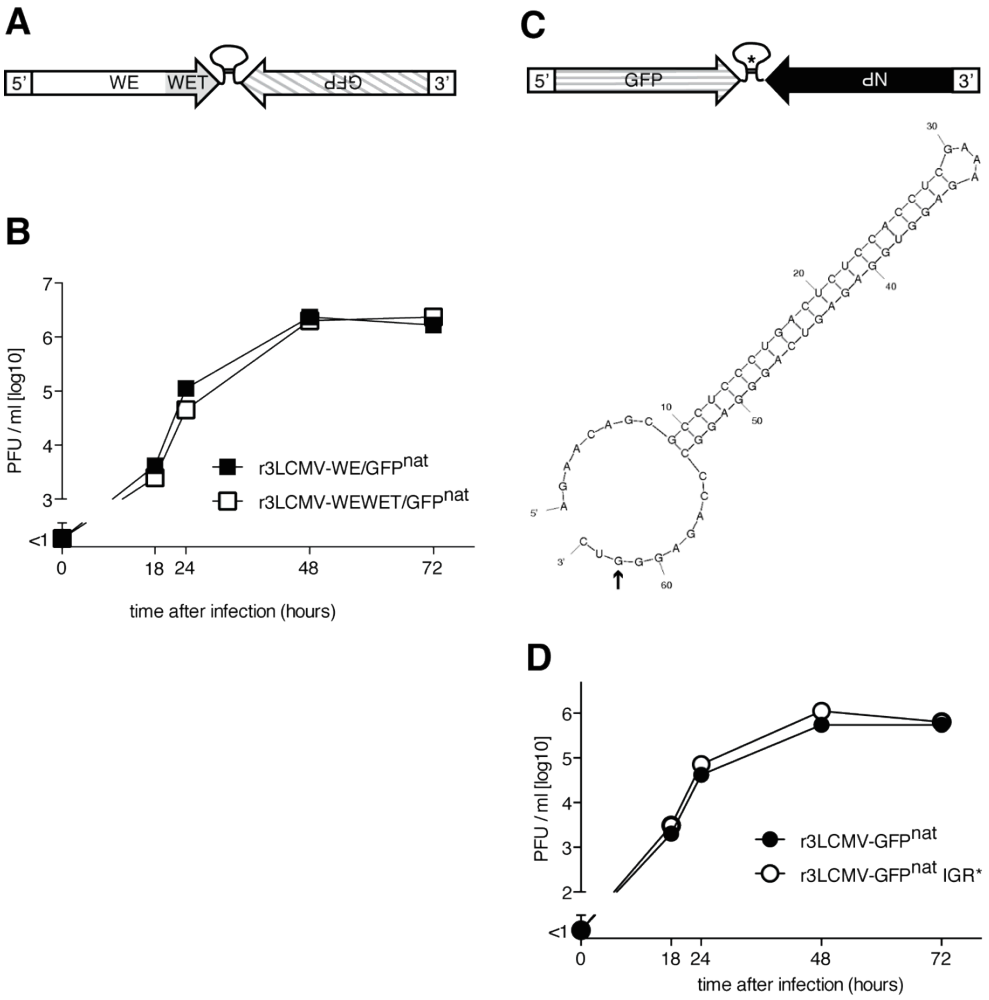

Figure 3.3: Design and growth kinetics of recombinant tri-segmented viruses carrying a partially codon-optimized GP ORF or a genetic tag in the IGR of the S segment.

(A) Schematic of genetically engineered S segment wherein the 255 C-terminal base pairs of GP are codon-optimized and NP is replaced for GFP (GP ORF referred to as "WE/WET"). Growth kinetics of the tri-segmented r3LCMV-WEWET/GFP^{nat} consisting of two S and one L segment as detailed in Fig. 3.1B, with modification of the GP-containing S segment as shown in (A) were performed on BHK-21 cells. Supernatant was taken at the indicated time points after infection at moi = 0.01 and viral titers were determined by focus forming assay (B). Symbols and bars represent the mean±SEM of three replicates per group are hidden in the symbol size. (C) Schematic of the NP-encoding S segment wherein one base pair of the IGR has been deleted in order to genetically "tag" this non-coding RNA element. The deleted residue (indicated by an arrow) lies outside the critical stem-loop structure of the IGR. Comparative growth kinetics of tri-segmented viruses with or without genetic tag in the IGR of the NP-encoding S segment (r3LCMV-GFP^{nat}: black circles; r3LCMV-GFP^{nat} IGR*: white circles) were performed on BHK-21 cells at a moi of 0.01. Supernatant was collected at the indicated time points after infection and viral titers were determined by focus forming assay. Symbols and bars represent the mean±SEM of three replicates per group. Representative data from one of two independent experiments are shown.

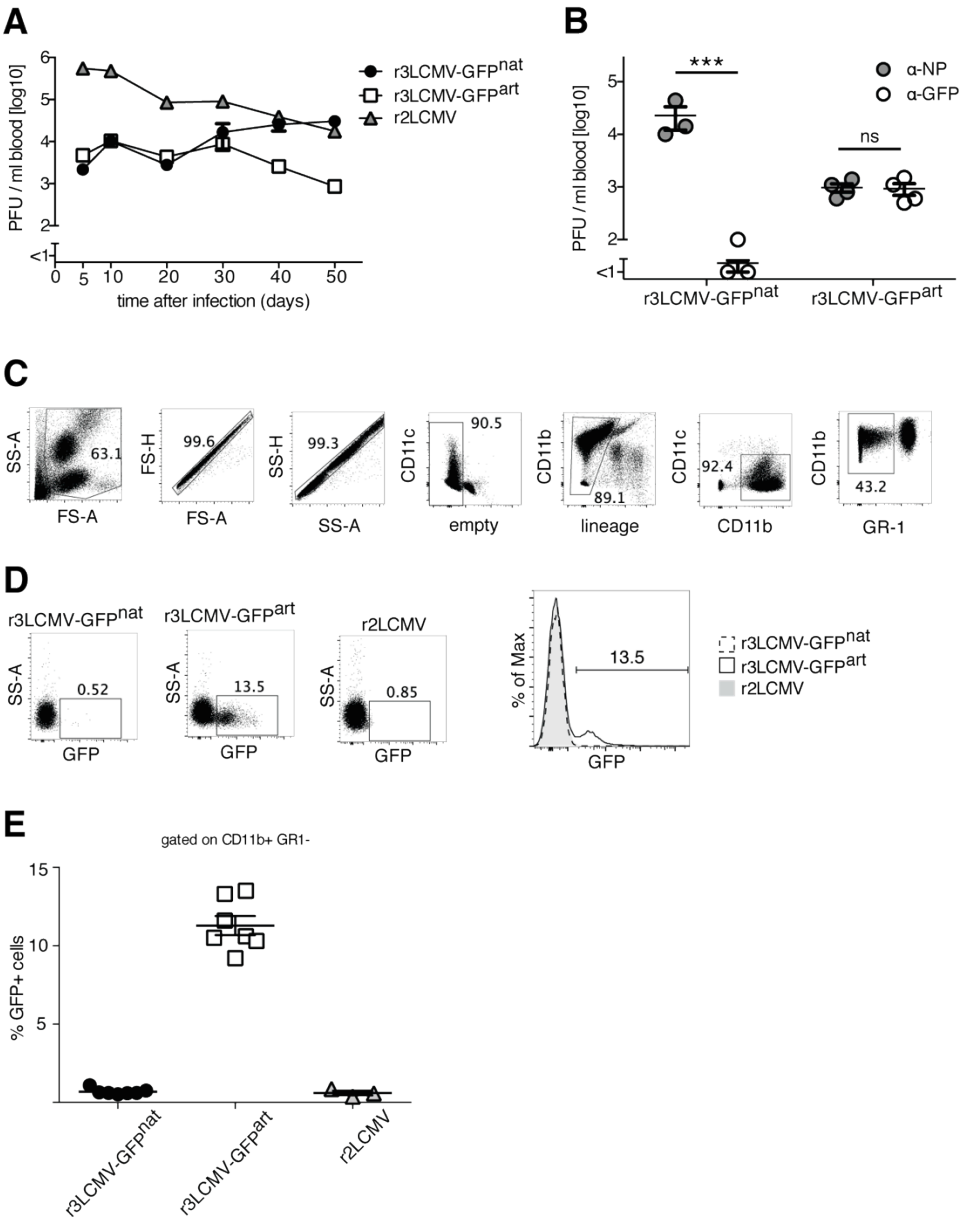

Figure 3.4: r3LCMV-GFP^{nat} but not r3LCMV-GFP^{art} persistent infection in mice reaches viremia levels equivalent to bi-segmented wild-type virus and results in loss of GFP expression.

(A) We infected AGRAG mice i.v. with 1x10^4 PFU of r3LCMV-GFP^{nat} (black circles), r3LCMV-GFP^{art} (white squares) or control bi-segmented r2LCMV (grey triangles) and monitored viremia over time. Symbols and bars represent the mean±SEM of 3-7 mice per group. Representative data from one out of two independent experiments are shown. (B) We determined LCMV viremia on day 127 after intravenous infection of AGRAG mice with 1x10^4 PFU of r3LCMV-GFP^{nat} or r3LCMV-GFP^{art}. Immunofocus assays were performed to detect either nucleoprotein NP (grey circles) or GFP (white circles). Symbols represent individual mice. ns: not statistically significant ($p \geq 0.05$); ***: $p < 0.001$ (unpaired two-tailed student's *t* test). (C-E) Blood from AGRAG mice infected with r3LCMV-GFP^{nat}, r3LCMV-GFP^{art} or r2LCMV was analyzed on day 120 after infection by flow cytometry for the presence of GFP+ cells. Monocytes/macrophages were identified using the gating strategy outlined in (C). One representative FACS plot for each group and one representative histogram overlay of the GFP expression is shown in (D). (E) Quantification of the GFP+ population within the CD11B+ GR1- monocytes/macrophage population. Symbols represent individual mice, bars represent the mean±SEM of 3-7 mice per group.

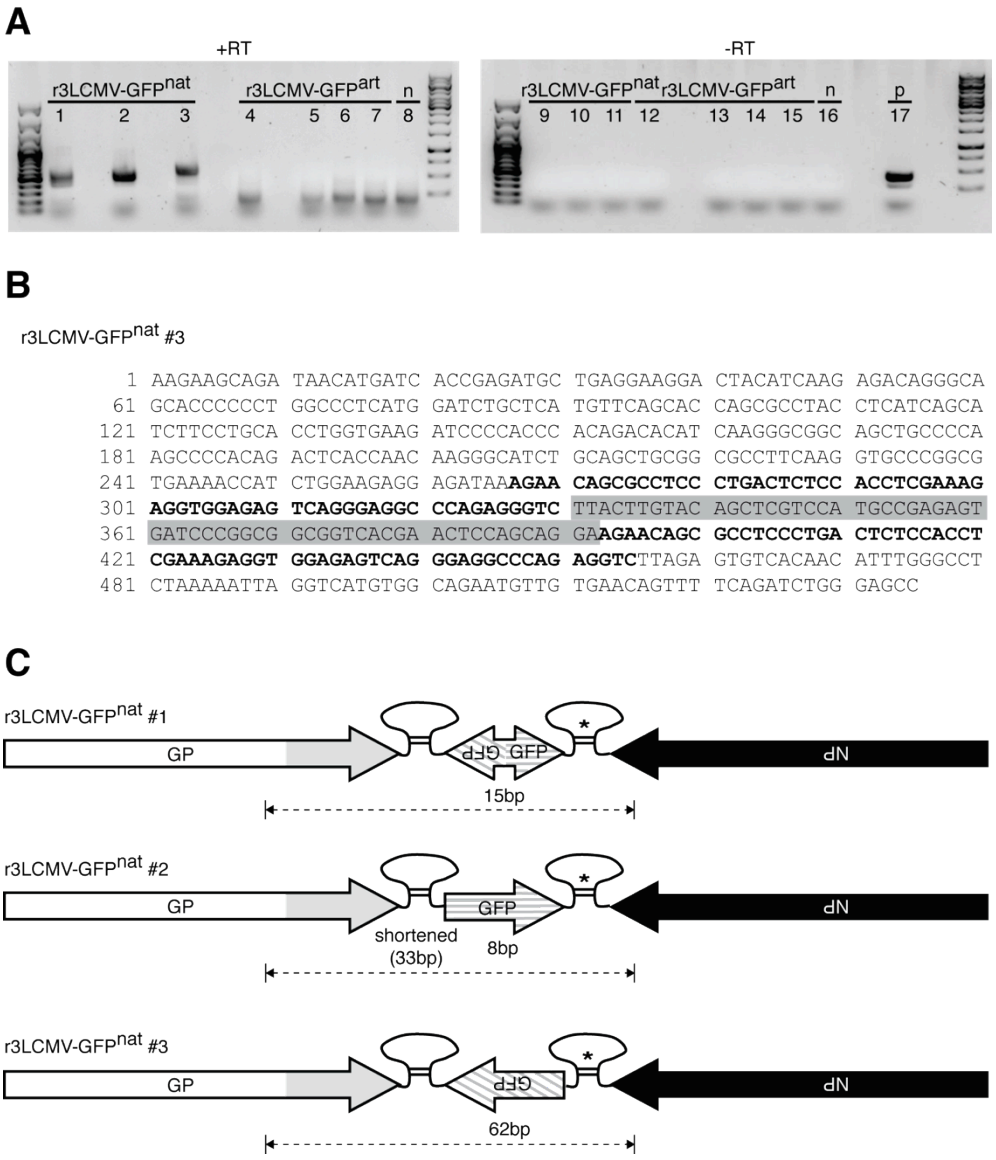

Figure 3.5: r3LCMV-GFP^{nat} persistent infection in mice results in S-segment recombination and loss of functional full-length transgenes.

Viral RNA was isolated from the serum of AGRAG mice on day 127 after i.v. infection with 1x10^4 PFU r3LCMV-GFP^{nat} or r3LCMV-GFP^{art}. Viral RNA was reverse transcribed and cDNA carrying both NP as well as GP sequences was PCR-amplified with appropriate gene-specific primers. (A) DNA electrophoresis of PCR products obtained subsequent to (+RT, lanes 1-8) or without prior reverse transcription of RNA template (-RT, negative control, lanes 9-16). Serum of a naive animal was used as negative control (n, lanes 8+16) and a plasmid encoding a wild-type LCMV S segment as positive control (p, lane 17). Amplicons of lanes 1-3 were subject to Sanger sequencing. (B) Representative cDNA sequence obtained from animal #3 (r3LCMV-GFP^{nat} #3) revealing a recombined S segment combining NP and GP sequences, two intergenic regions (IGRs, bold) and a C-terminal GFP portion (grey highlight). (C) Schematic of three recombined viral S segment sequences isolated on day 127 after infection, each of them dominating the viral population in one representative AGRAG mouse. The tagged IGR originating from the NP-carrying S segment is marked with a star (*). The stretch that has been sequenced is indicated by a double-arrow (|◄- - -►|).

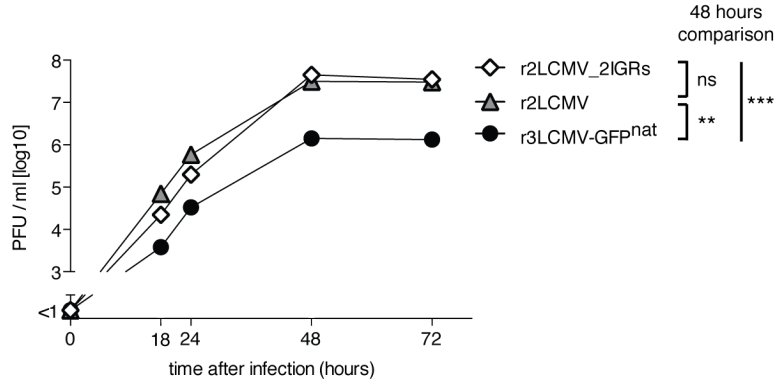

Figure 3.6: Growth kinetics of recombined virus with two IGRs on the S segment are similar to bi-segmented virus.

BHK-21 cells were infected at moi of 0.01 with either bi-segmented LCMV (grey triangles) carrying a wild type S segment, with tri-segmented r3LCMV-GFP^{nat} (black circles) or with r2LCMV_2IGRs (white diamonds) carrying one S segment corresponding to the recombination product recovered from infected AGRAG mice (compare Fig. 3.5). Supernatant was taken at the indicated time points and viral titers were determined by focus forming assay. Symbols and bars represent the mean±SEM of three replicates per group and are hidden in the symbol size. ns, not statistically significant ($p \geq 0.05$); ***: $p < 0.001$ (1-way ANOVA followed by Bonferroni's post-test for multiple comparisons). Representative data from one out of two independent experiments are shown.

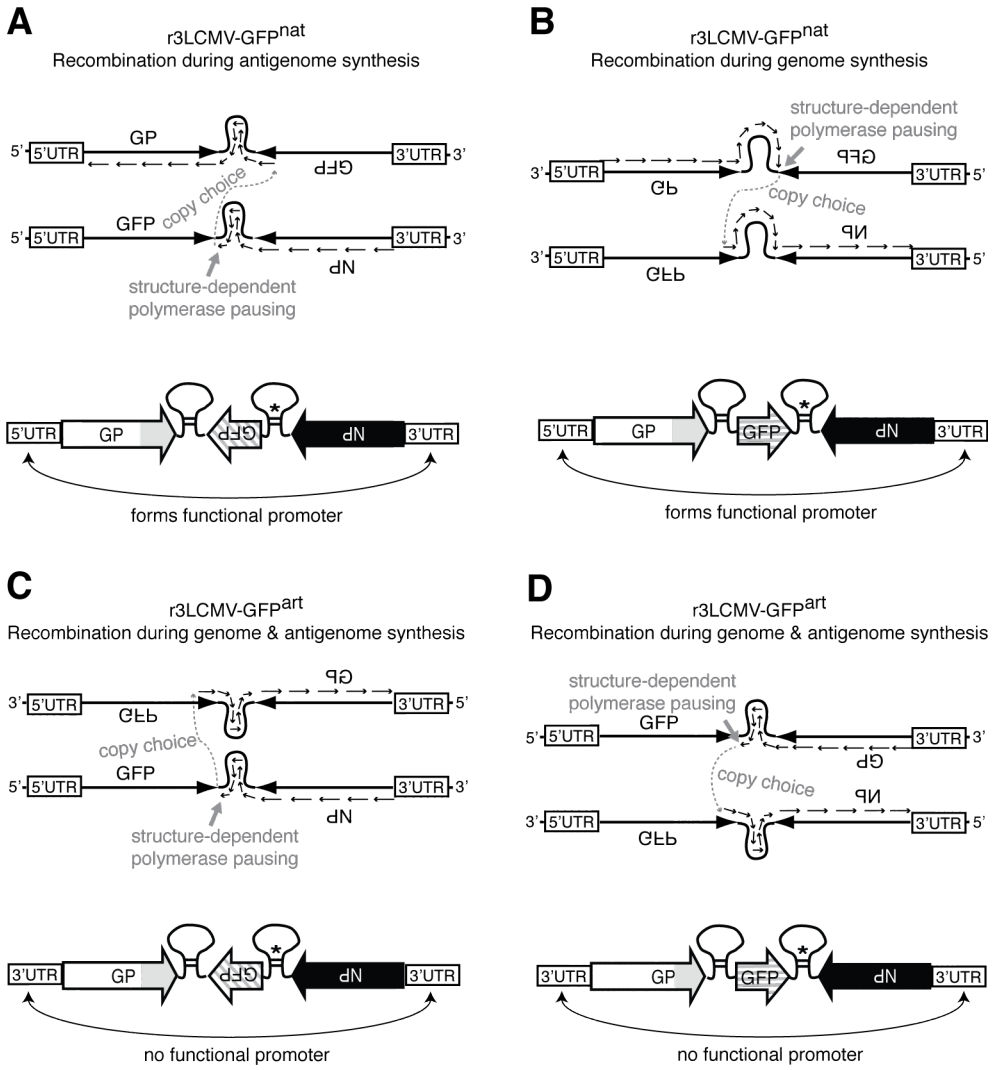

Figure 3.7: Model for the recombination events accountable for r3LCMV-GFP^{nat} transgene loss and postulated mechanism of r3LCMV-GFP^{art} genetic stability.

This model bases itself upon sequence data of LCMV transcription termination (Meyer and Southern 1993) combined with reverse genetic evidence for the IGR as transcription termination signal (Pinschewer, Perez et al. 2005). Together, these findings suggested structure-dependent polymerase pausing when completing the hairpin structure of the IGR. The GFP remnant between the two IGRs in recombined S segments was found to originate from either one or both S segments, fostering the model that polymerase template switch (also referred to as copy-choice) occurred when the polymerase paused, either during genome or antigenome synthesis (below scenarios A and B, respectively). (A) During antigenome synthesis the RNA dependent RNA polymerase (RdRp) initiates at the 3'UTR of a genomic S segment template and then reads through the NP ORF and IGR. At the end of the IGR the polymerase pauses due to the secondary structure ("structure-dependent polymerase pausing"). Stalling of the polymerase facilitates copy choice and continuation of RNA replication on an alternative template (here: GP-encoding S segment genome). Template switch must occur upstream of the GP STOP codon and apparently is most likely to target sequences close to or at the base of the IGR hairpin. Continuing its read through the C-terminus of the second template's GFP, the polymerase then synthesizes a second IGR, the GP ORF and the 5'UTR. (B) During genome synthesis the RdRp initiates RNA synthesis at the 3' end of an antigenomic S segment template containing GP, synthesizes the 5'UTR, GP and most or all of the IGR, followed by structure-dependent polymerase pausing. Copy choice occurs, switching into the C-terminal portion of the GFP ORF near the IGR of an NP-containing S segment. Replication thus adds a fragment of GFP, followed by

an IGR in full length, the NP and 3'UTR. (C – D) Template switch analogously to scenarios (A) and (B) can also occur during genome and antigenome synthesis of r3LCMV-GFP^{art}. This process also can combine NP and GP ORFs onto one RNA segment. The latter is, however, made up of two 3' UTRs instead of a 3'UTR and a 5'UTR, which only together form a functional viral promoter. Such molecules can therefore not be amplified by the RdRp and thus do not form recombined replication-competent virus.

III Global Discussion and Perspective

This work provides novel mechanistic insights into how to harness the immune system in the fight against chronic infection and cancer. We demonstrate that the IL-33/ST2 pathway plays an important role in driving potent effector CTL responses. We have provided a proof-of-principle that exogenous recombinant IL-33, serving as a mimic of damage-signals, can augment CTL responses to vaccination (Bonilla, Frohlich et al. 2012). These observations suggest IL-33 as an adjuvant in cancer immunotherapy. Further, we have shown that it essentially contributes to survival of T cells in the chronic infection context. Besides IL-21 (Elsaesser, Sauer et al. 2009, Frohlich, Kisielow et al. 2009, Yi, Du et al. 2009), IL-33 is currently the only cytokine known to specifically enhance survival of T cells in chronic viral infection. Therapeutic interventions that restore or augment T cell immunity are a promising approach in the fight against chronic viral infections and cancer. Immune responses against tumor cells and chronic viral infections share many similarities since both are underlying constant and high level exposure to their respective antigens, which heavily impacts potent T cell responses. Many studies are ongoing to counter suppressive cytokines like TGF-β (Gorelik and Flavell 2001), IL-10 (Brooks, Walsh et al. 2010) or LAG3 (Grosso, Kelleher et al. 2007) or inhibitory receptors like PD-1 in order to enhance T cell immunity and finally achieve better clinical prognosis. Expression of the inhibitory receptor PD-1 on the surface of functionally "exhausted" CTLs is associated with persistence of various viruses like LCMV or HIV, HBV and HCV in humans (Barber, Wherry et al. 2006, Day, Kaufmann et al. 2006, Trautmann, Janbazian et al. 2006, Radziewicz, Ibegbu et al. 2007, Ye, Weng et al. 2008) and blockade of the PD-1/PD-L1 pathway with specific antibodies correlates with enhanced CD8+ T cell functionality and improved virus control (Barber, Wherry et al. 2006, Velu, Titanji et al. 2009). This pathway has therapeutic potential both in chronic viral infections and in cancer and blockade of PD-1/PD-L1 has been shown to boost tumor-specific immunity in various malignant diseases (Chen, Wu et al. 2008, Fourcade, Sun et al. 2010, Matsuzaki, Gnjatic et al. 2010, Zhang, Huang et al. 2010, Sakthivel, Gereke et al. 2012). Targeting of the PD-1/PD-L1 pathway was demonstrated to be effective to enhance antitumor T cell immunity and the first PD-1 blocker has been licensed by the U.S. Food and Drug Administration (FDA) in early September 2014 for the treatment of melanoma (FDA 2014). In contrast to these immunomodulatory approaches, which target inhibitory pathways or suppressive cytokines to augment the

functionality and magnitude of T cell response IL-33 therapy offers a conceptually novel approach: It provides a survival and effector differentiation signal to specific CTLs rather than blocking inhibition, and thus represents an innovative strategy with great potential for synergy. The insights our studies provide into the role of IL-33 in T cell immunity should therefore help in refining treatments and improving disease outcome in cancer as well as in chronic microbial infections like, HIV, Malaria and tuberculosis.

An alternative approach to tackle these types of diseases consists in the induction of adaptive immunity. Virally vectored vaccines generally hold great promise in this regard because of their exquisite ability to not only induce protective antibodies but also strong CTL immunity. LCMV has been used for almost a century to elicit potent and long-lived CTL immunity in mice (Zinkernagel 2002) and it is known to do the same in humans (Kotturi, Swann et al. 2011). Our novel strategy for vectorization of replication-competent LCMV should thus become a useful vaccine platform that will be helpful in combatting the above-mentioned diseases. As we have learned from the work reported herein, replicating LCMV but not replication-deficient vectors benefit from the IL-33 pathway for effector CTL induction (Bonilla, Frohlich et al. 2012) and thus may be particularly valuable in the context of cancer vaccination. Viruses as vaccine candidates obviously have to be subject to the appropriate safety tests in order to evaluate their suitability for clinical use. The demonstration of stable attenuation and vaccine antigen expression is a key criterion in this context. This is a drawback of replicating viruses as vaccine vectors but it can rightfully be said that replication-competent recombinant viruses have recently gained acceptance. This change in the community's thinking is due, in large parts, to the protective capacity of recombinant CMV-based vectors in the HIV/SIV context (Hansen, Ford et al. 2011). The promising results of the chimeric replication-competent YF17D/Dengue Virus vaccine against Dengue virus infection (Sanofi-Pasteur 2014a, Sanofi-Pasteur 2014b) has also helped to renew the self-confidence of the biomedical community in that infectious diseases long thought of as "difficult targets" can be matched with vaccines. We are therefore confident that our viral vector has considerable translational potential and may open up new avenues in vaccination against persistent infections and tumors.

IV References

Adler, H., M. Messerle, M. Wagner and U. H. Koszinowski (2000). "Cloning and mutagenesis of the murine gammaherpesvirus 68 genome as an infectious bacterial artificial chromosome." J Virol **74**(15): 6964-6974.

Ahmed, R., L. D. Butler and L. Bhatti (1988). "T4+ T helper cell function in vivo: differential requirement for induction of antiviral cytotoxic T-cell and antibody responses." J Virol **62**(6): 2102-2106.

Ahmed, R., A. Salmi, L. D. Butler, J. M. Chiller and M. B. Oldstone (1984). "Selection of genetic variants of lymphocytic choriomeningitis virus in spleens of persistently infected mice. Role in suppression of cytotoxic T lymphocyte response and viral persistence." J Exp Med **160**(2): 521-540.

Ali, S., M. Huber, C. Kollewe, S. C. Bischoff, W. Falk and M. U. Martin (2007). "IL-1 receptor accessory protein is essential for IL-33-induced activation of T lymphocytes and mast cells." Proc Natl Acad Sci U S A **104**(47): 18660-18665.

Appay, V., R. A. van Lier, F. Sallusto and M. Roederer (2008). "Phenotype and function of human T lymphocyte subsets: consensus and issues." Cytometry A **73**(11): 975-983.

Archer, A. M. and R. Rico-Hesse (2002). "High genetic divergence and recombination in Arenaviruses from the Americas." Virology **304**(2): 274-281.

Auperin, D. D., M. Galinski and D. H. Bishop (1984). "The sequences of the N protein gene and intergenic region of the S RNA of pichinde arenavirus." Virology **134**(1): 208-219.

Baekkevold, E. S., M. Roussigne, T. Yamanaka, F. E. Johansen, F. L. Jahnsen, F. Amalric, P. Brandtzaeg, M. Erard, G. Haraldsen and J. P. Girard (2003). "Molecular characterization of NF-HEV, a nuclear factor preferentially expressed in human high endothelial venules." Am J Pathol **163**(1): 69-79.

Bajenoff, M., J. G. Egen, L. Y. Koo, J. P. Laugier, F. Brau, N. Glaichenhaus and R. N. Germain (2006). "Stromal cell networks regulate lymphocyte entry, migration, and territoriality in lymph nodes." Immunity **25**(6): 989-1001.

Bajenoff, M., N. Glaichenhaus and R. N. Germain (2008). "Fibroblastic reticular cells guide T lymphocyte entry into and migration within the splenic T cell zone." J Immunol **181**(6): 3947-3954.

Barber, D. L., E. J. Wherry, D. Masopust, B. Zhu, J. P. Allison, A. H. Sharpe, G. J. Freeman and R. Ahmed (2006). "Restoring function in exhausted CD8 T cells during chronic viral infection." Nature **439**(7077): 682-687.

Barton, L. L. (1996). "Lymphocytic choriomeningitis virus: a neglected central nervous system pathogen." Clin Infect Dis **22**(1): 197.

Battegay, M., S. Cooper, A. Althage, J. Banziger, H. Hengartner and R. M. Zinkernagel (1991). "Quantification of lymphocytic choriomeningitis virus with an immunological focus assay in 24- or 96-well plates." J Virol Methods **33**(1-2): 191-198.

Becerra, A., R. V. Warke, N. de Bosch, A. L. Rothman and I. Bosch (2008). "Elevated levels of soluble ST2 protein in dengue virus infected patients." Cytokine **41**(2): 114-120.

Bergthaler, A., L. Flatz, A. N. Hegazy, S. Johnson, E. Horvath, M. Lohning and D. D. Pinschewer (2010). "Viral replicative capacity is the primary determinant of lymphocytic choriomeningitis virus persistence and immunosuppression." Proc Natl Acad Sci U S A **107**(50): 21641-21646.

Bergthaler, A., L. Flatz, A. Verschoor, A. N. Hegazy, M. Holdener, K. Fink, B. Eschli, D. Merkler, R. Sommerstein, E. Horvath, M. Fernandez, A. Fitsche, B. M. Senn, J. S. Verbeek, B. Odermatt, C. A. Siegrist and D. D. Pinschewer (2009). "Impaired antibody response causes persistence of prototypic T cell-contained virus." PLoS Biol **7**(4): e1000080.

Bergthaler, A., N. U. Gerber, D. Merkler, E. Horvath, J. C. de la Torre and D. D. Pinschewer (2006). "Envelope exchange for the generation of live-attenuated arenavirus vaccines." PLoS Pathog **2**(6): e51.

Beutler, B., Z. Jiang, P. Georgel, K. Crozat, B. Croker, S. Rutschmann, X. Du and K. Hoebe (2006). "Genetic analysis of host resistance: Toll-like receptor signaling and immunity at large." Annu Rev Immunol **24**: 353-389.

Bianchi, M. E. (2007). "DAMPs, PAMPs and alarmins: all we need to know about danger." J Leukoc Biol **81**(1): 1-5.

Boni, M. F., M. D. de Jong, H. R. van Doorn and E. C. Holmes (2010). "Guidelines for identifying homologous recombination events in influenza A virus." PLoS One **5**(5): e10434.

Bonilla, W. V., A. Frohlich, K. Senn, S. Kallert, M. Fernandez, S. Johnson, M. Kreutzfeldt, A. N. Hegazy, C. Schrick, P. G. Fallon, R. Klemenz, S. Nakae, H. Adler, D. Merkler, M. Lohning and D. D. Pinschewer (2012). "The alarmin interleukin-33 drives protective antiviral CD8(+) T cell responses." Science **335**(6071): 984-989.

Bredenbeek, P. J., R. Molenkamp, W. J. Spaan, V. Deubel, P. Marianneau, M. S. Salvato, D. Moshkoff, J. Zapata, I. Tikhonov, J. Patterson, R. Carrion, A. Ticer, K. Brasky and I. S. Lukashevich (2006). "A recombinant Yellow Fever 17D vaccine expressing Lassa virus glycoproteins." Virology **345**(2): 299-304.

Brooks, D. G., D. B. McGavern and M. B. Oldstone (2006). "Reprogramming of antiviral T cells prevents inactivation and restores T cell activity during persistent viral infection." J Clin Invest **116**(6): 1675-1685.

Brooks, D. G., L. Teyton, M. B. Oldstone and D. B. McGavern (2005). "Intrinsic functional dysregulation of CD4 T cells occurs rapidly following persistent viral infection." J Virol **79**(16): 10514-10527.

Brooks, D. G., K. B. Walsh, H. Elsaesser and M. B. Oldstone (2010). "IL-10 directly suppresses CD4 but not CD8 T cell effector and memory responses following acute viral infection." Proc Natl Acad Sci U S A **107**(7): 3018-3023.

Buchmeier, M. J. and M. B. Oldstone (1979). "Protein structure of lymphocytic choriomeningitis virus: evidence for a cell-associated precursor of the virion glycopeptides." Virology **99**(1): 111-120.

Buller, R. M., G. L. Smith, K. Cremer, A. L. Notkins and B. Moss (1985). "Decreased virulence of recombinant vaccinia virus expression vectors is associated with a thymidine kinase-negative phenotype." Nature **317**(6040): 813-815.

Byrne, J. A., R. Ahmed and M. B. Oldstone (1984). "Biology of cloned cytotoxic T lymphocytes specific for lymphocytic choriomeningitis virus. I. Generation and recognition of virus strains and H-2b mutants." J Immunol **133**(1): 433-439.

Carriere, V., L. Roussel, N. Ortega, D. A. Lacorre, L. Americh, L. Aguilar, G. Bouche and J. P. Girard (2007). "IL-33, the IL-1-like cytokine ligand for ST2 receptor, is a chromatin-associated nuclear factor in vivo." Proc Natl Acad Sci U S A **104**(1): 282-287.

Cascone, P. J., T. F. Haydar and A. E. Simon (1993). "Sequences and structures required for recombination between virus-associated RNAs." Science **260**(5109): 801-805.

Cayrol, C. and J. P. Girard (2009). "The IL-1-like cytokine IL-33 is inactivated after maturation by caspase-1." Proc Natl Acad Sci U S A **106**(22): 9021-9026.

Chambers, T. J., Y. Liang, D. A. Droll, J. J. Schlesinger, A. D. Davidson, P. J. Wright and X. Jiang (2003). "Yellow fever virus/dengue-2 virus and yellow fever virus/dengue-4 virus chimeras: biological characterization, immunogenicity, and protection against dengue encephalitis in the mouse model." J Virol **77**(6): 3655-3668.

Chambers, T. J., A. Nestorowicz, P. W. Mason and C. M. Rice (1999). "Yellow fever/Japanese encephalitis chimeric viruses: construction and biological properties." J Virol **73**(4): 3095-3101.

Chare, E. R., E. A. Gould and E. C. Holmes (2003). "Phylogenetic analysis reveals a low rate of homologous recombination in negative-sense RNA viruses." J Gen Virol **84**(Pt 10): 2691-2703.

Charrel, R. N., X. de Lamballerie and C. F. Fulhorst (2001). "The Whitewater Arroyo virus: natural evidence for genetic recombination among Tacaribe serocomplex viruses (family Arenaviridae)." Virology **283**(2): 161-166.

Charrel, R. N., H. Feldmann, C. F. Fulhorst, R. Khelifa, R. de Chesse and X. de Lamballerie (2002). "Phylogeny of New World arenaviruses based on the

complete coding sequences of the small genomic segment identified an evolutionary lineage produced by intrasegmental recombination." Biochem Biophys Res Commun **296**(5): 1118-1124.

Chen, J., X. J. Wu and G. Q. Wang (2008). "Hepatoma cells up-regulate expression of programmed cell death-1 on T cells." World J Gastroenterol **14**(44): 6853-6857.

Chen, S. T., Y. L. Lin, M. T. Huang, M. F. Wu, S. C. Cheng, H. Y. Lei, C. K. Lee, T. W. Chiou, C. H. Wong and S. L. Hsieh (2008). "CLEC5A is critical for dengue-virus-induced lethal disease." Nature **453**(7195): 672-676.

Ciurea, A., L. Hunziker, P. Klenerman, H. Hengartner and R. M. Zinkernagel (2001). "Impairment of CD4(+) T cell responses during chronic virus infection prevents neutralizing antibody responses against virus escape mutants." J Exp Med **193**(3): 297-305.

Cohen, J. N., C. J. Guidi, E. F. Tewalt, H. Qiao, S. J. Rouhani, A. Ruddell, A. G. Farr, K. S. Tung and V. H. Engelhard (2010). "Lymph node-resident lymphatic endothelial cells mediate peripheral tolerance via Aire-independent direct antigen presentation." J Exp Med **207**(4): 681-688.

Cooper, M. D., H. G. Purchase, D. E. Bockman and W. E. Gathings (1974). "Studies on the nature of the abnormality of B cell differentiation in avian lymphoid leukosis: production of heterogeneous IgM by tumor cells." J Immunol **113**(4): 1210-1222.

Cooper, P. D., A. Steiner-Pryor, P. D. Scotti and D. D. (1974). "On the Nature of Poliovirus Genetic Recombinants." J. gen. Virol. **23**: 41-49.

Crotty, S. (2011). "Follicular helper CD4 T cells (TFH)." Annu Rev Immunol **29**: 621-663.

Crouse, J., G. Bedenikovic, M. Wiesel, M. Ibberson, I. Xenarios, D. Von Laer, U. Kalinke, E. Vivier, S. Jonjic and A. Oxenius (2014). "Type I interferons protect T cells against NK cell attack mediated by the activating receptor NCR1." Immunity **40**(6): 961-973.

Day, C. L., D. E. Kaufmann, P. Kiepiela, J. A. Brown, E. S. Moodley, S. Reddy, E. W. Mackey, J. D. Miller, A. J. Leslie, C. DePierres, Z. Mncube, J. Duraiswamy, B. Zhu, Q. Eichbaum, M. Altfeld, E. J. Wherry, H. M. Coovadia, P. J. Goulder, P. Klenerman, R. Ahmed, G. J. Freeman and B. D. Walker (2006). "PD-1 expression on HIV-specific T cells is associated with T-cell exhaustion and disease progression." Nature **443**(7109): 350-354.

Dinarello, C. A. (2009). "Immunological and inflammatory functions of the interleukin-1 family." Annu Rev Immunol **27**: 519-550.

Dobrzanski, M. J., J. B. Reome, J. A. Hollenbaugh and R. W. Dutton (2004). "Tc1 and Tc2 effector cell therapy elicit long-term tumor immunity by contrasting mechanisms that result in complementary endogenous type 1 antitumor responses." J Immunol **172**(3): 1380-1390.

Doherty, P. C., W. Allan, M. Eichelberger and S. R. Carding (1992). "Roles of alpha beta and gamma delta T cell subsets in viral immunity." Annu Rev Immunol **10**: 123-151.

Doherty, P. C. and J. P. Christensen (2000). "Accessing complexity: the dynamics of virus-specific T cell responses." Annu Rev Immunol **18**: 561-592.

Drummond, R. A. and G. D. Brown (2011). "The role of Dectin-1 in the host defence against fungal infections." Curr Opin Microbiol **14**(4): 392-399.

Duffy, S., L. A. Shackelton and E. C. Holmes (2008). "Rates of evolutionary change in viruses: patterns and determinants." Nat Rev Genet **9**(4): 267-276.

Ehtisham, S., N. P. Sunil-Chandra and A. A. Nash (1993). "Pathogenesis of murine gammaherpesvirus infection in mice deficient in CD4 and CD8 T cells." J Virol **67**(9): 5247-5252.

Elsaesser, H., K. Sauer and D. G. Brooks (2009). "IL-21 is required to control chronic viral infection." Science **324**(5934): 1569-1572.

Emonet, S. F., L. Garidou, D. B. McGavern and J. C. de la Torre (2009). "Generation of recombinant lymphocytic choriomeningitis viruses with trisegmented genomes stably expressing two additional genes of interest." Proc Natl Acad Sci U S A **106**(9): 3473-3478.

Fahey, L. M., E. B. Wilson, H. Elsaesser, C. D. Fistonich, D. B. McGavern and D. G. Brooks (2011). "Viral persistence redirects CD4 T cell differentiation toward T follicular helper cells." J Exp Med **208**(5): 987-999.

FDA (2014). FDA approves Keytruda for advanced melanoma. First PD-1 blocking drug ro receive agency approval; retrieved from http://www.fda.gov/newsevents/newsroom/pressannouncements/ucm412802.htm. U. F. a. D. Administration.

Flatz, L., A. Bergthaler, J. C. de la Torre and D. D. Pinschewer (2006). "Recovery of an arenavirus entirely from RNA polymerase I/II-driven cDNA." Proc Natl Acad Sci U S A **103**(12): 4663-4668.

Flatz, L., A. N. Hegazy, A. Bergthaler, A. Verschoor, C. Claus, M. Fernandez, L. Gattinoni, S. Johnson, F. Kreppel, S. Kochanek, M. Broek, A. Radbruch, F. Levy, P. H. Lambert, C. A. Siegrist, N. P. Restifo, M. Lohning, A. F. Ochsenbein, G. J. Nabel and D. D. Pinschewer (2010). "Development of replication-defective lymphocytic choriomeningitis virus vectors for the induction of potent CD8+ T cell immunity." Nat Med **16**(3): 339-345.

Fletcher, A. L., V. Lukacs-Kornek, E. D. Reynoso, S. E. Pinner, A. Bellemare-Pelletier, M. S. Curry, A. R. Collier, R. L. Boyd and S. J. Turley (2010). "Lymph node fibroblastic reticular cells directly present peripheral tissue antigen under steady-state and inflammatory conditions." J Exp Med **207**(4): 689-697.

Flick, R. and G. Hobom (1999). "Transient bicistronic vRNA segments for indirect selection of recombinant influenza viruses." Virology **262**(1): 93-103.

Fourcade, J., Z. Sun, M. Benallaoua, P. Guillaume, I. F. Luescher, C. Sander, J. M. Kirkwood, V. Kuchroo and H. M. Zarour (2010). "Upregulation of Tim-3 and PD-1 expression is associated with tumor antigen-specific CD8+ T cell dysfunction in melanoma patients." J Exp Med **207**(10): 2175-2186.

Frebel, H., V. Nindl, R. A. Schuepbach, T. Braunschweiler, K. Richter, J. Vogel, C. A. Wagner, D. Loffing-Cueni, M. Kurrer, B. Ludewig and A. Oxenius (2012). "Programmed death 1 protects from fatal circulatory failure during systemic virus infection of mice." J Exp Med **209**(13): 2485-2499.

Frohlich, A., J. Kisielow, I. Schmitz, S. Freigang, A. T. Shamshiev, J. Weber, B. J. Marsland, A. Oxenius and M. Kopf (2009). "IL-21R on T cells is critical for sustained functionality and control of chronic viral infection." Science **324**(5934): 1576-1580.

Fuller, M. J. and A. J. Zajac (2003). "Ablation of CD8 and CD4 T cell responses by high viral loads." J Immunol **170**(1): 477-486.

Fuller-Pace, F. V. and P. J. Southern (1988). "Temporal analysis of transcription and replication during acute infection with lymphocytic choriomeningitis virus." Virology **162**(1): 260-263.

Fung-Leung, W. P., T. M. Kundig, R. M. Zinkernagel and T. W. Mak (1991). "Immune response against lymphocytic choriomeningitis virus infection in mice without CD8 expression." J Exp Med **174**(6): 1425-1429.

Gallimore, A., A. Glithero, A. Godkin, A. C. Tissot, A. Pluckthun, T. Elliott, H. Hengartner and R. Zinkernagel (1998). "Induction and exhaustion of lymphocytic choriomeningitis virus-specific cytotoxic T lymphocytes visualized using soluble tetrameric major histocompatibility complex class I-peptide complexes." J Exp Med **187**(9): 1383-1393.

Gallucci, S. and P. Matzinger (2001). "Danger signals: SOS to the immune system." Curr Opin Immunol **13**(1): 114-119.

Garbutt, M., R. Liebscher, V. Wahl-Jensen, S. Jones, P. Moller, R. Wagner, V. Volchkov, H. D. Klenk, H. Feldmann and U. Stroher (2004). "Properties of replication-competent vesicular stomatitis virus vectors expressing glycoproteins of filoviruses and arenaviruses." J Virol **78**(10): 5458-5465.

Garcia-Sastre, A., T. Muster, W. S. Barclay, N. Percy and P. Palese (1994). "Use of a mammalian internal ribosomal entry site element for expression of a foreign protein by a transfectant influenza virus." J Virol **68**(10): 6254-6261.

Gazi, U. and L. Martinez-Pomares (2009). "Influence of the mannose receptor in host immune responses." Immunobiology **214**(7): 554-561.

Geisbert, T. W. and P. B. Jahrling (2004). "Exotic emerging viral diseases: progress and challenges." Nat Med **10**(12 Suppl): S110-121.

Geisbert, T. W., S. Jones, E. A. Fritz, A. C. Shurtleff, J. B. Geisbert, R. Liebscher, A. Grolla, U. Stroher, L. Fernando, K. M. Daddario, M. C. Guttieri, B. R. Mothe, T. Larsen, L. E. Hensley, P. B. Jahrling and H. Feldmann (2005). "Development of a new vaccine for the prevention of Lassa fever." PLoS Med **2**(6): e183.

Gorelik, L. and R. A. Flavell (2001). "Immune-mediated eradication of tumors through the blockade of transforming growth factor-beta signaling in T cells." Nat Med **7**(10): 1118-1122.

Grosso, J. F., C. C. Kelleher, T. J. Harris, C. H. Maris, E. L. Hipkiss, A. De Marzo, R. Anders, G. Netto, D. Getnet, T. C. Bruno, M. V. Goldberg, D. M. Pardoll and C. G. Drake (2007). "LAG-3 regulates CD8+ T cell accumulation and effector function in murine self- and tumor-tolerance systems." J Clin Invest **117**(11): 3383-3392.

Guirakhoo, F., R. Weltzin, T. J. Chambers, Z. X. Zhang, K. Soike, M. Ratterree, J. Arroyo, K. Georgakopoulos, J. Catalan and T. P. Monath (2000). "Recombinant chimeric yellow fever-dengue type 2 virus is immunogenic and protective in nonhuman primates." J Virol **74**(12): 5477-5485.

Guirakhoo, F., Z. X. Zhang, T. J. Chambers, S. Delagrave, J. Arroyo, A. D. Barrett and T. P. Monath (1999). "Immunogenicity, genetic stability, and protective efficacy of a recombinant, chimeric yellow fever-Japanese encephalitis virus (ChimeriVax-JE) as a live, attenuated vaccine candidate against Japanese encephalitis." Virology **257**(2): 363-372.

Hahn, C. S., S. Lustig, E. G. Strauss and J. H. Strauss (1988). "Western equine encephalitis virus is a recombinant virus." Proc Natl Acad Sci U S A **85**(16): 5997-6001.

Hansen, S. G., J. C. Ford, M. S. Lewis, A. B. Ventura, C. M. Hughes, L. Coyne-Johnson, N. Whizin, K. Oswald, R. Shoemaker, T. Swanson, A. W. Legasse, M. J. Chiuchiolo, C. L. Parks, M. K. Axthelm, J. A. Nelson, M. A. Jarvis, M. Piatak, Jr., J. D. Lifson and L. J. Picker (2011). "Profound early control of highly pathogenic SIV by an effector memory T-cell vaccine." Nature **473**(7348): 523-527.

Haraldsen, G., J. Balogh, J. Pollheimer, J. Sponheim and A. M. Kuchler (2009). "Interleukin-33 - cytokine of dual function or novel alarmin?" Trends Immunol **30**(5): 227-233.

Harari, A., P. A. Bart, W. Stohr, G. Tapia, M. Garcia, E. Medjitna-Rais, S. Burnet, C. Cellerai, O. Erlwein, T. Barber, C. Moog, P. Liljestrom, R. Wagner, H. Wolf, J. P. Kraehenbuhl, M. Esteban, J. Heeney, M. J. Frachette, J. Tartaglia, S. McCormack, A. Babiker, J. Weber and G. Pantaleo (2008). "An HIV-1 clade C DNA prime, NYVAC boost vaccine regimen induces reliable, polyfunctional, and long-lasting T cell responses." J Exp Med **205**(1): 63-77.

Hardison, S. E. and G. D. Brown (2012). "C-type lectin receptors orchestrate antifungal immunity." Nat Immunol **13**(9): 817-822.

Hardman, C. S., V. Panova and A. N. McKenzie (2013). "IL-33 citrine reporter mice reveal the temporal and spatial expression of IL-33 during allergic lung inflammation." Eur J Immunol **43**(2): 488-498.

Hass, M., U. Golnitz, S. Muller, B. Becker-Ziaja and S. Gunther (2004). "Replicon system for Lassa virus." J Virol **78**(24): 13793-13803.

Holland, J., K. Spindler, F. Horodyski, E. Grabau, S. Nichol and S. VandePol (1982). "Rapid evolution of RNA genomes." Science **215**(4540): 1577-1585.

Holmes, E. C., M. Worobey and A. Rambaut (1999). "Phylogenetic evidence for recombination in dengue virus." Mol Biol Evol **16**(3): 405-409.

Homann, D., L. Teyton and M. B. Oldstone (2001). "Differential regulation of antiviral T-cell immunity results in stable CD8+ but declining CD4+ T-cell memory." Nat Med **7**(8): 913-919.

Hornung, V., J. Ellegast, S. Kim, K. Brzozka, A. Jung, H. Kato, H. Poeck, S. Akira, K. K. Conzelmann, M. Schlee, S. Endres and G. Hartmann (2006). "5'-Triphosphate RNA is the ligand for RIG-I." Science **314**(5801): 994-997.

Jarvis, T. C. and K. Kirkegaard (1991). "The polymerase in its labyrinth: mechanisms and implications of RNA recombination." Trends Genet **7**(6): 186-191.

Jiang, X., T. J. Dalebout, P. J. Bredenbeek, R. Carrion, Jr., K. Brasky, J. Patterson, M. Goicochea, J. Bryant, M. S. Salvato and I. S. Lukashevich (2011). "Yellow fever 17D-vectored vaccines expressing Lassa virus GP1 and GP2 glycoproteins provide protection against fatal disease in guinea pigs." Vaccine **29**(6): 1248-1257.

Joffre, O., M. A. Nolte, R. Sporri and C. Reis e Sousa (2009). "Inflammatory signals in dendritic cell activation and the induction of adaptive immunity." Immunol Rev **227**(1): 234-247.

Johnson, K. M., M. L. Kuns, R. B. Mackenzie, P. A. Webb and C. E. Yunker (1966). "Isolation of Machupo virus from wild rodent Calomys callosus." Am J Trop Med Hyg **15**(1): 103-106.

Joshi, N. S., W. Cui, A. Chandele, H. K. Lee, D. R. Urso, J. Hagman, L. Gapin and S. M. Kaech (2007). "Inflammation directs memory precursor and short-lived effector CD8(+) T cell fates via the graded expression of T-bet transcription factor." Immunity **27**(2): 281-295.

Kagi, D., B. Ledermann, K. Burki, P. Seiler, B. Odermatt, K. J. Olsen, E. R. Podack, R. M. Zinkernagel and H. Hengartner (1994). "Cytotoxicity mediated by T cells and natural killer cells is greatly impaired in perforin-deficient mice." Nature **369**(6475): 31-37.

Kang, D. C., R. V. Gopalkrishnan, Q. Wu, E. Jankowsky, A. M. Pyle and P. B. Fisher (2002). "mda-5: An interferon-inducible putative RNA helicase with double-

stranded RNA-dependent ATPase activity and melanoma growth-suppressive properties." Proc Natl Acad Sci U S A **99**(2): 637-642.

King, A. M. (1988). "Preferred sites of recombination in poliovirus RNA: an analysis of 40 intertypic cross-over sequences." Nucleic Acids Res **16**(24): 11705-11723.

Kirkegaard, K. and D. Baltimore (1986). "The mechanism of RNA recombination in poliovirus." Cell **47**(3): 433-443.

Klempa, B., H. A. Schmidt, R. Ulrich, S. Kaluz, M. Labuda, H. Meisel, B. Hjelle and D. H. Kruger (2003). "Genetic interaction between distinct Dobrava hantavirus subtypes in Apodemus agrarius and A. flavicollis in nature." J Virol **77**(1): 804-809.

Kolumam, G. A., S. Thomas, L. J. Thompson, J. Sprent and K. Murali-Krishna (2005). "Type I interferons act directly on CD8 T cells to allow clonal expansion and memory formation in response to viral infection." J Exp Med **202**(5): 637-650.

Koopman, L. A., H. D. Kopcow, B. Rybalov, J. E. Boyson, J. S. Orange, F. Schatz, R. Masch, C. J. Lockwood, A. D. Schachter, P. J. Park and J. L. Strominger (2003). "Human decidual natural killer cells are a unique NK cell subset with immunomodulatory potential." J Exp Med **198**(8): 1201-1212.

Kotturi, M. F., J. A. Swann, B. Peters, C. L. Arlehamn, J. Sidney, R. V. Kolla, E. A. James, R. S. Akondy, R. Ahmed, W. W. Kwok, M. J. Buchmeier and A. Sette (2011). "Human CD8(+) and CD4(+) T cell memory to lymphocytic choriomeningitis virus infection." J Virol **85**(22): 11770-11780.

Lai, M. M. (1992). "RNA recombination in animal and plant viruses." Microbiol Rev **56**(1): 61-79.

Lazzarini, R. A., J. D. Keene and M. Schubert (1981). "The origins of defective interfering particles of the negative-strand RNA viruses." Cell **26**(2 Pt 2): 145-154.

Le Goffic, R., M. I. Arshad, M. Rauch, A. L'Helgoualc'h, B. Delmas, C. Piquet-Pellorce and M. Samson (2011). "Infection with influenza virus induces IL-33 in murine lungs." Am J Respir Cell Mol Biol **45**(6): 1125-1132.

Lee, J. W., M. Epardaud, J. Sun, J. E. Becker, A. C. Cheng, A. R. Yonekura, J. K. Heath and S. J. Turley (2007). "Peripheral antigen display by lymph node stroma promotes T cell tolerance to intestinal self." Nat Immunol **8**(2): 181-190.

Lee, K. J., I. S. Novella, M. N. Teng, M. B. Oldstone and J. C. de La Torre (2000). "NP and L proteins of lymphocytic choriomeningitis virus (LCMV) are sufficient for efficient transcription and replication of LCMV genomic RNA analogs." J Virol **74**(8): 3470-3477.

Lee, K. J., M. Perez, D. D. Pinschewer and J. C. de la Torre (2002). "Identification of the lymphocytic choriomeningitis virus (LCMV) proteins required to rescue LCMV RNA analogs into LCMV-like particles." J Virol **76**(12): 6393-6397.

Lewandoski, M., K. M. Wassarman and G. R. Martin (1997). "Zp3-cre, a transgenic mouse line for the activation or inactivation of loxP-flanked target genes specifically in the female germ line." Curr Biol **7**(2): 148-151.

Liew, F. Y., N. I. Pitman and I. B. McInnes (2010). "Disease-associated functions of IL-33: the new kid in the IL-1 family." Nat Rev Immunol **10**(2): 103-110.

Link, A., T. K. Vogt, S. Favre, M. R. Britschgi, H. Acha-Orbea, B. Hinz, J. G. Cyster and S. A. Luther (2007). "Fibroblastic reticular cells in lymph nodes regulate the homeostasis of naive T cells." Nature immunology **8**(11): 1255-1265.

Linterman, M. A., L. Beaton, D. Yu, R. R. Ramiscal, M. Srivastava, J. J. Hogan, N. K. Verma, M. J. Smyth, R. J. Rigby and C. G. Vinuesa (2010). "IL-21 acts directly on B cells to regulate Bcl-6 expression and germinal center responses." J Exp Med **207**(2): 353-363.

Ljutic, B., J. R. Carlyle, D. Filipp, R. Nakagawa, M. Julius and J. C. Zuniga-Pflucker (2005). "Functional requirements for signaling through the stimulatory and inhibitory mouse NKR-P1 (CD161) NK cell receptors." J Immunol **174**(8): 4789-4796.

Lohning, M., A. Stroehmann, A. J. Coyle, J. L. Grogan, S. Lin, J. C. Gutierrez-Ramos, D. Levinson, A. Radbruch and T. Kamradt (1998). "T1/ST2 is preferentially expressed on murine Th2 cells, independent of interleukin 4, interleukin 5, and interleukin 10, and important for Th2 effector function." Proc Natl Acad Sci U S A **95**(12): 6930-6935.

Lopez, N., R. Jacamo and M. T. Franze-Fernandez (2001). "Transcription and RNA replication of tacaribe virus genome and antigenome analogs require N and L proteins: Z protein is an inhibitor of these processes." J Virol **75**(24): 12241-12251.

Lukashevich, I. S., J. Patterson, R. Carrion, D. Moshkoff, A. Ticer, J. Zapata, K. Brasky, R. Geiger, G. B. Hubbard, J. Bryant and M. S. Salvato (2005). "A live attenuated vaccine for Lassa fever made by reassortment of Lassa and Mopeia viruses." J Virol **79**(22): 13934-13942.

Luthi, A. U., S. P. Cullen, E. A. McNeela, P. J. Duriez, I. S. Afonina, C. Sheridan, G. Brumatti, R. C. Taylor, K. Kersse, P. Vandenabeele, E. C. Lavelle and S. J. Martin (2009). "Suppression of interleukin-33 bioactivity through proteolysis by apoptotic caspases." Immunity **31**(1): 84-98.

Machado, A. V., N. Naffakh, S. van der Werf and N. Escriou (2003). "Expression of a foreign gene by stable recombinant influenza viruses harboring a dicistronic genomic segment with an internal promoter." Virology **313**(1): 235-249.

Mackett, M., G. L. Smith and B. Moss (1982). "Vaccinia virus: a selectable eukaryotic cloning and expression vector." Proc Natl Acad Sci U S A **79**(23): 7415-7419.

Matloubian, M., R. J. Concepcion and R. Ahmed (1994). "CD4+ T cells are required to sustain CD8+ cytotoxic T-cell responses during chronic viral infection." J Virol **68**(12): 8056-8063.

Matsuzaki, J., S. Gnjatic, P. Mhawech-Fauceglia, A. Beck, A. Miller, T. Tsuji, C. Eppolito, F. Qian, S. Lele, P. Shrikant, L. J. Old and K. Odunsi (2010). "Tumor-infiltrating NY-ESO-1-specific CD8+ T cells are negatively regulated by LAG-3 and PD-1 in human ovarian cancer." Proc Natl Acad Sci U S A **107**(17): 7875-7880.

Matter, M., V. Pavelic, D. D. Pinschewer, S. Mumprecht, B. Eschli, T. Giroglou, D. von Laer and A. F. Ochsenbein (2007). "Decreased tumor surveillance after adoptive T-cell therapy." Cancer Res **67**(15): 7467-7476.

Mebius, R. E. and G. Kraal (2005). "Structure and function of the spleen." Nat Rev Immunol **5**(8): 606-616.

Meyer, B. J. and P. J. Southern (1993). "Concurrent sequence analysis of 5' and 3' RNA termini by intramolecular circularization reveals 5' nontemplated bases and 3' terminal heterogeneity for lymphocytic choriomeningitis virus mRNAs." J Virol **67**(5): 2621-2627.

Mikkelsen, J. G. and F. S. Pedersen (2000). "Genetic reassortment and patch repair by recombination in retroviruses." J Biomed Sci **7**(2): 77-99.

Mills, J. N., B. A. Ellis, J. E. Childs, K. T. McKee, Jr., J. I. Maiztegui, C. J. Peters, T. G. Ksiazek and P. B. Jahrling (1994). "Prevalence of infection with Junin virus in rodent populations in the epidemic area of Argentine hemorrhagic fever." Am J Trop Med Hyg **51**(5): 554-562.

Moskophidis, D., S. P. Cobbold, H. Waldmann and F. Lehmann-Grube (1987). "Mechanism of recovery from acute virus infection: treatment of lymphocytic choriomeningitis virus-infected mice with monoclonal antibodies reveals that Lyt-2+ T lymphocytes mediate clearance of virus and regulate the antiviral antibody response." J Virol **61**(6): 1867-1874.

Moskophidis, D., F. Lechner, H. Pircher and R. M. Zinkernagel (1993). "Virus persistence in acutely infected immunocompetent mice by exhaustion of antiviral cytotoxic effector T cells." Nature **362**(6422): 758-761.

Moussion, C., N. Ortega and J. P. Girard (2008). "The IL-1-like cytokine IL-33 is constitutively expressed in the nucleus of endothelial cells and epithelial cells in vivo: a novel 'alarmin'?" PLoS One **3**(10): e3331.

Mueller, S. N., M. Matloubian, D. M. Clemens, A. H. Sharpe, G. J. Freeman, S. Gangappa, C. P. Larsen and R. Ahmed (2007). "Viral targeting of fibroblastic reticular cells contributes to immunosuppression and persistence during chronic infection." Proc Natl Acad Sci U S A **104**(39): 15430-15435.

Nagy, P. D., A. Dzianott, P. Ahlquist and J. J. Bujarski (1995). "Mutations in the helicase-like domain of protein 1a alter the sites of RNA-RNA recombination in brome mosaic virus." J Virol **69**(4): 2547-2556.

Nagy, P. D. and A. E. Simon (1997). "New insights into the mechanisms of RNA recombination." Virology **235**(1): 1-9.

Nichols, L. A., Y. Chen, T. A. Colella, C. L. Bennett, B. E. Clausen and V. H. Engelhard (2007). "Deletional self-tolerance to a melanocyte/melanoma antigen derived from tyrosinase is mediated by a radio-resistant cell in peripheral and mesenteric lymph nodes." J Immunol **179**(2): 993-1003.

Nolte, M. A., J. A. Belien, I. Schadee-Eestermans, W. Jansen, W. W. Unger, N. van Rooijen, G. Kraal and R. E. Mebius (2003). "A conduit system distributes chemokines and small blood-borne molecules through the splenic white pulp." J Exp Med **198**(3): 505-512.

Oboki, K., T. Ohno, N. Kajiwara, K. Arae, H. Morita, A. Ishii, A. Nambu, T. Abe, H. Kiyonari, K. Matsumoto, K. Sudo, K. Okumura, H. Saito and S. Nakae (2010). "IL-33 is a crucial amplifier of innate rather than acquired immunity." Proc Natl Acad Sci U S A **107**(43): 18581-18586.

Odermatt, B., M. Eppler, T. P. Leist, H. Hengartner and R. M. Zinkernagel (1991). "Virus-triggered acquired immunodeficiency by cytotoxic T-cell-dependent destruction of antigen-presenting cells and lymph follicle structure." Proc Natl Acad Sci U S A **88**(18): 8252-8256.

Oldstone, M. B. (2002). "Biology and pathogenesis of lymphocytic choriomeningitis virus infection." Curr Top Microbiol Immunol **263**: 83-117.

Olschlager, S. and L. Flatz (2013). "Vaccination strategies against highly pathogenic arenaviruses: the next steps toward clinical trials." PLoS Pathog **9**(4): e1003212.

Oppenheim, J. J. and D. Yang (2005). "Alarmins: chemotactic activators of immune responses." Curr Opin Immunol **17**(4): 359-365.

Osokine, I., L. M. Snell, C. R. Cunningham, D. H. Yamada, E. B. Wilson, H. J. Elsaesser, J. C. de la Torre and D. Brooks (2014). "Type I interferon suppresses de novo virus-specific CD4 Th1 immunity during an established persistent viral infection." Proc Natl Acad Sci U S A **111**(20): 7409-7414.

Ou, R., S. Zhou, L. Huang and D. Moskophidis (2001). "Critical role for alpha/beta and gamma interferons in persistence of lymphocytic choriomeningitis virus by clonal exhaustion of cytotoxic T cells." J Virol **75**(18): 8407-8423.

Oxenius, A., M. F. Bachmann, R. M. Zinkernagel and H. Hengartner (1998). "Virus-specific MHC-class II-restricted TCR-transgenic mice: effects on humoral and cellular immune responses after viral infection." Eur J Immunol **28**(1): 390-400.

Ozaki, K., R. Spolski, C. G. Feng, C. F. Qi, J. Cheng, A. Sher, H. C. Morse, 3rd, C. Liu, P. L. Schwartzberg and W. J. Leonard (2002). "A critical role for IL-21 in regulating immunoglobulin production." Science **298**(5598): 1630-1634.

Palmer, G. and C. Gabay (2011). "Interleukin-33 biology with potential insights into human diseases." Nat Rev Rheumatol **7**(6): 321-329.

Paveley, R. A., S. A. Aynsley, J. D. Turner, C. D. Bourke, S. J. Jenkins, P. C. Cook, L. Martinez-Pomares and A. P. Mountford (2011). "The Mannose Receptor (CD206) is an important pattern recognition receptor (PRR) in the detection of the infective stage of the helminth Schistosoma mansoni and modulates IFNgamma production." Int J Parasitol **41**(13-14): 1335-1345.

Percy, N., W. S. Barclay, A. Garcia-Sastre and P. Palese (1994). "Expression of a foreign protein by influenza A virus." J Virol **68**(7): 4486-4492.

Perez, M. and J. C. de la Torre (2003). "Characterization of the genomic promoter of the prototypic arenavirus lymphocytic choriomeningitis virus." J Virol **77**(2): 1184-1194.

Peters, B. S., W. Jaoko, E. Vardas, G. Panayotakopoulos, P. Fast, C. Schmidt, J. Gilmour, M. Bogoshi, G. Omosa-Manyonyi, L. Dally, L. Klavinskis, B. Farah, T. Tarragona, P. A. Bart, A. Robinson, C. Pieterse, W. Stevens, R. Thomas, B. Barin, A. J. McMichael, J. A. McIntyre, G. Pantaleo, T. Hanke and J. Bwayo (2007). "Studies of a prophylactic HIV-1 vaccine candidate based on modified vaccinia virus Ankara (MVA) with and without DNA priming: effects of dosage and route on safety and immunogenicity." Vaccine **25**(11): 2120-2127.

Pichery, M., E. Mirey, P. Mercier, E. Lefrancais, A. Dujardin, N. Ortega and J. P. Girard (2012). "Endogenous IL-33 is highly expressed in mouse epithelial barrier tissues, lymphoid organs, brain, embryos, and inflamed tissues: in situ analysis using a novel Il-33-LacZ gene trap reporter strain." J Immunol **188**(7): 3488-3495.

Pinschewer, D. D., L. Flatz, R. Steinborn, E. Horvath, M. Fernandez, H. Lutz, M. Suter and A. Bergthaler (2010). "Innate and adaptive immune control of genetically engineered live-attenuated arenavirus vaccine prototypes." Int Immunol **22**(9): 749-756.

Pinschewer, D. D., M. Perez and J. C. de la Torre (2003). "Role of the virus nucleoprotein in the regulation of lymphocytic choriomeningitis virus transcription and RNA replication." J Virol **77**(6): 3882-3887.

Pinschewer, D. D., M. Perez and J. C. de la Torre (2005). "Dual role of the lymphocytic choriomeningitis virus intergenic region in transcription termination and virus propagation." J Virol **79**(7): 4519-4526.

Pinschewer, D. D., M. Perez, E. Jeetendra, T. Bachi, E. Horvath, H. Hengartner, M. A. Whitt, J. C. de la Torre and R. M. Zinkernagel (2004). "Kinetics of protective antibodies are determined by the viral surface antigen." J Clin Invest **114**(7): 988-993.

Pinschewer, D. D., M. Perez, E. Jeetendra, T. Bächi, E. Horvath, H. Hengartner, M. A. Whitt, J. C. de la Torre and R. M. Zinkernagel (2004). "Kinetics of protective antibodies are determined by the viral surface antigen." J. Clin. Invest. **114**: 988-993.

Pircher, H., K. Burki, R. Lang, H. Hengartner and R. M. Zinkernagel (1989). "Tolerance induction in double specific T-cell receptor transgenic mice varies with antigen." Nature **342**(6249): 559-561.

Plyusnin, A., S. K. Kukkonen, A. Plyusnina, O. Vapalahti and A. Vaheri (2002). "Transfection-mediated generation of functionally competent Tula hantavirus with recombinant S RNA segment." EMBO J **21**(6): 1497-1503.

Popkin, D. L., J. R. Teijaro, A. M. Lee, H. Lewicki, S. Emonet, J. C. de la Torre and M. Oldstone (2011). "Expanded potential for recombinant trisegmented lymphocytic choriomeningitis viruses: protein production, antibody production, and in vivo assessment of biological function of genes of interest." J Virol **85**(15): 7928-7932.

Probst, H. C., J. Lagnel, G. Kollias and M. van den Broek (2003). "Inducible transgenic mice reveal resting dendritic cells as potent inducers of CD8+ T cell tolerance." Immunity **18**(5): 713-720.

Radziewicz, H., C. C. Ibegbu, M. L. Fernandez, K. A. Workowski, K. Obideen, M. Wehbi, H. L. Hanson, J. P. Steinberg, D. Masopust, E. J. Wherry, J. D. Altman, B. T. Rouse, G. J. Freeman, R. Ahmed and A. Grakoui (2007). "Liver-infiltrating lymphocytes in chronic human hepatitis C virus infection display an exhausted phenotype with high levels of PD-1 and low levels of CD127 expression." J Virol **81**(6): 2545-2553.

Rahemtulla, A., W. P. Fung-Leung, M. W. Schilham, T. M. Kundig, S. R. Sambhara, A. Narendran, A. Arabian, A. Wakeham, C. J. Paige, R. M. Zinkernagel and et al. (1991). "Normal development and function of CD8+ cells but markedly decreased helper cell activity in mice lacking CD4." Nature **353**(6340): 180-184.

Rahman, A. H., W. Cui, D. F. Larosa, D. K. Taylor, J. Zhang, D. R. Goldstein, E. J. Wherry, S. M. Kaech and L. A. Turka (2008). "MyD88 plays a critical T cell-intrinsic role in supporting CD8 T cell expansion during acute lymphocytic choriomeningitis virus infection." J Immunol **181**(6): 3804-3810.

Rahman, A. H., R. Zhang, C. D. Blosser, B. Hou, A. L. Defranco, J. S. Maltzman, E. J. Wherry and L. A. Turka (2011). "Antiviral memory CD8 T-cell differentiation, maintenance, and secondary expansion occur independently of MyD88." Blood **117**(11): 3123-3130.

Rivers, T. M. and T. F. McNair Scott (1935). "Meningitis in Man Caused by a Filterable Virus." Science **81**(2105): 439-440.

Ruddle, N. H. and E. M. Akirav (2009). "Secondary lymphoid organs: responding to genetic and environmental cues in ontogeny and the immune response." J Immunol **183**(4): 2205-2212.

Runge, S., K. M. Sparrer, C. Lassig, K. Hembach, A. Baum, A. Garcia-Sastre, J. Soding, K. K. Conzelmann and K. P. Hopfner (2014). "In vivo ligands of MDA5 and RIG-I in measles virus-infected cells." PLoS Pathog **10**(4): e1004081.

Sakthivel, P., M. Gereke and D. Bruder (2012). "Therapeutic intervention in cancer and chronic viral infections: antibody mediated manipulation of PD-1/PD-L1 interaction." Rev Recent Clin Trials **7**(1): 10-23.

Salvato, M., E. Shimomaye and M. B. Oldstone (1989). "The primary structure of the lymphocytic choriomeningitis virus L gene encodes a putative RNA polymerase." Virology **169**(2): 377-384.

Salvato, M., E. Shimomaye, P. Southern and M. B. Oldstone (1988). "Virus-lymphocyte interactions. IV. Molecular characterization of LCMV Armstrong (CTL+) small genomic segment and that of its variant, Clone 13 (CTL-)." Virology **164**(2): 517-522.

Salvato, M. S. and E. M. Shimomaye (1989). "The completed sequence of lymphocytic choriomeningitis virus reveals a unique RNA structure and a gene for a zinc finger protein." Virology **173**(1): 1-10.

Sanchez, A. B. and J. C. de la Torre (2006). "Rescue of the prototypic Arenavirus LCMV entirely from plasmid." Virology **350**(2): 370-380.

Sanofi-Pasteur (2014a). The World's First, Large-Scale Dengue Efficacy Study Successfully Achieved Its Primary Clinical Endpoint; retrieved from http://www.sanofipasteur.com/en/articles/theworld-s-first-large-scale-dengue-vaccine-efficacy-study-successfully-achieved-its-primary-clinical-endpoint.aspx.

Sanofi-Pasteur (2014b). Sanofi Pasteur's Dengue Vaccine Candidate Successfully Completes Final Landmark Phase III Clinical Efficacy Study In Latin America; retrieved from http://www.sanofipasteur.com/en/articles/sanofi-pasteur-s-dengue-vaccine-candidate-successfully-completes-final-landmark-phase-3-clinical-efficacy-study-in-latin-america.aspx.

Scandella, E., B. Bolinger, E. Lattmann, S. Miller, S. Favre, D. R. Littman, D. Finke, S. A. Luther, T. Junt and B. Ludewig (2008). "Restoration of lymphoid organ integrity through the interaction of lymphoid tissue-inducer cells with stroma of the T cell zone." Nat Immunol **9**(6): 667-675.

Schenten, D. and R. Medzhitov (2011). "The control of adaptive immune responses by the innate immune system." Adv Immunol **109**: 87-124.

Schmitz, J., A. Owyang, E. Oldham, Y. Song, E. Murphy, T. K. McClanahan, G. Zurawski, M. Moshrefi, J. Qin, X. Li, D. M. Gorman, J. F. Bazan and R. A. Kastelein (2005). "IL-33, an interleukin-1-like cytokine that signals via the IL-1 receptor-related protein ST2 and induces T helper type 2-associated cytokines." Immunity **23**(5): 479-490.

Scott, T. F. M. and T. M. Rivers (1936). "Meningitis in man caused by a filterable virus I. Two cases and the method of obtaining a virus from their spinal fluids." Journal of Experimental Medicine **63**(3): 397-414.

Senn, K. A., K. D. McCoy, K. J. Maloy, G. Stark, E. Frohli, T. Rulicke and R. Klemenz (2000). "T1-deficient and T1-Fc-transgenic mice develop a normal protective Th2-type immune response following infection with Nippostrongylus brasiliensis." Eur J Immunol **30**(7): 1929-1938.

Sevilla, N., S. Kunz, A. Holz, H. Lewicki, D. Homann, H. Yamada, K. P. Campbell, J. C. de La Torre and M. B. Oldstone (2000). "Immunosuppression and resultant viral persistence by specific viral targeting of dendritic cells." J Exp Med **192**(9): 1249-1260.

Sevilla, N., S. Kunz, D. McGavern and M. B. Oldstone (2003). "Infection of dendritic cells by lymphocytic choriomeningitis virus." Curr Top Microbiol Immunol **276**: 125-144.

Sevilla, N., D. B. McGavern, C. Teng, S. Kunz and M. B. Oldstone (2004). "Viral targeting of hematopoietic progenitors and inhibition of DC maturation as a dual strategy for immune subversion." J Clin Invest **113**(5): 737-745.

Sibold, C., H. Meisel, D. H. Kruger, M. Labuda, J. Lysy, O. Kozuch, M. Pejcoch, A. Vaheri and A. Plyusnin (1999). "Recombination in Tula hantavirus evolution: analysis of genetic lineages from Slovakia." J Virol **73**(1): 667-675.

Sironen, T., A. Vaheri and A. Plyusnin (2001). "Molecular evolution of Puumala hantavirus." J Virol **75**(23): 11803-11810.

Spann, K. M., P. L. Collins and M. N. Teng (2003). "Genetic recombination during coinfection of two mutants of human respiratory syncytial virus." J Virol **77**(20): 11201-11211.

Steinman, R. M. (2007). "Lasker Basic Medical Research Award. Dendritic cells: versatile controllers of the immune system." Nat Med **13**(10): 1155-1159.

Storni, T., F. Lechner, I. Erdmann, T. Bachi, A. Jegerlehner, T. Dumrese, T. M. Kundig, C. Ruedl and M. F. Bachmann (2002). "Critical role for activation of antigen-presenting cells in priming of cytotoxic T cell responses after vaccination with virus-like particles." J Immunol **168**(6): 2880-2886.

Talabot-Ayer, D., C. Lamacchia, C. Gabay and G. Palmer (2009). "Interleukin-33 is biologically active independently of caspase-1 cleavage." J Biol Chem **284**(29): 19420-19426.

Tesh, R. B., M. L. Wilson, R. Salas, N. M. De Manzione, D. Tovar, T. G. Ksiazek and C. J. Peters (1993). "Field studies on the epidemiology of Venezuelan hemorrhagic fever: implication of the cotton rat Sigmodon alstoni as the probable rodent reservoir." Am J Trop Med Hyg **49**(2): 227-235.

Thummel, C., R. Tjian and T. Grodzicker (1981). "Expression of SV40 T antigen under control of adenovirus promoters." Cell **23**(3): 825-836.

Tian, W., R. Nunez, S. Cheng, Y. Ding, J. Tumang, C. Lyddane, C. Roman and H. C. Liou (2005). "C-type lectin OCILRP2/Clr-g and its ligand NKRP1f costimulate T cell proliferation and IL-2 production." Cell Immunol **234**(1): 39-53.

Townsend, M. J., P. G. Fallon, D. J. Matthews, H. E. Jolin and A. N. McKenzie (2000). "T1/ST2-deficient mice demonstrate the importance of T1/ST2 in developing primary T helper cell type 2 responses." J Exp Med **191**(6): 1069-1076.

Traub, E. (1935). "A Filterable Virus Recovered from White Mice." Science **81**(2099): 298-299.

Trautmann, L., L. Janbazian, N. Chomont, E. A. Said, S. Gimmig, B. Bessette, M. R. Boulassel, E. Delwart, H. Sepulveda, R. S. Balderas, J. P. Routy, E. K. Haddad and R. P. Sekaly (2006). "Upregulation of PD-1 expression on HIV-specific CD8+ T cells leads to reversible immune dysfunction." Nat Med **12**(10): 1198-1202.

Turley, S. J., A. L. Fletcher and K. G. Elpek (2010). "The stromal and haematopoietic antigen-presenting cells that reside in secondary lymphoid organs." Nat Rev Immunol **10**(12): 813-825.

Velu, V., K. Titanji, B. Zhu, S. Husain, A. Pladevega, L. Lai, T. H. Vanderford, L. Chennareddi, G. Silvestri, G. J. Freeman, R. Ahmed and R. R. Amara (2009). "Enhancing SIV-specific immunity in vivo by PD-1 blockade." Nature **458**(7235): 206-210.

Vigil, A., M. S. Park, O. Martinez, M. A. Chua, S. Xiao, J. F. Cros, L. Martinez-Sobrido, S. L. Woo and A. Garcia-Sastre (2007). "Use of reverse genetics to enhance the oncolytic properties of Newcastle disease virus." Cancer Res **67**(17): 8285-8292.

von Messling, V. and R. Cattaneo (2004). "Toward novel vaccines and therapies based on negative-strand RNA viruses." Curr Top Microbiol Immunol **283**: 281-312.

Walker, D. H. and F. A. Murphy (1987). "Pathology and pathogenesis of arenavirus infections." Curr Top Microbiol Immunol **133**: 89-113.

Wherry, E. J. and R. Ahmed (2004). "Memory CD8 T-cell differentiation during viral infection." J Virol **78**(11): 5535-5545.

Wherry, E. J., J. N. Blattman, K. Murali-Krishna, R. van der Most and R. Ahmed (2003). "Viral persistence alters CD8 T-cell immunodominance and tissue distribution and results in distinct stages of functional impairment." J Virol **77**(8): 4911-4927.

Wherry, E. J., S. J. Ha, S. M. Kaech, W. N. Haining, S. Sarkar, V. Kalia, S. Subramaniam, J. N. Blattman, D. L. Barber and R. Ahmed (2007). "Molecular signature of CD8+ T cell exhaustion during chronic viral infection." Immunity **27**(4): 670-684.

Wilson, S. M. and J. C. Clegg (1991). "Sequence analysis of the S RNA of the African arenavirus Mopeia: an unusual secondary structure feature in the intergenic region." Virology **180**(2): 543-552.

Wittmann, T. J., R. Biek, A. Hassanin, P. Rouquet, P. Reed, P. Yaba, X. Pourrut, L. A. Real, J. P. Gonzalez and E. M. Leroy (2007). "Isolates of Zaire ebolavirus from wild apes reveal genetic lineage and recombinants." Proc Natl Acad Sci U S A **104**(43): 17123-17127.

Worobey, M. and E. C. Holmes (1999). "Evolutionary aspects of recombination in RNA viruses." J Gen Virol **80 (Pt 10)**: 2535-2543.

Wright, R., D. Johnson, M. Neumann, T. G. Ksiazek, P. Rollin, R. V. Keech, D. J. Bonthius, P. Hitchon, C. F. Grose, W. E. Bell and J. F. Bale, Jr. (1997). "Congenital lymphocytic choriomeningitis virus syndrome: a disease that mimics congenital toxoplasmosis or Cytomegalovirus infection." Pediatrics **100**(1): E9.

Xu, D., W. L. Chan, B. P. Leung, F. Huang, R. Wheeler, D. Piedrafita, J. H. Robinson and F. Y. Liew (1998). "Selective expression of a stable cell surface molecule on type 2 but not type 1 helper T cells." J Exp Med **187**(5): 787-794.

Yang, Q., G. Li, Y. Zhu, L. Liu, E. Chen, H. Turnquist, X. Zhang, O. J. Finn, X. Chen and B. Lu (2011). "IL-33 synergizes with TCR and IL-12 signaling to promote the effector function of CD8+ T cells." Eur J Immunol **41**(11): 3351-3360.

Ye, P., Z. H. Weng, S. L. Zhang, J. A. Zhang, L. Zhao, J. H. Dong, S. H. Jie, R. Pang and R. H. Wei (2008). "Programmed death-1 expression is associated with the disease status in hepatitis B virus infection." World J Gastroenterol **14**(28): 4551-4557.

Yewdell, J. W. and S. M. Haeryfar (2005). "Understanding presentation of viral antigens to CD8+ T cells in vivo: the key to rational vaccine design." Annu Rev Immunol **23**: 651-682.

Yi, J. S., M. Du and A. J. Zajac (2009). "A vital role for interleukin-21 in the control of a chronic viral infection." Science **324**(5934): 1572-1576.

Yoneyama, M., M. Kikuchi, T. Natsukawa, N. Shinobu, T. Imaizumi, M. Miyagishi, K. Taira, S. Akira and T. Fujita (2004). "The RNA helicase RIG-I has an essential function in double-stranded RNA-induced innate antiviral responses." Nat Immunol **5**(7): 730-737.

Zajac, A. J., J. N. Blattman, K. Murali-Krishna, D. J. Sourdive, M. Suresh, J. D. Altman and R. Ahmed (1998). "Viral immune evasion due to persistence of activated T cells without effector function." J Exp Med **188**(12): 2205-2213.

Zhang, Y., S. Huang, D. Gong, Y. Qin and Q. Shen (2010). "Programmed death-1 upregulation is correlated with dysfunction of tumor-infiltrating CD8+ T lymphocytes in human non-small cell lung cancer." Cell Mol Immunol **7**(5): 389-395.

Zhao, W. and Z. Hu (2010). "The enigmatic processing and secretion of interleukin-33." Cell Mol Immunol **7**(4): 260-262.

Zinkernagel, R. M. (2002). "Lymphocytic choriomeningitis virus and immunology." Curr Top Microbiol Immunol **263**: 1-5.

Zinkernagel, R. M., C. J. Pfau, H. Hengartner and A. Althage (1985). "Susceptibility to murine lymphocytic choriomeningitis maps to class I MHC genes--a model for MHC/disease associations." Nature **316**(6031): 814-817.

Zotos, D., J. M. Coquet, Y. Zhang, A. Light, K. D'Costa, A. Kallies, L. M. Corcoran, D. I. Godfrey, K. M. Toellner, M. J. Smyth, S. L. Nutt and D. M. Tarlinton (2010). "IL-21 regulates germinal center B cell differentiation and proliferation through a B cell-intrinsic mechanism." J Exp Med **207**(2): 365-378.

Contributions to the work

The article “The alarmin Interleukin-33 drives protective antiviral CD8+ T cell responses” (Chapter 1) was achieved in close collaboration of our lab with the group of Prof. Max Löhning at the DRFZ and Charité-University Hospital in Berlin, Germany. I performed experiments and analyses, which contributed to Figure 1.1E+F, 1.2C, 1.3D-F, 1.4A, 1.S1E, 1.S3B-E, as well as the genome wide cDNA expression analyses leading to Supplementary Tables 1.S1 and 1.S2.

The big majority of experiments presented in Chapter 2 and 3 were done by myself with the following exceptions. The validation of the IL-33 reporter mouse line by immunofluorescence (shown in Figure 2.2) was done in the laboratory of Prof. Sanjiv Luther at University of Lausanne by Hsin-Ying Huang and Stephanie Favre. Immunofluorescence stainings of LCMV-infected BECs shown in Figure 2.3G were conducted in the laboratory of Prof. Doron Merkler at University of Geneva by Ingrid Wagner. Experiments and analyses for Figure 3.2A were done by Stephanie Darbre, a former member of the lab.

Acknowledgments

First and foremost I would like to thank Daniel for the last four years; thanks for giving me the opportunity to work in your lab on such interesting projects. I am very grateful for your passionate and excellent supervision and your never-ending optimism even throughout tricky times. You always manage to see things in a positive way and I really appreciate your confidence in my work, which allowed me to plan and perform experiments independently and develop my own way of thinking. I also truly value that you enabled me to get hands-on experience in so many different fields of research all the range from molecular cloning to my beloved stroma isolations and in vivo experiments with lots of FACS.

I would like to thank the members of my PhD committee: Prof. Christoph Dehio, thank you for kindly accepting to be my representative supervisor for the faculty and to evaluate my work. Thank you also for supporting Daniel and me with your experience with all administrative hurdles related to our moving to Basel. Sincere thanks also to Prof. Benjamin Marsland for accepting to be a member in my PhD jury and taking the time to come to Basel to attend my defense.

A big THANK YOU to all present and past lab members. Thanks especially to Ben and Melissa, the good old Geneva crew that made it all the way to Basel. Ben, thanks for always being supportive and helpful and for staying patient and calm also in hectic times (and sorry for missing so many of your data sessions..). And thanks for your chocolate emergency stock, which prevented me from quite some hypoglycemic madness. Melissa, thanks for the great times we had in the lab, the mountains and elsewhere. I am glad we met and hope to keep in touch. MERCI to all past lab members Stephanie, Dimitri, Gregg, Marylise, Linda, Susan, Béné and Bastien. It has always been a pleasure to work with you guys! And last but not least many thanks to all the current lab members. Min, thank you for your endless patience and the constant smile on your face. You've been a great support for me during these last stressful months. Maggie, Mehmet, Micael and of course Weldy (thanks for the productive collaboration and all the discussions on the ST2 project!): it has been quite a change for us to jump over the Röschtigraben - thanks for being there and bringing some life to the lab. Thanks also to Cornelia and Karsten, two very important persons that keep the lab running.

During the time in Geneva I always considered Doron's and Daniel's group as one big team so I'd also like to express my gratitude to you, Doron, for very helpful discussions and input during lab meetings and the collaboration on the recombination part. Mario, Tanja, Ingrid and Karin, thanks for many shared croissants and laughs especially on Tuesday mornings.

I would like to thank our collaborators in Lausanne, Prof. Sanjiv Luther and Hsin-Ying Huang at the University of Lausanne, for great scientific discussions and experiments on the stroma project – To be continued!

Finally, I would like to thank all the friends I've made in Geneva and who have made these years so memorable and special. Thanks to Praxi, Patrick, Mario, Carmen, Melissa, Stephanie, Ben and Boris for all the fun evenings, weekends, adventures and coffee breaks – for sharing frustrations as much as legendary Café Cuba nights and mountain escapes! OBRIGADA to Fernanda (newly called Dr. Fe), the best flatmate I've ever had. Thanks for being there and sharing all these moments, it was amazing. I'll keep the peupliers-times always in best memory.

Particularly in hard times, the support I got from my friends back in Germany was priceless. Danke Johannes und Lisa für die vielen Jahre unserer Freundschaft seit Kindertagen, für alle gemeinsamen Abende und Erinnerungen. Ich weiss, dass ich immer auf Euch zählen kann und das bedeutet mir extrem viel. Auch Dir, Eva, möchte ich danken. Wir haben schon so viele Etappen unseres Lebens gemeinsam gemacht. Jetzt also die nächste! Es tut immer gut mit Dir zu reden. Danke für all die girls nights! Und bis bald an deiner Defense ☺

Un grand merci aussi à Laurence et Alexis - ma deuxième famille ici à Bâle. Merci de toujours essayer de comprendre ce que je fais et de me demander "Alors est-ce que t'as trouvé quelque chose maintenant?". Merci aussi pour tous les weekends en montagne. Ça a toujours été un grand plaisir de fuir mon quotidien pour quelques jours au grand air.

My sincere and wholehearted thanks go to my parents. Danke, dass Ihr immer an mich geglaubt habt und für Eure bedingungslose Unterstützung egal in welcher Lebenslage. Ihr habt niemals an mir gezweifelt und ohne Euch hätte ich all dies nicht erreichen können.

Danke auch für euer Vertrauen und eure Lässigkeit, dass am Ende schon alles immer irgendwie klappt und für all die Umzugshilfen in den letzten Jahren. Vielen Dank auch an Dich, Markus. Du warst immer eine sichere Stütze und es tut gut zu wissen, dass ich mich immer auf Dich verlassen und Dich nerven kann.

And last but not least of course I want to thank you, Philippe. You went through the entire PhD with me and you've always supported me in all situations. Thanks for your listening and understanding, for being my partner and my best friend and for your ability to make me laugh almost anytime. Thank you for all the things we've experienced and grown with together. I won't miss the airports and morning flights back from Gatwick, but those memories are hidden somewhere in between all the amazing weekends, travels and adventures that we've spend together between Geneva, London, Zurich and Basel. Next stop? ☺